SISSA
Scuola
Internazionale
Superiore di
Studi Avanzati

Physics Area - PhD course in
Theoretical Particle Physics

Precision microstate counting of black hole entropy from $\mathcal{N} = 1$ toric quiver gauge theories

Candidate:
Alfredo González Lezcano

Advisor: Leopoldo A. Pando Zayas
Co-advisor: Kyriakos Papadodimas

Academic Year 2020-21



A mi hermana Anabel

Acknowledgements

I would like to start by expressing my deepest gratitude to my family from Cuba: Nereida Lezcano Mató, Alfredo González Rodríguez, Anabel González Lezcano, Julio Cesar Lezcano Blanco and Olga Rodríguez Márquez, whose constant love and unconditional support has been fundamental for the completion of this wonderful journey.

Next I want to thank my supervisor Leopoldo Pando Zayas, whose great passion and dedication were crucial for my growth as a physicist. Thank you for your contagious excitement about physics and your continuous guidance during the past five years.

During these four years PhD I had the pleasure to share many hours of excellent discussion with Kyriakos Papadodimas. For that, and your infinite patience, I am very grateful.

I would also like to thank my collaborators, James Liu and Junho Hong, for the very productive interchanges from which I have profited a lot and learned every step of the way.

I have also had the opportunity to discuss with and learn from many colleagues to whom I would like to thank: Alejandro Cabo Bizet, Alejandra Castro, Marina David, Francesca Ferrari, Paolo Milan, Jun Nian, Arnab Rudra, Antonello Scardicchio and Christoph Uhlemann. As a student of the joint ICTP-SISSA PhD program I am highly indebted to many people who made my participation possible, specially Alejandro Cabo Montes de Oca, who guided my very first steps into the high energy physics world. Thanks to Giulio Bonelli and Matteo Bertolini for their encouragement during difficult times. Special thanks go also to all the ICTP staff, both faculty and administrative, for making ICTP feel like home since my arrival in 2016 for the Diploma program. Specially I thank Patrizia and Sandra, for helping me and guiding me through adaptation process when I first arrived to Trieste.

The completion of a journey full of challenges like this one, would have been impossible without the support and friendship of so many people. I thank Etien Martínez for his faith in me and his unwavering example of perseverance. I thank Cesar Reigosa and his family for all the countless unforgettable moments. Thanks to Uriel Luviano, for the music and for Reinaldo Arenas. Thanks to Alfredo Reyes, for bringing with you a piece of Havana to Trieste. Thanks to Mateo, Ana and their lovely family, for making Istria a second home for so many of us. I would like to thank: Tristram Acuña, Osbel Almora Rodríguez, José Enrique Álvarez, Claudia Artiaco, Alessio Baldazzi, Camilo Bravo, Alexandru Dima, Valerio Gherardi, Eduardo González, Shani Meynet, Alessandro Morandini, Ernesto Lopez Fune, Adu Offei-Danso, Paolo Spezzati and Vicharit Yingcharoenrat for every good memory shared along the way.

It is my pleasure to thank Andrés, Marita and Rodrigo for transforming Monfalcone from the train stop before Trieste into a warm and welcoming home. Finally, I offer my heartfelt appreciation to Noelia Cicuttin, whose support and company have been the greatest fuel that kept me running through good and bad moments during the last two years.

Abstract

The AdS/CFT correspondence, which conjectures a mathematical equivalence between string theories and field theories, has proven to be extremely successful in probing the microscopic structure of black holes. In this thesis we apply the AdS/CFT correspondence to investigate the entropy of five-dimensional, electrically charged rotating black holes. We do so by computing a field theoretical observable called the superconformal index. Specifically, we first study the superconfomal index of a large class of four-dimensional toric quiver gauge theories using a Bethe-Ansatz approach. Relying on a particular set of solutions to the corresponding Bethe-Ansatz equations we evaluate the superconformal index in the limit where the rank N of the gauge group of the field theory is large. We present explicit results for field theories arising from a stack of N D3 branes at the tip of toric Calabi-Yau cones whose gravity dual are IIB string theories on $\mathrm{AdS}_5 \times \mathrm{SE}_5$, where $\mathrm{SE}_5 = Y^{p,q}, X^{p,q}, L^{a,b,c}$ are Sasaki-Einstein manifolds. For a suitable choice of the chemical potentials of the theory we find agreement of the superconformal index and the function whose Legendre transform yields the black hole entropy, even in those situations where the explicit black hole supergravity solution is not known.

Furthermore, we systematically study various sub-leading structures in the superconformal index of $\mathcal{N} = 4$ supersymmetric Yang-Mills theory with $SU(N)$ gauge group. We concentrate in the two descriptions of the superconformal index, one as a matrix model of elliptic gamma functions, another in the Bethe-Ansatz presentation. Our saddle-point approximation goes beyond the Cardy-like limit and we uncover various saddles governed by a matrix model corresponding to $SU(N)$ Chern-Simons theory. The dominant saddle, however, leads to perfect agreement with the Bethe-Ansatz approach. We also determine the logarithmic correction to the superconformal index to be $\log N$, finding precise agreement between the saddle-point and Bethe-Ansatz approaches in their respective approximations. We generalize the two approaches to cover a large class of 4d $\mathcal{N} = 1$ toric quiver gauge theories. We find that also in this case both approximations agree all the way down to a universal contribution of the form $\log N$. The universality of this last result constitutes a robust signature of this ultraviolet description of asymptotically AdS_5 black holes and could be tested by low-energy IIB one-loop supergravity.

Contents

Dedication i

Acknowledgements ii

Abstract iii

List of Figures ix

List of Tables xi

1 Motivation, statement of the problem and summary of results 2

1.1 Introduction 3

1.2 Black holes microstate counting in string theory 4

1.3 The microscopic entropy of asymptotically AdS black holes 5

2 The $4d$ Superconformal Index and a large class of $\mathcal{N}=1$ toric quiver gauge theories 10

2.1 The 4d Superconformal Index 11

2.1.1 The structure of poles in the Superconformal Index 13

2.1.2 The Bethe-Ansatz formulation of the SCI 14

2.2 Construction of $\mathcal{N}=1$ theories dual to $\mathbf{AdS}_5\times\mathbf{SE}_5$ 17

2.2.1 The $Y^{p,q}$ geometries 17

2.2.2 Field theory dual of $Y^{p,q}$ geometries 26

2.2.3 The $Y^{p,q}$ quivers generated iteratively from the $Y^{p,p}$ quiver 28

2.2.4 The $X^{p,q}$ theories 30

2.2.5 The $L^{a,b,c}$ geometries 33

2.2.6 The field theory dual to $L^{a,b,c}$ 34

2.2.7 Generic properties of toric quiver gauge theories 35

2.3 The entropy function of $\mathcal{N}=1$ SCFT's 38

3 The SCI and the entropy function at leading N^2 order 40

3.1 Bethe Ansatz solutions for $\mathcal{N}=1$ toric quiver gauge theories **41**
3.1.1 Evaluation of the index 43

3.2 The superconformal index of various $\mathcal{N}=1$ toric quiver gauge theories **48**
3.2.1 The conifold theory 48
3.2.2 The Suspended Pinch Point 50
3.2.3 The $\mathbf{dP}_1$ theory 51
3.2.4 $Y^{p,q}$ quiver gauge theories 52
3.2.5 The $X^{p,q}$ theories 53
3.2.6 The $L^{a,b,c}$ theories 53

3.3 Conclusions I **54**

4 Logarithmic contribution to the SCI and underlying Chern-Simons matrix model **56**

4.1 Saddle-point approach to the SCI **57**
4.1.1 Saddle point approximation for $\mathcal{N}=4$ SYM 58
4.1.2 Leading term in the Cardy-like limit 59
4.1.3 Sub-leading terms in the Cardy-like expansion 60
4.1.4 Saddle point approximation for $\mathcal{N}=1$ toric quiver gauge theories 65

4.2 Bethe-Ansatz approach **70**
4.2.1 Bethe Ansatz approximation for $\mathcal{N}=4$ SYM 70
4.2.2 Bethe Ansatz approximation for generic $\mathcal{N}=1$ SCFT 76

4.3 Conclusions II **80**

5 Appendix A **83**

A Elliptic functions **84**
A.1 Definitions 84
A.2 Basic properties 84
A.3 Asymptotic behaviors 85

B Contribution from C-center solutions **87**
B.1 Saddle point approach 87
B.2 Bethe-Ansatz approach 89

C Saddle point solutions of 3d Chern-Simons theory **92**
C.1 The dominant saddle point 92
C.1.1 The solution for $t>0$ 94
C.1.2 The solution for $t=2\pi i/\eta$ with $\eta=\pm 1$ 94
C.2 The sub-leading saddle point 96

C.2.1 The solution for $t > 0$ 96
C.2.2 The solution for $t = 2\pi i/\eta$ with $\eta = \pm 1$ 97
C.3 Saddle point solutions of $\mathcal{N} = 4$ SYM from direct numerical evaluation 98

D The S^3 partition function of $SU(N)$ Chern-Simons theory **100**

List of Figures

1 This figure shows the two complex domains for the holonomies related through the map $z = e^{2\pi i u}$. The z plane is represented such that the unit circle over which the integration is originally performed is the boundary between the gray and white regions. The complex variable u lives on a cylinder. The unit circle on the z plane is mapped to the circle in the middle of the cylinder (both represented in red) where $\mathrm{Re}(u) \in [0,1]$ and $0 \sim 1$. 14

2 The figure shows the pairs of contours added and subtracted in order to obtain the final form of integration contour and the integrand for the SCI using the BA approach. The final integration contour is simply $\mathcal{C} \bigcup \mathcal{C}^1$. 16

3 Example of a cone in $\mathbb{R}^3$ whose base is a Delzant polytope. The normal vectors to the facets are represented in the figure by arrows and they are necessarily rational and describe which $U(1)$ subgroup of $\mathbb{T}^3$ is vanishing over the corresponding co-dimension two submanifold of $C\left(Y^{p,q}\right)$. 21

4 Toric diagrams associated to $Y^{1,0}$ (the conifold), $Y^{2,1}$ and $Y^{3,1}$ respectively. All of them are embedded in the corresponding orbifold $\mathbb{C}^3/\mathbb{Z}_{p+1} \times \mathbb{Z}_{p+1}$. 25

5 Triangulation of the toric diagram of $Y^{4,2}$ (embedded in the orbifold $\mathbb{C}^3/\mathbb{Z}_5 \times \mathbb{Z}_5$) where the number of simple triangles gives the value of $n_{\mathrm{v}} = 8$. Note also that, for a fixed p, as we decrease q, the node at the upper left side of the diagram moves up along the hypotenuse (see red dots) until it reaches $q = 0$ to form a parallelogram. 26

6 Example of a (p,q)-web for $Y^{4,2}$ and we have defined $a = p - q$. We obtain the reciprocal diagram by simply tracing orthogonal lines to each side of the toric diagram (represented here with dashed lines). We represent with the same color and continuous line the dual to each side. We keep the length of the reciprocal line to be the same as the original, hence the endpoints labeled in gray are easily determined if we make all reciprocal lines meet at the origin of the lattice. We refer to the reciprocal lines as external legs and they serve to fix the number of chiral fields n_χ in the quiver gauge theory. 27

7 Quiver diagram for $\mathbb{C}/\mathbb{Z}_8$ orbifold corresponding to the $Y^{4,4}$ geometry. Superpotential terms appear in the quiver diagram as triangles combining a green, a blue and a red arrow. 28

8 Quiver diagram corresponding to the $Y^{4,3}$ and $Y^{4,2}$ geometries. Superpotential terms appear in the quiver diagram as triangles combining a green, a blue and a red arrow and Z singlets are colored in violet. 30

9 Quiver diagram corresponding to the $Y^{4,1}$ and the $Y^{4,0}$ geometries. 30

10 Example of toric diagrams for $\mathbb{F}_0$, $d\mathbf{P}_1$ and $d\mathbf{P}_2$. The figure illustrates the Higgsing process from the point of view of the toric diagram. Vertices of iqual color are hose which are preserved from $d\mathbf{P}_2$ to either $d\mathbf{P}_1$(we preserve the black vertex and eliminate the blue one) or $\mathbb{F}_0$ (we preserve the blue vertex and eliminate the black one). 31

11 Relevant portion of quiver diagram for $X^{p,q}$ theory. The remaining part of the quiver is represented by a dotted line. New nodes k_1 and k_2 and fields $X_{k_{(1,2),j}}$, $X_{j,k_{(1,2)}}$ are drawn in orange. New superpotential terms appear in the quiver diagram as parallelograms. The labeling follows a counter-clockwise order. 32

12 Relevant portion of quiver diagram for $X^{p,p}$ theory. The remaining part of the quiver is represented by a dotted line. New nodes and fields are drawn in orange and new superpotential terms appear in the quiver diagram as parallelograms contaning at least one orange line. 33

13 Generic toric diagram for $X^{p,q}$ theory on the right as a simple generalization of the case of $d\mathbf{P}_2$ shown in figure 10. Here $a = p-q$ and we show the $Y^{p,q-1}$ toric diagram on the left and the $Y^{p,q}$ toric diagram on the center. 33

14 Example of a (p,q)-web for $X^{p,q}$ and we have defined $a = p - q$. We obtain the reciprocal diagram by simply tracing orthogonal lines to each side of the toric diagram (represented here with dashed lines). We represent with the same color and continuous line the dual to each side. We keep the length of the reciprocal line to be the same as the original, hence the endpoints labeled in gray are easily determined if we make all reciprocal lines meet at the origin of the lattice. 34

15 A generic four sided toric diagram of $L^{a,b,c}$ with the (p,q)-web included following the same color code used in section 2.2.2. The values of m and n have to satisfy the Diophantine equation $b = n(a+b-c) - am$. To this diagram corresponds one baryonic symmetry, however, generically, one has that $\#-$ of baryonic symmetries $+3 = \#$-of external legs of (p,q)-web. From this data we extract $n_{\mathrm{v}} = a + b$ and $n_\chi = a + 3b$. 35

16 The figure shows the complex plane of chemical potentials for a generic Δ where the region specified by (3.2.2) is shown in gray. 48

17 Numerical leading saddle points (blue dots) discussed in Appendix C.3 with $N = 30$ and $\tau = \frac{ie^{\pi i/6}}{\pi}$. There must be $N = 30$ distinct sets of holonomies in the above figure but here only 5 copies of them are shown for presentation. Orange crosses denote $\pm\tau + \frac{m}{N}$ $(m = 2, 8, 14, 20, 26)$ and therefore it is straightforward to see that each set of holonomies collapses to $\frac{m}{N}$ as $|\tau| \to 0$. 63

18 In the left hand side, blue dots represent numerical values of the real part of the Jacobian contribution $\mathrm{Re}\log H(\hat{u};\Delta,\tau)$ and an orange line shows the first two leading terms read from (4.2.26), namely $N\log N - (N-1)\log|\tau|$. The figure in the right hand side shows numerical values of $\mathrm{Re}\log\det(I_{N-1} + \tilde{H})$, obtained by subtracting an orange line from blue dots in the left hand side. It converges to a certain finite value and therefore we can conclude it is of order $\mathcal{O}(N^0)$. 75

19 Orange (red) crosses are branch points and green (blue) lines are branch cuts of $h_+(x)$ and $h_-(x)$, respectively. Here we chose $\epsilon = 1/10$ for presentation. 95

20 The numerically determined eigenvalue density, $\rho(x)$, for $N = 50$ and $t = 5$ (red dots) along with the large-N analytic solution (blue line), (C.33). The numerical density is obtained by finite differencing. 97

21 The numerically determined eigenvalues, $-iu_j$ for $N = 50$. The family of solutions correspond to $t = 5$ (red), $t = 5 + \pi i/2$ (orange), $t = 5 + 2\pi i$ (yellow), $t = 3 + 2\pi i$ (green), and $t = 2\pi i$ (blue), respectively. 98

22 Comparison between the $\mathcal{N} = 4$ SYM (blue dots) and 3d Chern-Simons (orange diamonds) solutions for the dominant saddle point. Here we have taken $N = 100$ along with $\tau = ie^{i\pi/6}$ and $\Delta_a = (2/3, 2/3, 2/3 + 2\tau)$, which maps to $t = 2\pi i$ in the Chern-Simons theory. As seen in the figure on the right, the exponentiated eigenvalues go twice around the circle. The 3d Chern-Simons eigenvalues u_i are given as in (C.3), while the $\mathcal{N} = 4$ SYM eigenvalues $\tilde{u}_i$ are mapped according to $u_i = 2\pi i\tilde{u}_i/\tau$. 99

23 Comparison between the $\mathcal{N} = 4$ SYM (blue dots) and 3d Chern-Simons (orange diamonds) solutions for the sub-leading saddle point. The parameters are the same as in Figure 22, but for the sub-leading saddle the exponentiated eigenvalues go only once around the (distorted) circle. 99

List of Tables

1 Charge assignment and multiplicities of fields for $Y^{p,q}$ theory where $k = 1, 2, 3$ and two of the global charges are really enhanced to $SU(2)$ as we discussed in section 2.2.2. 37

2 Charge assignment and multiplicities for $X^{p,q}$ theory where $k = 1, 2, 3, 4$. 37

3 Charge assignment and multiplicities of fields for $L^{a,b,c}$ theory where $k = 1, 2, 3$. 37

4 Charge assignment and fields for the conifold theory. 49

5 Charge assignment and fields associated to the Suspended Pinched Point theory. 50

6 Charge assignment and fields of the $d\mathbf{P}_1$ theory, which corresponds to $Y^{2,1}$. 52

7 Charge assignment and multiplicities for $Y^{p,q}$ theory. 52

8 Charge assignment and multiplicities for $X^{p,q}$ theory. 53

9 Charge assignment and multiplicities for $L^{a,b,c}$ theory. 54

Preface

In this thesis we present the results of [1] and [2]. The research of the candidate during his PhD has also lead to the publication [3].

CHAPTER 1
Motivation, statement of the problem and summary of results

1.1 Introduction

Understanding the microscopic structure of black holes is one of the greatest scientific problems in modern science. There is a lot more to gain by tackling this problem than the mere satisfaction of answering technically challenging questions. Indeed, the quest to accomplish a unified theory to describe nature has driven the scientific community since ancient times. Black holes can be thought of as "theoretical laboratories" since they force our known theories to their limits of validity, thus giving us the chance to systematically tests our candidates to fundamental theories of nature.

Looking into the last century we see that one of the most fruitful attempts of unification brought Einstein's Special Theory of Relativity and Quantum Mechanics into the same footing, which resulted in the quantum theory of fields, or quantum field theory (QFT), as we know it today. The Standard Model of Elementary Particles is, so far, the most complete and experimentally validated theory describing all interactions of matter (except gravity) at the fundamental level and it is entirely formulated in the framework of QFT, in particular gauge field theories. Another major achievement of the last century is the general theory of relativity which describes the evolution of space-time in the presence of matter and energy, that is, gravitational interaction.

It is then natural to ask if there exist an even more fundamental theory in which gravitational interaction appears properly quantized. Such theory would be a theory of quantum gravity. String theory has successfully accommodated both general relativity (GR) and QFT harmoniously into a single theoretical framework. As any other candidate for quantum gravity, string theory must face, eventually, experimental scrutiny whose implementation currently lays beyond technological reach. In the meantime we must try our best to make predictions that can either recover known results or be experimentally tested in the future.

Typically one ignores gravitational effects when describing phenomena involving elementary particles. However, in situations where the radius of curvature of space-time is comparable to the Planck length $L_P = \left(G_N\hbar/c^3\right)^{1/2} \approx 10^{-33}$cm, one could no longer ignore gravitational effects. It is in such situations where it becomes relevant to have a quantum description of gravity.

Black holes can be the ideal scenario to attempt a description including the interplay between GR and QFT precisely because they are very massive objects which make it no longer viable to ignore gravitational interaction even at scales typically governed by QFT. In practice, the radius of curvature of space-time outside (and near) a black hole is still very large compared to L_P, hence the energy density of particles created by the gravitational field is large compared to the space-time curvature. Quantum effects are locally small, still, as emphasized by Hawking in [4], they can have an overall effect over the lifetime of the Universe $\approx 10^{17}s$, which is very long compared to the Planck time $\approx 10^{-43}s$.

The physics of black holes is deeply connected to the laws of thermodynamics [4–8]. Bekenstein provided in 1973 a nice generalization of the second law of thermodynamics which required the black hole to carry entropy. The entropy of a black hole with horizon area A is proportional to A [5, 6]. The proportionality factor was pinned down by Hawking [7, 8] by studying the quantum thermal radiation in the black hole background. The black hole entropy is finally given by the celebrated Bekenstein-Hawking entropy formula:

$$S_{BH} = k_B \frac{c^3}{G_N\hbar}\frac{A}{4}, \tag{1.1.1}$$

where k_B is the Boltzmann constant, c is the speed of light and G_N is the Newton constant. From now on we shall use natural units by setting $k_B = \hbar = c = 1$, however, let us notice here that this is a very illustrative formula where, at least at an intuitive level, we identify the coalescence of the fundamental constants both from gravity (G_N) and from quantum mechanics ($\hbar$). Even though (1.1.1) was obtained through a quasi-classical computation, the appearance of $\hbar$ clearly indicates the inevitability of full quantum mechanics and the need for an underlying more fundamental theory.

Entropy is a quantity that establishes a bridge between the microscopic composition of a system and the macroscopic (thermodynamic) description of the system. Therefore, any candidate for theory of quantum gravity should be able to provide a successful counting of the microstates which give rise to the entropy of black holes. A first stage would require to reproduce the result (1.1.1) (including the proportionality factor 1/4), which has to be done in a quasi-classical regime. In field theoretical language this means that all interactions considered are evaluated only up to tree level and loops corrections are negligible. As we depart from the quasi-classical regime, the entropy (1.1.1) receives quantum corrections which a theory of quantum gravity should reproduce. The work here presented contains contributions in both of these directions. Before explicitly formulating our problem, we shall elaborate some more on the different results obtained in the counting of black holes microstates from string theory.

1.2 Black holes microstate counting in string theory

In 1996, Strominger and Vafa made a breakthrough in the direction of counting black holes microstates in the context of string theory [9]. It was the first time the precise factor of 1/4 in (1.1.1) was reproduced from a direct counting of states. The authors of [9] considered phases of string theory with five non-compact dimensions and $\mathcal{N} = 4$ supersymmetry. The result was attained by looking for black holes with non vanishing horizon area which had non-vanishing both electric and axion charges Q_F, Q_H respectively and at the same time saturated the Bogomol'nyi-Prasad-Sommerfield (BPS) condition. Such BPS states may be viewed as bound states of minimally charged BPS solitons, and their exact degeneracy can be computed by counting soliton bound states [10–16].

The counting process reduced to finding degeneracies of 1/4 BPS states of a supersymmetric sigma model defined on a symmetric tensor product of the compact manifold on which the compactification was performed. Such degeneracies were known to be bound by the elliptic genus of the sigma model [17, 18] and in the large charge limit was indistinguishable from it. Precisely in this large charge limit, the leading degeneracy of the logarithm of bound state degeneracy reproduces the Bekenstein-Hawking entropy formula for a $5d$ extremal Reissner-Nordstrom black hole with charge $Q = \sqrt{3}\left(\frac{8Q_H Q_F^2}{\pi}\right)^{1/3}$.

In [19] an 11-dimensional M-theory formulation where the spectrum of five-branes BPS states was found and satisfactory connected to the entropy of the corresponding black holes. Further developments in [20, 21] made more precise the connection between the elliptic genus on symmetric tensor product of a manifold $\mathcal{M}$ and the partition function of a second quantized string theory on $\mathcal{M} \times S^1$. This result uncovered deep connections between black hole microstates and modular properties through the elliptic genus.

The results of [19–21] essentially solved the problem of microstate counting of asymptotically flat single centered dyonic black holes. In fact, tackling the same question for multi-centered black holes opened a very fruitful new avenue where unsuspected beautiful relations with mock modular forms were encountered [22][1].

One significant limitation of Strominger-Vafa's approach is that no off-shell calculation can be performed, since there is no an off-shell formulation of string theory. The results reviewed so far refer only to asymptotically flat black holes. The problem of counting black holes microstates in asymptotically AdS black holes has been developed more recently and this constitutes the subject of the next section. In fact, we will see that from a holographic perspective one can also make off-shell statements about black hole entropy.

1.3 The microscopic entropy of asymptotically AdS black holes

The Anti de Sitter/ Conformal Field Theory (AdS/CFT) correspondence [25] conjectures a mathematical equivalence between string theory on asymptotically AdS spaces and conformal field theory (CFT). The prototypical example is the case of a $\mathcal{N}=4$, Supersymmetric Yang-Mills (SYM) gauge theory with gauge group $SU(N)$ and coupling constant g_{YM}, it has been argued that the such theory can be precisely reformulated as string theory in $\mathrm{AdS}_5\times S^5$ with N units of Ramond-Ramond five-form flux [26].

So far the most useful regime in the correspondence has been the classical gravity approximation, which can be put in correspondence with the field theory side restricted to the regime $N\to\infty$ keeping fixed a large value of $g^2_{YM}N$, known as 't Hooft limit. The AdS/CFT correspondence allows to address difficult problems of strongly coupled field theory dynamics using weakly couple gravity. Furthermore, it answers implicitly a great puzzle formulated in gravity like Hawking's information paradox. By establishing such a deep link between gravity and a well defined QFT, the AdS/CFT resolves, at least conceptually speaking, the puzzle of information, since unitarity of the QFT implies no information loss. Our community is finally at a stage where we can explicitly see how solving these conceptual puzzles can be realized through concrete calculations.

In the context of counting black holes microstates from AdS/CFT one is actually counting field theoretical degrees of freedom, hence it was natural to expect that the Bekenstein-Hawking entropy formula could be reproduced for asymptotically AdS black holes using a holographic approach. In fact, for the specific case of asymptotically AdS_3 black holes the counting of states can be done in the $2d$ CFT related to AdS_3 through the AdS/CFT correspondence by making use of the Cardy formula [27], which counts the asymptotic growth of CFT states for large charges. The problem for $\mathrm{AdS}_{d\geq 4}$ remained open for a long time and it was not until approximately twenty years after [9], with the paper by Benini, Hristov and Zaffaroni [28, 29] that this problem was solved for static dyonic BPS in $\mathrm{AdS}_4\times S^7$ M-theory consistently truncated on S^7 to a $4d$ $\mathcal{N}=2$ gauged supergravity with three Abelian vector multiplets [30]. The result was obtained in the large rank limit of the Aharony-Bergman-Jafferis-Maldacena (ABJM) theory [31] living in the boundary of AdS_4. The black hole microstates are mapped by holography to the ground state of the dual CFT quantized on S^2 with a topological twist [32] which takes care of the magnetic charges of the black hole. Specifically, such states can be counted by means of a refined version of the Witten index [33],

[1] See [23, 24] for a pedagogical and detailed introduction to these subjects.

called the topologically twisted index, which has the form:

$$\mathcal{I}_{TT}(p,\Delta) = \mathrm{Tr}_{\mathcal{H}_{S^2}}\,(-1)^F\, e^{-\beta H} e^{2\pi i \sum_a \Delta_a Q_a}, \tag{1.3.1}$$

where Δ_a is the chemical potential associated to the electric charges Q_a, p are integer numbers associated to the magnetic charge of the black hole, H is the Hamiltonian, F is the fermion number and β is the inverse temperature.

Supersymmetry ensures that only the ground states contribute to $\mathcal{I}_{TT}$ and it remains unchanged under continuous deformations of the coupling of the theory [33]. The presence of the $(-1)^F$ in (1.3.1) implies the possibility of significant cancellation between fermionic and bosonic states and poses a potential obstruction to argue that an index can indeed have the correct asymptotic growth of states as to account for black hole entropy. However, operating under the assumption that no such cancellation would happen, the authors of [28, 29] where able to show that $\mathcal{I}_{TT}$ has the correct asymptotic growth of states in the large N limit (where N is the rank of the gauge group of ABJM theory). In such limit, the black hole entropy can be extracted from it via a Legendre transform:

$$S_{BH} = \log \mathcal{I}_{TT}(\tilde{\Delta}) - 2\pi i \sum_a \tilde{\Delta}_a Q_a, \tag{1.3.2}$$

where $\tilde{\Delta}$ are values that extremize the right hand side of (1.3.2).

Before the work of [28, 29] there was another attempt in [34] to attack the problem of black holes microstate counting for asymptotically AdS black holes for the holographic pair of $\mathcal{N}=4$ SYM theory and Type IIB supergravity on $\mathrm{AdS}_5 \times S^5$. In [34], the authors constructed and evaluated a $4d$ Superconformal Index (SCI) whose precise definition we shall give presently. The SCI counts (with sign) BPS states that can not combine to form long representations of the superconformal algebra. For $\mathcal{N}=1$ theories on $S^1 \times S^3$, the SCI was defined in [34, 35] and takes the form:

$$\mathcal{I}(p,q;v) = \mathrm{Tr}_{\mathcal{H}(S^1\times S^3)}\left[(-1)^F\, e^{-\beta\{\mathcal{Q},\mathcal{Q}^\dagger\}} v_a^{Q_a} p^{J_1+\frac{r}{2}} q^{J_2+\frac{r}{2}}\right], \tag{1.3.3}$$

where Q_a are the charges associated to flavor symmetries and r is the R-charge. The angular momenta on S^3 are denoted as $J_{1,2}$ and the combination $J_{1,2}+\frac{r}{2}$ commutes with the supercharge $\mathcal{Q}$. The fugacities p and q are associated to $J_{1,2}+\frac{r}{2}$. We have that, $\mathcal{I}(p,q;v)$ counts $\frac{1}{16}-$BPS states for $\mathcal{N}=4$ SYM theory and $\frac{1}{4}-$BPS states for more generic $\mathcal{N}=1$ superconformal field theories (SCFT's). Details on the different forms (1.3.3) takes will be given in chapter 2. The asymptotic growth of states in the large N limit of the SCI resulted to be $\mathcal{O}(e^{N^0})$ (which was too small to reproduce black hole entropy correctly) when using real fugacities.

There has been a recent revival of the problem of giving a microscopic explanation of the entropy of electrically charged, rotating black holes in AdS_5 using the SCI of $\mathcal{N}=4$ SYM theory. Three recent works have provided microscopic foundations for the black hole entropy using the dual supersymmetric field theory [36–38]. The answer was obtained simultaneously by three groups using slightly different starting points, however all of them shared the idea of permitting chemical potentials to be complex.

The first goal of this thesis is to investigate the SCI of a large class of $\mathcal{N}=1$ toric quiver gauge theories in the large N limit. This extends the results of [38]. We address these matters in chapter 3. The approach put forward by Benini and Milan in [38], attacked the SCI using a Bethe-Ansatz (BA) approach developed in [39]. Understanding that the SCI can be written as a sum

over solutions to BA equations was demonstrated in [40] based on interesting relations between observables on manifolds of different topologies developed in [41]. Previous works studied the SCI in the limit of very small angular velocities, known as the Cardy-like limit. The main result was the demonstration that the Cardy-like limit of the SCI of 4d $\mathcal{N}=4$ SYM accounts for the entropy function, whose Legendre transform corresponds to the entropy of the holographically dual AdS_5 rotating black holes were presented in [42, 43]. Such analysis has by now been extended to generic $\mathcal{N}=1$ supersymmetric gauge theories [44, 45] including a particular description specialized to arbitrary $\mathcal{N}=1$ toric quiver gauge theories, observing that the corresponding entropy function can be interpreted in terms of the toric data [46]. These powerful results rest on systematic studies of the Cardy limit developed in, for example, [47–51].

One key advantage of the BA approach is that it probes the large N behavior of the SCI for all values of angular velocities, and thus opens the door for a more in-depth understanding of the SCI.

We can summarize our first result as follows: By selecting a set of chemical potentials that ensures an optimal obstruction of cancellations between bosonic and fermionic contributions to the SCI, one can always find a region of chemical potentials where the index accounts for the black hole entropy. Concretely, for $p=q=e^{2\pi i\tau}$ in (1.3.3), we obtain that the index reproduces the expected entropy function of the form:

$$\log \mathcal{I}(\tau;\Delta) = -\frac{i\pi N^2}{6\tau^2} C_{IJK}\Delta_I\Delta_J\Delta_K, \tag{1.3.4}$$

whose functional from was first conjectured in [52]. The coefficients C_{IJK} in (1.3.4) correspond, as pointed out originally in [53] and later in [46], to the Chern-Simons couplings of the holographic dual gravitational description as elucidated in [54]. The quantities Δ_I are related to the chemical potential of flavor charges and will be defined more precisely in chapter 2.

In chapter 3 we proceed to evaluate the SCI for various models, some of them recently discussed in a similar context in [46], and compare our results with (3.1.36) on a case by case basis.

The results we will discuss in chapter 3 were reported in [1] where we extend the results of [38] to a large class of $\mathcal{N}=1$ toric quiver gauge theories. These results where also reported in a later publication [55].

The second goal of this thesis is to systematically study the SCI both from the BA approach and the saddle point approximation to evaluate the integral expression for SCI. Specifically, we keep track of logarithmic corrections in the rank of the gauge group and refine the Cardy-like limit computations by finding all perturbative corrections in inverse powers of the angular velocity. The results here summarized were published in [2] and there have been follow up research by other authors ever since (see for example [56–59]).

The scenario we faced was the following: Initially, there were three approaches to the question of AdS_5 black hole entropy: (i) The collaboration in [36] exploited a supersymmetric localization argument; (ii) The work [37] started from the physical partition function at weak coupling; (iii) The authors of [38] started from a Bethe-Ansatz (BA) presentation of the SCI.

Soon after these original works, it became evident that these groups basically proposed different approaches to the SCI whose leading term is (1.3.4). Naturally, the ideas put forward in those works have inspired similar computations that have been carried out in various field theories with the resounding outcome of providing microscopic foundations for the entropy of rotating, electrically

charged, asymptotically AdS black holes in various dimensions including AdS_4, AdS_6 and AdS_7, see for example, [60–67]; this collective body of work reinforces the original intuition.

One question that follows from this embarrassment of richness is to determine the precise relation between the different approaches. This situation motivates us to embark on a systematic study of those presentations at leading and sub-leading orders. We demonstrate explicitly that the two main presentations are different approximations schemes to the index which result, nevertheless, in the same answer including sub-leading terms all the way down to a universal logarithmic correction. This process helps us clarify a number of central elements and provides a glimpse into an effective matrix model theory governed by a $SU(N)$ Chern-Simons theory. This result leads to a deeper understanding of the effective field theory approach to the SCI [58, 59].

Let us briefly describe some of our main results. Recall that the index counts (with sign) $\frac{1}{16}$-BPS states and depends on the fugacity τ and chemical potentials Δ_a. When written as a matrix model, we discuss the saddle-point approach to the SCI. In this approach we consider a Cardy-like limit but extend it to include all terms up to exponentially suppressed ones, $\mathcal{O}(e^{-1/|\tau|})$. The τ independent term appears as the action of a matrix model which can be studied in the large-N limit to obtain the following result:

$$\boxed{\begin{aligned}\mathcal{I}(\tau;\Delta) &= \mathcal{I}(\tau;\Delta)\big|_{\text{Dominat Saddle Point}} + (\text{contribution from other saddles})\\ \log\mathcal{I}(\tau;\Delta)\big|_{\text{Dominant Saddle Point}} &= -\frac{\pi i(N^2-1)}{\tau^2}\prod_{a=1}^{3}\left(\{\Delta_a\}_\tau - \frac{1+\eta}{2}\right) + \log N + \mathcal{O}(e^{-1/|\tau|}).\end{aligned}} \tag{1.3.5}$$

The value of $\eta = \pm 1$ is determined by the domain of Δ_a. We are also able to compute explicitly the contribution from other saddles, one of which turns out to be subdominant compared to (1.3.5) by an N^2-leading order term independent of chemical potentials.

The matrix model we obtain exactly reproduces the action of a matrix model associated to a $SU(N)$ Chern-Simons theory on S^3. The exact partition function of such theory is known at finite N (see appendix D), rendering our result valid for all N. Our result can be expressed as:

$$\boxed{\log\mathcal{I}(\tau;\Delta) = -\frac{\pi i(N^2-1)}{\tau^2}\prod_{a=1}^{3}\left(\{\Delta_a\}_\tau - \frac{1+\eta}{2}\right) + \log N + \mathcal{O}(e^{-1/|\tau|}).} \tag{1.3.6}$$

Note that the result in (1.3.6) coincides with the leading saddle point contribution in (1.3.5), moreover, since (1.3.6) is exact in N, it seems to suggest that contributions from other saddles in (1.3.5) should cancel each other, however we only analyzed one of such subdominant saddles (see Appendix (C.2.2)). Analogous results were obtained for a large class of $\mathcal{N}=1$ toric quiver gauge theories. We obtain an analogous expression for a wide class of $\mathcal{N}=1$ 4d SCFT's.

The other approach to the index that we scrutinize in chapter 4 is the BA approach. In this approximation the index is written as the sum of contributions from BA solutions and we focus on the contribution of the so-called basic solution. This solution to the eigenvalues first appeared in the high temperature limit of the the topologically twisted index of $\mathcal{N}=4$ SYM on $T^2\times S^2$ [52]. It

was later shown in [68] that it provides an exact solution for the topologically twisted index without the need of the high temperature approximation. This solution was also used by Benini and Milan in their discussion of the SCI [38] and it was further extended in [1, 55] where it was shown that it furnishes a solution for a generic class of $\mathcal{N}=1$ supersymmetric field theories[2] . More recently, the BA approach to the index based on the basic solution was extended to include two different angular velocities [69], thus covering the most general type of asymptotically $AdS_5 \times S^5$ black holes. Our results for the BA approach goes beyond the leading N^2 order in the large-N limit and takes the form

$$\boxed{\begin{aligned} \mathcal{I}(\tau;\Delta) &= \mathcal{I}(\tau;\Delta)\big|_{\text{Basic BA}} + (\text{contribution from other BA solutions}) \\ \log \mathcal{I}(\tau;\Delta)\big|_{\text{Basic BA}} &= -\frac{\pi i (N^2-1)}{\tau^2} \prod_{a=1}^{3} \left(\{\Delta_a\}_\tau - \frac{1+\eta}{2} \right) + \log N + \mathcal{O}(N^0). \end{aligned}} \tag{1.3.7}$$

We are also able to compute explicitly the contribution from other BA solutions in Appendix B.2. We obtain an analogous expression for a wide class of $\mathcal{N}=1$ 4d SCFT's.

There are two important lessons that we provide:

- The expressions (1.3.6) and (1.3.7) explicitly demonstrate that both approaches are consistent with each other and yield the same contribution to the SCI up to exponentially suppressed terms of the form $e^{-1/|\tau|}$ in the Cardy-like limit, filling a gap in the literature regarding all possible perturbative sub-leading corrections, namely $o(|\tau|^{-1})$[3] in (1.3.6) and $o(N^2)$ in (1.3.7).

- One of our main results is finding the logarithmic corrections which required control beyond the Cardy-like limit. In both approximations we find the same term, $\log N$. The $\log N$ terms constitute, as remarked by Ashoke Sen [70], a litmus test for any theory aspiring to be the ultraviolet complete description of gravity and such term should match the corresponding supergravity one-loop computation, presenting a unique UV/IR connection. The robustness of this term in the two approaches to the index is an important UV signature that we derive.

The rest of the thesis is organized as follows: In **chapter** 2 we review the necessary background we will need. Firstly we present the BA approach to the SCI. Since we are interested in evaluate the SCI of a wider class of $\mathcal{N}=1$ toric quiver gauge theories, we give a detailed presentation of these theories and their main properties that will be of use during our derivations. **Chapter** 3 presents the evaluation of the SCI at leading order in N^2 for a $\mathcal{N}=1$ toric quiver gauge theories using the BA approach [1]. **Chapter** 4 shows with both the Saddle point approach to the SCI and the BA including logarithmic corrections in N [2]. When needed, we offer separated conclusions at the end of each chapter. Given the technical nature of our investigation we relegate a number of calculations and results to a series of appendices.

[2] In fact this is the content of chapter 3 of this thesis.
[3] Contributions of $\mathcal{O}(|\tau|^{-1})$ were found in [44].

CHAPTER 2

The $4d$ Superconformal Index and a large class of $\mathcal{N} = 1$ toric quiver gauge theories

In this chapter we shall review known results of immediate interest for further developments. The matter here presented should serve as a background and reference for next chapters. We first give, in (2.1), a detailed presentation of the SCI, its definition, and its analytical explicit formula. We discuss the BA approach to evaluating the SCI which will be applied in chapters 3 and 4 to evaluate the SCI of $\mathcal{N}=1$ toric quiver gauge theories. We then proceed in section (2.2) to discuss the construction of $\mathcal{N}=1$ toric quiver gauge theories dual to the product AdS_5 times a 5d Sasaki-Einstein manifold. Section (2.3) is devoted to motivate the functional form of log(SCI) at leading order and the extremization process that should be carried in order to extract the black hole entropy.

2.1 The 4d Superconformal Index

The SCI counts (with sign) BPS states that can not combine to form long representations of the superconformal algebra. For $\mathcal{N}=1$ theories on $S^1\times S^3$, the SCI was defined in [34, 35] and takes the form:

$$\mathcal{I}(p,q;v)=\mathrm{Tr}_{\mathcal{H}(S^1\times S^3)}\left[(-1)^F e^{-\beta\{\mathcal{Q},\mathcal{Q}^\dagger\}}v_a^{Q_a}p^{J_1+\frac{r}{2}}q^{J_2+\frac{r}{2}}\right], \tag{2.1.1}$$

where Q_a are the flavor charges with fugacities v_a. The the combination $J_{1,2}+\frac{r}{2}$, where $J_{1,2}$ are the angular momenta on S^3 and r is the R-charge, commute with the supercharge $\mathcal{Q}$. The fugacities p and q are associated to $J_1+\frac{r}{2}$ and $J_2+\frac{r}{2}$ respectively. We have that, $\mathcal{I}(p,q;v)$ counts $\frac{1}{16}-$BPS states for $\mathcal{N}=4$ SYM theory and $\frac{1}{4}-$BPS states for more generic $\mathcal{N}=1$ SCFT's. To count such states we need the single letter partition function of the non-interacting theory which is define exactly like (2.1.1) but the trace is taken over the space of single letters:

$$f(p,q;v)=\mathrm{Tr}_{\text{Sinlge letters}}\left[(-1)^F e^{-\beta\{\mathcal{Q},\mathcal{Q}^\dagger\}}v_a^{Q_a}p^{J_1+\frac{r}{2}}q^{J_2+\frac{r}{2}}\right] \tag{2.1.2}$$

To generate the multi-trace partition function $g(p,q;v)$ from $f(p,q;v)$ we have to use the Plethystic exponentiation [71–73]:

$$g(p,q;v)=\exp\left(\sum_n^\infty\frac{1}{n}f(p^n,q^n;v^n)\right). \tag{2.1.3}$$

Recalling that we want to only count gauge singlets, then we can use the algebraic property that the number of singlets in a product of representations is simply the integral over the group manifold of the product of characters for these representations. Then we have that the SCI (2.1.1) for $\mathcal{N}=1$ Superconformal gauge theories can be expressed as a complex integral [74]:

$$\mathcal{I}(p,q;v)=\int[\mathcal{D}U]\exp\left(\sum_{n=1}^\infty\sum_{i,\mathrm{R}_i}\frac{1}{n}f_i(p^n,q^n;v^n)\chi_{\mathrm{R}_i}(U^n)\right), \tag{2.1.4}$$

where U is the holonomy of the gauge field around S^1, $[\mathcal{D}U]$ is the invariant group measure and i runs over the matter and gauge fields transforming in representations R_i. The character of such representation is denoted as $\chi_{\mathrm{R}}(\cdot)$. The single letter partition function of the i-th field is denoted as $f_i(p,q;v)$. Specifically, for chiral matter, the single letter index has the form [74]

$$f_\Phi(p,q;v)=\frac{v-pq/v}{(1-q)(1-p)}, \tag{2.1.5}$$

whereas the vector multiplet single letter index is given by:

$$f_{\mathrm{V}}(p,q) = 1 - \frac{1-pq}{(1-p)(1-q)}. \tag{2.1.6}$$

Inserting (2.1.5) and (2.1.6) in (2.1.4) will generate terms of the form:

$$\begin{aligned}
\exp\left(\sum_{n=1}^{\infty}\frac{1}{n}f_{\Phi}(p^n,q^n;v^n)\right) &= \prod_{j,k\geq 0}\frac{1-v^{-1}p^{j+1}q^{k+1}}{1-vp^jq^k} = \Gamma\left(v;p,q\right)\\
\exp\left[\sum_{n=1}^{\infty}\frac{1}{n}f_{\mathrm{V}}(p^n,q^n)\left(z^n+z^{-n}\right)\right] &= \frac{1}{(1-z)(1-z^{-1})}\frac{1}{\Gamma(z;p,q)\Gamma(z^{-1};p,q)}\\
\exp\left(\sum_{n=1}^{\infty}\frac{1}{n}f_{\mathrm{V}}(p^n,q^n)\right) &= (p;p)_{\infty}\,(q;q)_{\infty}\,,
\end{aligned} \tag{2.1.7}$$

which hold in the domain where $|p|,|q|<1$ for $p,q\in\mathbb{R}$. The function $\Gamma(x;y,z)$ is the elliptic gamma function and $(q;q)_{\infty}$ is the q-Pochhammer symbol, both of which we define in appendix A together with some of the properties that will be useful for our study. One main ingredient in the successful account for the asymptotic growth of the SCI in the large-N limit has been to allow the chemical potentials to be complex [36–38], therefore, we consider the analytic continuation of (2.1.8) below in the fugacities p,q,v. Equation (2.1.4) becomes a contour integral over complex eigenvalues z_i ($|z_i|=1$) upon diagonalization of the unitary matrix U.

Consider now a generic $\mathcal{N}=1$ theory with semi-simple gauge group G with rank $\mathrm{rk}(G)$, flavor symmetry G_F and non-anomalous $U(1)_R$ R-symmetry. In practice the gauge groups we will consider will be of the form $SU(N)^{n_{\mathrm{v}}}$ with $n_{\mathrm{v}}\in\mathbb{Z}^{>0}$, however, in order to fix notation and keep the discussion generic we still denote the gauge group as G. The matter content of this theory is taken to be n_χ chiral multiplets Φ_a in representations $\mathfrak{R}_a$ of G having weight ρ_a, with flavor weights ω_a in some representation $\mathfrak{R}_F$ of G_F and superconformal R-charge r_a.

Using (2.1.7) the complex integral for the SCI (2.1.4) can be written as [74, 75]

$$\begin{aligned}
\mathcal{I}\left(p,q;v\right) &= \bar{\kappa}_G\oint_{\mathbb{T}^{\mathrm{rk}(G)}}\frac{\prod_{a=1}^{n_\chi}\prod_{\rho_a\in\mathfrak{R}_a}\Gamma\left((pq)^{r_a/2}\,z^{\rho_a}v^{\omega_a};p,q\right)}{\prod_{\alpha\in D}\Gamma\left(z^{\alpha};p,q\right)}\prod_{i=1}^{\mathrm{rk}(G)}\frac{dz_i}{2\pi i z_i},\\
\bar{\kappa}_G &\equiv \frac{(p;p)_{\infty}^{\mathrm{rk}(G)}\,(q;q)_{\infty}^{\mathrm{rk}(G)}}{|\mathcal{W}_G|}.
\end{aligned} \tag{2.1.8}$$

In (2.1.8) we have adopted the notation of [39] in which $z^{\rho_a}=\prod_{i=1}^{\mathrm{rk}(G)}z_i^{\rho_a^i}$ and $v^{\omega_a}=\prod_{l=1}^{\mathrm{rk}(G_F)}v_a^{\omega_l}$. With D we denote the set of all simple roots of the Lie algebra of G. The integration contour is the product of $\mathrm{rk}(G)$ unit circles $|z_i|=1,\ i=1,\cdots\mathrm{rk}(G)$. The order of the Weyl group is denoted as $|W_G|$.

For later convenience, we introduce the following quantities:

$$p=e^{2\pi i\tau},\quad q=e^{2\pi i\sigma},\quad v_a=e^{2\pi i\xi_a},\quad z_i=e^{2\pi i u_i} \tag{2.1.9}$$

and the R-charge chemical potential which is fixed by supersymmetry to:

$$\nu_R=\frac{1}{2}\left(\tau+\sigma\right). \tag{2.1.10}$$

In terms of these quantities we use a modified version of the elliptic gamma function $\widetilde{\Gamma}(u;\tau,\sigma)$ defined in appendix A. We can further define

$$y_a \equiv e^{2\pi i \Delta_a} \equiv v^{\omega_a}(pq)^{\frac{r_a}{2}} \quad \Rightarrow \quad \Delta_a = \xi_a + r_a \nu_R, \tag{2.1.11}$$

which allows to write (2.1.8) as

$$\mathcal{I}(\tau,\sigma;\Delta) = \bar{\kappa}_G \int_{\mathcal{C}} \frac{\prod_{a=1}^{n_\chi} \prod_{\rho_a \in \mathfrak{R}_a} \widetilde{\Gamma}\left(\rho^a(u) + \Delta_a;\tau,\sigma\right)}{\prod_{\alpha \in D} \widetilde{\Gamma}\left(\rho^\alpha(u);\tau,\sigma\right)} \prod_{i=1}^{\mathrm{rk}(G)} du_i, \tag{2.1.12}$$

where $\mathcal{C} = \bigcup_{i=1}^{\mathrm{rk}(G)}(0,1]$ and we have defined $\rho^a(u)$ such that $z^{\rho_a} = e^{2\pi i \rho^a(u)}$. We shall be interested only in the case of equal angular momenta $J_1 = J_2 = J$, thus we set $\sigma = \tau$, which yields:

$$\mathcal{I}(\tau;\Delta) = \bar{\kappa}_G \int_{\mathcal{C}} \frac{\prod_{a=1}^{n_\chi} \prod_{\rho_a \in \mathfrak{R}_a} \widetilde{\Gamma}\left(\rho^a(u) + \Delta_a;\tau\right)}{\prod_{\alpha \in D} \widetilde{\Gamma}\left(\rho^\alpha(u);\tau\right)} \prod_{i=1}^{\mathrm{rk}(G)} du_i, \tag{2.1.13}$$

where we have replaced $\mathcal{I}(\tau,\tau;\Delta)$ and $\widetilde{\Gamma}(u;\tau,\tau)$ with $\mathcal{I}(\tau;\Delta)$ and $\widetilde{\Gamma}(u;\tau)$ respectively for notational convenience. Particularizing for the $\mathcal{N}=4$ SYM theory with $SU(N)$ gauge group in which $\rho^a(u) = u_{ij} \equiv u_i - u_j$, equation (2.1.13) takes the form:

$$\begin{aligned} \mathcal{I}(\tau;\Delta) &= \kappa_N \int_{\mathcal{C}} \prod_{\mu=1}^{N-1} du_\mu \frac{\prod_{a=1}^{3} \prod_{i \neq j} \widetilde{\Gamma}\left(u_{ij} + \Delta_a;\tau\right)}{\prod_{i \neq j} \widetilde{\Gamma}\left(u_{ij};\tau\right)}, \\ \kappa_N &= \bar{\kappa}_{SU(N)} \prod_{a=1}^{3} \left(\widetilde{\Gamma}(\Delta_a;\tau)\right)^{N-1}. \end{aligned} \tag{2.1.14}$$

2.1.1 The structure of poles in the Superconformal Index

As emphasized already in [39], the only singularities of the integrand of (2.1.8) come from the elliptic gamma functions associated to the chiral multiplets and in the z_i variables take the form:

$$z^{\rho_a} = v^{-\omega_a} q^{-r_a - k}, \quad k \in \mathbb{Z}^{\geq 0}. \tag{2.1.15}$$

The map $z = e^{2\pi i u}$ preserves the singularity structure of the integrand in (2.1.13), therefore any deformation of the contour even in the variables u has to keep track of possible poles being crossed while deforming the contour. In Figure 1 we illustrate how the domains transform under $z = e^{2\pi i u}$, where the periodicity of u implies it takes values on a cylinder. With the u-variables is easier to visualize the location of the poles: for a fixed value of $\rho^a(u)$, the poles are separated from each other by τ translations on the surface of the $u-$cylinder as

$$\rho^a(u) + \Delta_a + k\tau = 0, \tag{2.1.16}$$

which can be read from the integrand of (2.1.13).

We will study $\mathcal{N}=4$ SYM theory, thus we can write:

$$u_{ij} + \Delta_a + k\tau = 0. \tag{2.1.17}$$

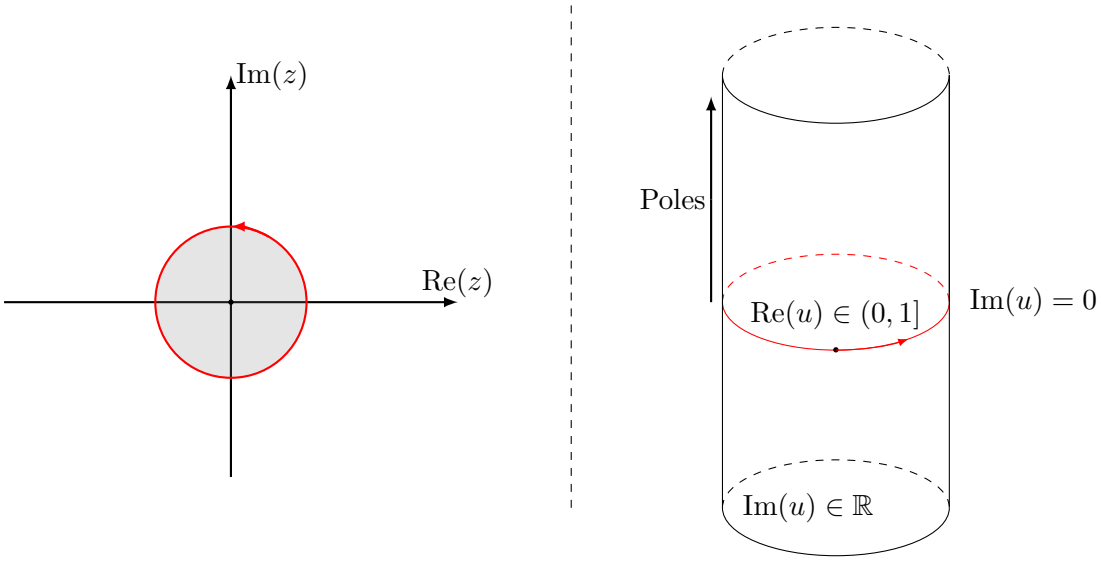


Figure 1: This figure shows the two complex domains for the holonomies related through the map $z = e^{2\pi i u}$. The z plane is represented such that the unit circle over which the integration is originally performed is the boundary between the gray and white regions. The complex variable u lives on a cylinder. The unit circle on the z plane is mapped to the circle in the middle of the cylinder (both represented in red) where $\mathrm{Re}(u) \in [0, 1]$ and $0 \sim 1$.

Note that, even when applying the saddle point method we will eventually have to deform the contours, therefore we want to make sure not to cross non-trivial poles in this process. By non-trivial pole we mean a point $P = \{u_1, \cdots, u_N\} \in \mathbb{C}^N$ whose residue contribution to (2.1.13) is different from 0. Given a point $P \in \mathbb{C}^N$, if there is at least one coordinate u_i not satisfying (2.1.17), then the integral over that coordinate in (2.1.13) vanishes. Thus, we call non-trivial poles those satisfying that $\forall\ i = 1, \cdots, N$ there is at least one point of the form (2.1.17) through which the holonomy u_i passes.

2.1.2 The Bethe-Ansatz formulation of the SCI

Benini and Milan in [38], represented the SCI using a BA approach developed in [39]. The conceptual basis for writing the SCI as a sum over solutions to Bethe-Ansatz Equations (BAEs) were originally clarified in [40] based on interesting relations between observables on manifolds of different topologies developed in [41]. For completeness, we present a derivation of the BAEs in which they arise as the outcome of properly organizing the residues contributing to (2.1.13). Let us define the integrand of (2.1.14) such that we can write the integral as:

$$\begin{aligned} \mathcal{I}(\tau; \Delta) &= \kappa_N \int_{\mathcal{C}} \prod_{\mu=1}^{N-1} du_\mu \mathcal{Z}(u; \Delta, \tau), \\ \mathcal{Z}(u; \Delta, \tau) &\equiv \prod_{i \neq j} \mathcal{Z}_{ij}(u_{ij}; \Delta, \tau). \end{aligned} \tag{2.1.18}$$

Under shifting by τ the argument of $\mathcal{Z}(u;\Delta,\tau)$ we have the following property:

$$\begin{gathered}\mathcal{Z}(u-\delta_k\tau;\Delta,\tau)=Q_k(u;\Delta,\tau)\mathcal{Z}(u;\Delta,\tau)\\ \delta_k\equiv(\delta_{kl})_{l=1}^{N-1},\end{gathered}\tag{2.1.19}$$

where the function $Q_k(u;\Delta,\tau)$ measures the lack of periodicity of $\mathcal{Z}(u;\Delta,\tau)$ in the variable u_k under shifting by τ and is defined in [39] as:

$$Q_k(u;\Delta,\tau)=e^{2\pi i\lambda}\prod_{l=1(\neq k)}^{N}\prod_{a=1}^{3}\frac{\theta_1(-u_{kl}+\Delta_a;\tau)}{\theta_1(u_{kl}+\Delta_a;\tau)},\tag{2.1.20}$$

where λ is a Lagrange multiplier implementing the $SU(N)$ constraint on the holonomies and $\theta_1(u;\tau)$ is the elliptic theta function defined in appendix A. These functions are called BA operators and have the crucial property of being doubly periodic with periods 1 and τ as proved in [39], namely

$$Q_k(u+n+m\tau;\Delta,\tau)=Q_k(u;\Delta,\tau).\tag{2.1.21}$$

Another important property of the BA operator is that, wherever $\mathcal{Z}(u;\Delta,\tau)$ has a pole, $Q_k(u;\Delta,\tau)$ has a pole of higher order. Specifically, as demonstrated in [39], the points (2.1.17) are such that $Q_k(u;\Delta,\tau)$ have stronger singularities than the integrand $\mathcal{Z}(u;\Delta,\tau)$. Using the change of variable $u_k\to u_k+\tau$, a contour $\mathcal{C}_k^0=(0,1]$ transforms into $\mathcal{C}_k^1=(\tau,\tau+1]$. Defining $\mathcal{C}_{i_1\cdots i_n}$ as

$$\mathcal{C}_{i_1\cdots i_n}=\left(\bigcup_{i=1}^{N-1-n}\mathcal{C}_i^0\right)\times\left(\bigcup_{j=1}^{n}\mathcal{C}_{i_j}^1\right),\tag{2.1.22}$$

the following relation holds:

$$\sum_{n=1}^{N-1}\frac{(-1)^n}{n!}\bigcup_{i_1\neq\cdots\neq i_n}\mathcal{C}_{i_1,\cdots,i_n}=-\bigcup_{k=1}^{N-1}\mathcal{C}_k^1\equiv\mathcal{C}^1.\tag{2.1.23}$$

Using (2.1.20) with the corresponding change of variables and (2.1.23), we can define the shifting operator:

$$Q(u;\Delta,\tau)=\sum_{n=1}^{N-1}\frac{(-1)^n}{n!}Q_{i_1}(u;\Delta,\tau)\cdots Q_{i_n}(u;\Delta,\tau).\tag{2.1.24}$$

Therefore we can write:

$$\begin{gathered}\mathcal{Z}(u-\tau;\Delta,\tau)=Q(u;\Delta,\tau)\mathcal{Z}(u;\Delta,\tau)\\ \Downarrow\\ \mathcal{Z}(u-m\tau;\Delta,\tau)=(Q(u;\Delta,\tau))^m\mathcal{Z}(u;\Delta,\tau).\end{gathered}\tag{2.1.25}$$

A way to systematically collect all non-trivial poles is to sum the contribution of poles located in strips slicing up the upper half cylinder in Figure 1. Using properties (2.1.21) and (2.1.25), one can add and subtract infinitely many times the same integral taken over contours successively

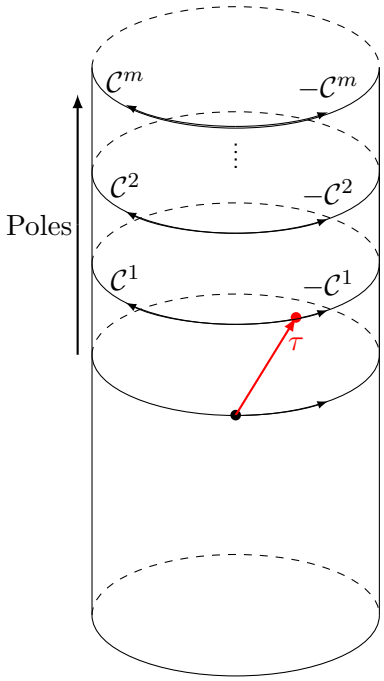


Figure 2: The figure shows the pairs of contours added and subtracted in order to obtain the final form of integration contour and the integrand for the SCI using the BA approach. The final integration contour is simply $\mathcal{C}\bigcup\mathcal{C}^1$.

τ-shifted as shown in Figure 2. This yields

$$\begin{aligned}\mathcal{I}(\tau;\Delta) &= \kappa_N \int_{\mathcal{C}\bigcup\mathcal{C}^1} \prod_{\mu=1}^{N-1} du_\mu \sum_{m=0}^{\infty} (Q(u;\Delta,\tau))^m \mathcal{Z}(u;\Delta,\tau) \\ &= \kappa_N \int_{\mathcal{C}\bigcup\mathcal{C}^1} \prod_{\mu=1}^{N-1} du_\mu \frac{1}{1-Q(u;\Delta,\tau)} \mathcal{Z}(u;\Delta,\tau) \\ &= \kappa_N \int_{\mathcal{C}\bigcup\mathcal{C}^1} \prod_{\mu=1}^{N-1} du_\mu \frac{\mathcal{Z}(u;\Delta,\tau)}{\prod_{k=1}^{N-1}(1-Q_k(u;\Delta,\tau))}.\end{aligned} \tag{2.1.26}$$

Since points of the form (2.1.17) are stronger singularities for $Q_k(u;\Delta,\tau)$, then the only singularities contributing to $\mathcal{I}(\tau;\Delta)$ are those satisfying the BAEs which take the form:

$$Q_k(\hat{u};\Delta,\tau) = 1, \ \ \forall\ k = 1,\cdots,N. \tag{2.1.27}$$

The values $\hat{u}$ satisfying (2.1.27) are called BA solutions. Upon direct application of the residue theorem, $\mathcal{I}(\tau,\Delta)$ can be rewritten in terms of a discrete sum as:

$$\begin{aligned}\mathcal{I}(\tau;\Delta) &= \kappa_N \sum_{\hat{u}\in \mathrm{BA}} \mathcal{Z}(\hat{u};\Delta,\tau) H(\hat{u};\Delta,\tau)^{-1}, \\ H(\hat{u};\Delta,\tau) &= \det\left[\frac{1}{2\pi i}\frac{\partial(Q_1,\cdots,Q_N)}{\partial(u_1,\cdots,u_{N-1},\lambda)}\right].\end{aligned} \tag{2.1.28}$$

2.2 Construction of $\mathcal{N}=1$ theories dual to $\mathbf{AdS}_5\times\mathbf{SE}_5$

Since we are interested in the computation of black hole entropy in gravitational configurations with dual field theories, we will now come to describe the process of construction of $\mathcal{N}=1$ supersymmetric filed theories dual to $\mathrm{AdS}_5\times\mathrm{SE}_5$ which are toric quiver gauge theories.

There has been a very enriching feedback between string theory constructions and the supersymmetric field theories defined in brane world-volumes. One of the most used approaches to construct interesting gauge theories is to probe singular geometries with D-branes. All relevant data for the gauge theory living on the D-brane world-volume, namely the amount of supersymmetry, matter content, gauge group and superpotential interaction, is encoded in the geometry of the singularity. In what follows we will explain how to extract such information.

Consider the specific case of a stack of N D3-branes which exhibit an $\mathrm{AdS}_5\times Y_5$ near horizon behavior with Y_5 being a 5-dimensional Einstein manifold. In [76], the authors studied the constraints supersymmetry imposes on the geometry of the Einstein manifolds Y_5 (the analysis in [76] was in fact for Dp-branes and the Einstein manifold was more generic Y_d but we focus here on the case $d=5$ of interest to us). Furthermore, they used the geometry of these manifolds in order to identify the superconformal symmetries which are required under the AdS/CFT correspondence. A prototypical example is the case of $\mathrm{AdS}_5\times S^5$ which arises as the near horizon geometry of $D3$-branes on $M_4\times\mathbb{R}^6$, interpolating between $\mathrm{AdS}_5\times S^5$ and $M_4\times\mathbb{R}^6$ where M_4 is 4-dimensional Minkowski space. In the same fashion, any solution of the form $\mathrm{AdS}_5\times Y_5$ is the near-horizon geometry of a $D3$-brane solution which will be supersymmetric if the near-horizon geometry is, and which interpolates between $\mathrm{AdS}_5\times Y_5$ and a vacuum $M_4\times C(Y_5)$ where $C(Y_5)$ is the cone over Y_5 with metric given by:

$$ds_C^2=dr^2+r^2ds_{Y_5}^2, \tag{2.2.1}$$

with $ds_{Y_5}^2$ being the line element of Y_5. The cone $C(Y_5)$ is Ricci-flat and the number of supersymmetries of the $M_4\times C(Y_5)$ vacuum depends on the number of covariantly constant spinors. This is determined by the holonomy group of $C(Y_5)$, and such holonomies have been classified in [77]. The number of supersymmetries on $\mathrm{AdS}_5\times Y_5$ depends on the number of Killing spinors on Y_5, but these all arise from covariantly constant spinors on $C(Y_5)$ [78], leading to a characterization of supersymmetric anti-de Sitter solutions. The upshot of this work was essentially that for those vacua $\mathrm{AdS}_5\times Y_5$ which are supersymmetric the geometry of Y_5 has to be Sasaki-Einstein, which means that its cone $C(Y_5)$ is both Kähler and Ricci flat (hence Calabi-Yau). In what follows we shall refer to a generic Sasaki-Einstein manifold as SE_5 and only when referring to specific classes of SE_5 we will use other nomenclature.

2.2.1 The $Y^{p,q}$ geometries

Surprisingly, for a long time there were only two cases where the explicit form of the metric for the Sasaki-Einstein manifolds SE_5 was known, namely the round five sphere S^5(or its orbifold quotient $S^5/\mathbb{Z}_3$) and the homogeneous metric on $T^{1,1}$ on $S^2\times S^3$ or $T^{1,1}/\mathbb{Z}_2$. The cones of these geometries are, respectively, $\mathbb{C}^3$ and the conifold. Within this family of Sasaki-Einstein geometries there are two classes which are dubbed *quasi-regular* and *irregular* referring to properties of the orbits of a Killing vector field:

$$K = 3\frac{\partial}{\partial\psi} - \frac{1}{2}\frac{\partial}{\partial\alpha} \tag{2.2.2}$$

called Reeb vector and the coordinates ψ and α will be specified below when we display the explicit metric. The manifold SE_5 is said to be *quasi-regular* if the orbits of K are closed (which implies that there is a locally free $U(1)$ action on SE_5). The Sasaki-Einstein manifold is said to be *irregular* if the orbits of the Reeb vector do not close (in such situation, there is a $\mathbb{R}$ action on SE_5). In [79], a countably infinite number of co-homogeneity one[4] Sasaki–Einstein metrics on $S^2 \times S^3$ was found. Consider the Einstein and locally Sasaki metric given by:

$$\begin{aligned} ds^2_{SE_5} &= \frac{1-cy}{6}\left(d\theta^2 + \sin^2 d\phi^2\right) + \frac{1}{W(y)Q(y)}dy^2 + \frac{Q(y)}{9}\left[d\psi - \cos\theta d\phi\right]^2 \\ &\quad + W(y)\left[d\alpha + \frac{ac - 2y + cy^2}{6(a-y^2)}\left(d\psi - \cos\theta d\phi\right)\right]^2 \end{aligned} \tag{2.2.3}$$

$$ds^2 = ds^2\left(B_4\right) + W(y)\left(d\alpha + A\right)^2 \tag{2.2.4}$$

$$A = \frac{a - 2y + y^2}{6(a-y^2)}\left(d\psi - \cos\theta d\phi\right), \tag{2.2.5}$$

where:

$$W(y) = \frac{2\left(a-y^2\right)}{1-cy} \tag{2.2.6}$$

$$Q(y) = \frac{a - 3y^2 + 2cy^3}{a-y^2}. \tag{2.2.7}$$

It is possible to argue that such a metric can be globally extended to the $S^2 \times S^3$ manifold and so it can be done with its Sasaki structure since it has globally well defined Killing spinors. The space B_4 in (2.2.4) can be considered as a smooth complete compact manifold by making a suitable choice of the range of variables. The variable y has to obey the following constraints $y < 1$, $a - y^2 > 0$, $W(y) > 0$, $Q(y) \geq 0$. Defining y_1, y_2, y_3 such that:

$$(y - y_1)(y - y_2)(y - y_3) = a - 3y^2 + 2y^3, \tag{2.2.8}$$

where for $0 < a < 1$, we have $y_1 < 0$ and $y_{2,3} > 0$. Then, for $y_1 < y < y_2$, $0 \leq \theta \leq \pi$, $0 \leq \phi \leq 2\pi$, $0 \leq \psi \leq 2\pi$ which makes B_4 an axially squashed S^2 bundle over S^2 which can be shown to be trivial [80], hence $B_4 \cong S^2 \times S^2$. Note that for $c = 0$, then (2.2.3) is the standard homogeneous metric for $T^{1,1}$:

$$\begin{aligned} ds^2_{T^{1,1}} &= \frac{1}{6}\left(d\theta^2 + \sin^2\theta d\phi^2 + d\omega^2 + \sin^2\omega d\nu^2\right) + \frac{1}{9}\left[d\psi - \cos\theta d\phi - \cos\omega d\nu\right]^2 \\ a = 3,\ \ \cos\omega = y,\ \ \nu = 6\alpha,\ \ \nu \sim \nu + 2\pi\ \ \psi \sim \psi + 4\pi,\ \ &\left(\psi \sim \psi + 2\pi \text{ gives } ds^2_{T^{1,1}/\mathbb{Z}_2}\right). \end{aligned} \tag{2.2.9}$$

Therefore, if we only concern ourselves with $c \neq 0$, by a simple rescaling of y and a it is possible to set $c = 1$ and we see that geometries we are interested in are described by a single parameter a.

[4] This means that the corresponding isometry group acts with generic orbit of co-dimension one.

The other particular case of the round five sphere is obtained by setting $a = 1$, which yields:

$$\begin{aligned} ds^2_{S^5} &= d\sigma^2 + \frac{1}{4}\sin^2\sigma\left(d\theta^2 + \sin^2\theta d\phi^2\right) + \frac{1}{4}\cos^2\sigma\sin^2\sigma\left(d\beta + \cos\theta d\phi\right)^2 \\ &+ \frac{1}{2}\left[d\psi' - \frac{3}{2}\sin^2\sigma\left(d\beta + \cos\theta d\phi\right)\right]^2 \\ y &= 1 - \frac{3}{2}\sin^2\sigma, \quad \psi = \psi' - \beta, \quad \alpha = -\frac{\psi'}{6} \\ \beta &\sim \beta + 4\pi, \quad \psi' \sim \psi' + 6\pi, \quad \left(\psi' \sim \psi' + 2\pi \text{ gives } ds^2_{S^5/\mathbb{Z}_3}\right). \end{aligned} \tag{2.2.10}$$

Furthermore, as it was shown in [79], for a countably infinity set of values of the parameter a $(0 < a < 1)$, the total space can be considered as a S^1 fibration over B_4 where α is regarded as the S^1 coordinate. The resulting space turns out to be topologically $S^2 \times S^3$. To obtain a compact five dimensional manifold we want ds^2 to describe a S^1 bundle over B_4, hence the coordinate α has to be $2\pi\ell$ periodic and, upon a ℓ^{-1} rescaling, then $\ell^{-1}A$ is a gauge connection on a $U(1)$ bundle over B_4. Gauge connections A are chracterized by the Chern numbers in $H^2\left(S^2;\mathbb{Z}\right) = \mathbb{Z}$ denoted as p and q which motivates the labeling of the five dimensional total space as $Y^{p,q}$. The result of [79] is essentially that $0 < q/p < 1$ and that values of ℓ and $0 < a < 1$ can be always found such that $\ell^{-1}A$ is a good $U(1)$ gauge connection. In particular, for p, q relative primes, it can be shown that $Y^{p,q}$ is topologically $S^2 \times S^3$. The values of the roots (2.2.8) in terms of p and q are:

$$y_1 = \frac{1}{4p}\left(2p - 3q - \sqrt{4p^2 - 3q^2}\right) \tag{2.2.11}$$

$$y_2 = \frac{1}{4p}\left(2p + 3q - \sqrt{4p^2 - 3q^2}\right) \tag{2.2.12}$$

$$y_3 = \frac{3}{2} - y_1 - y_2. \tag{2.2.13}$$

The value of ℓ can be written:

$$\ell = \frac{q}{3q^2 - 2p^2 + p(4p^2 - 3q^2)^{1/2}}. \tag{2.2.14}$$

Moreover, the volume of the $Y^{p,q}$ space will be:

$$\mathrm{Vol}\left(Y^{p,q}\right) = \frac{4\pi^3}{9}\ell\left(y_1 - y_2\right)\left(y_1 + y_2 - 2\right) \tag{2.2.15}$$

$$= \frac{q^2\left[2p + (4p^2 - 3q^2)^{1/2}\right]}{3q^2 - 2p^2 + p(4p^2 - 3q^2)^{1/2}}\pi^3. \tag{2.2.16}$$

An important observation is that $\mathrm{Vol}\left(Y^{p,q}\right)$ is a monotonic function of q for fixed p and it is bounded in the following way:

$$\mathrm{Vol}\left(T^{1,1}/\mathbb{Z}_p\right) > \mathrm{Vol}\left(Y^{p,q}\right) > \mathrm{Vol}\left(S^5/\mathbb{Z}_2 \times \mathbb{Z}_p\right). \tag{2.2.17}$$

These properties allow to connect $Y^{p,0}$ and $Y^{p,p}$ to quotients of $T^{1,1}$ and $S^5/\mathbb{Z}_2$ by $\mathbb{Z}_p$ respectively, which becomes a useful property when obtaining the field theory dual to $Y^{p,q}$ from those theories which are already known. The field theories dual to the type IIB supergravity solutions associated to the $Y^{p,q}$ geometries should be $\mathcal{N} = 1$ quiver gauge theories, that is, supersymmetric gauge theories

where each field transforms in representations of the gauge group with two indices. Specifically, the superconformal field theory may be thought of as arising from a stack of N $D3$–branes sitting at the tip of the Calabi–Yau cone $C(\mathrm{SE}_5)$:

$$ds^2_C = dr^2 + r^2 ds^2_{\mathrm{SE}_5}, \tag{2.2.18}$$

which is mildly singular at the tip $r = 0$ unless $\mathrm{SE}_5 = S^5$. In fact, the cone of the five-sphere is $\mathbb{C}^3$ and its dual superconformal field theory is $SU(N)$ $\mathcal{N} = 4$ SYM theory. The cone associated to $T^{1,1}$ is the conifold and its field theory dual was obtained in [81, 82]. The construction of the $\mathcal{N} = 1$ quiver gauge theories associated to the full family of $Y^{p,q}$ geometries was developed in [83], although all the dual theories for $p \leq 2$ where already known and respectively studied in [80, 82, 84–86]. Before entering into details about such construction, we list some other important properties of the $Y^{p,q}$ geometries presented in [80].

It was shown in [80] that located at the two roots (2.2.8) $y_{1,2}$ there were two submanifolds of $Y^{p,q}$ which we denote as $\Sigma_{1,2} = S^3/\mathbb{Z}_{p\pm q}$ (the positive sign corresponds to Σ_1 and the negative to Σ_2). Such submanifolds have cones $C(\Sigma_{1,2})$ which are calibrated manifolds[5] in the Calabi-Yau cone $C(Y^{p,q})$ which renders $\Sigma_{1,2}$ supersymmetric. The volumes of $\Sigma_{1,2}$ are given by:

$$\mathrm{Vol}(\Sigma_{1,2}) = \frac{q^2(p \pm q)\left(\mp 2p + 3q \pm \sqrt{4p^2 - 3q^2}\right)^2}{2p^2\left(3q^2 - 2p^2 + p\sqrt{4p^2 - 3q^2}\right)^2}\pi^2. \tag{2.2.19}$$

As we can see from equations (2.2.16) and (2.2.19), the volumes are only rational fractions of $\mathrm{Vol}(S^5)$ and $\mathrm{Vol}(S^3)$ respectively if and only if $4p^2 - 3q^2 = n^2$ for $n \in \mathbb{Z}$. When this condition is met, then ℓ is also a rational number (see (2.2.14)) and this, together with the fact that the period of ψ is 2π and α has period $2\pi\ell$ implies that the orbits of the Reeb vector (2.2.2) do close, hence the Sasaki-Einstein manifold $Y^{p,q}$ is said to be quasi-regular. In contrast, if $4p^2 - 3q^2 \neq n^2$ then the orbits of the Reeb vector (2.2.2) do not close, but instead densely fill the orbits of the torus generated by the Killing vectors $\frac{\partial}{\partial\psi}$ and $\frac{\partial}{\partial\alpha}$ and the Sasaki-Einstein manifold $Y^{p,q}$ is irregular.

Since $C(Y^{p,q})$ is a symplectic manifold we can define the associated symplectic form ω which can be written as:

$$\omega = d\phi \wedge d\left[r^2\frac{1-y}{6}\cos\theta\right] + d\psi \wedge d\left[-r^2\frac{1-y}{6}\right] + d\alpha \wedge d\left[r^2 y\right]. \tag{2.2.20}$$

The $Y^{p,q}$ manifold has an isometry group whose maximal torus[6] has dimension 3, which is half the dimension of $C(Y^{p,q})$. This implies, by definition, that the cone is *toric*. This is a crucial property, since it connects the $Y^{p,q}$ manifolds to a very rich branch of algebraic geometry which studies toric varieties. This is a very well studied subject and a comprehensive treatment of toric varieties can be found, for example, in [87, 88]. An algebraic variety is essentially the set of solutions of a system

[5] A calibrated manifold $\mathcal{M}_D$ is a D-dimensional manifold equipped with a differential p–form ϕ, $(0 \leq p \leq D)$ which is a calibration. This means that $d\phi = 0$ and for any point $x \in \mathcal{M}_D$ and any p-dimensional subspace V_p of $T\mathcal{M}_{D_x}$, then $\phi|_{V_p} = \lambda \mathrm{Vol}(V_p)$ with $\lambda \leq 1$.

[6] A torus T on a compact Lie group G is a compact, connected and Abelian Lie subgroup of G. A torus T is maximal if for any other torus T' containing T then we have $T = T'$. T is isomorphic to a standard torus $\mathbb{T}^n$, where n is the dimension of T.

of polynomial equations over a field, say $\mathbb{C}$, to fix ideas. In particular, toric varieties are algebraic varieties which contain an algebraic torus as an open dense subset. The geometry of toric varieties is purely determined by the combinatorics of a polytope (recall that a polytope is a convex hull of a finite number of points generically in $\mathbb{R}^n$, however we only focus here on $n = 3$) which is precisely the base of the convex cone in figure 3. In the present manuscript we mainly focus on the toric diagram, in terms of which all relevant information of the SE_5 manifolds can be encoded. Let us focus now, for concreteness, in the case of $Y^{p,q}$ manifolds.

The fact that $C\left(Y^{p,q}\right)$ is toric implies that it is the pre-image, through a moment map which we define below, of a convex cone in $\mathbb{R}^3$ formed by four intersecting planes passing through the origin as represented in figure 3.

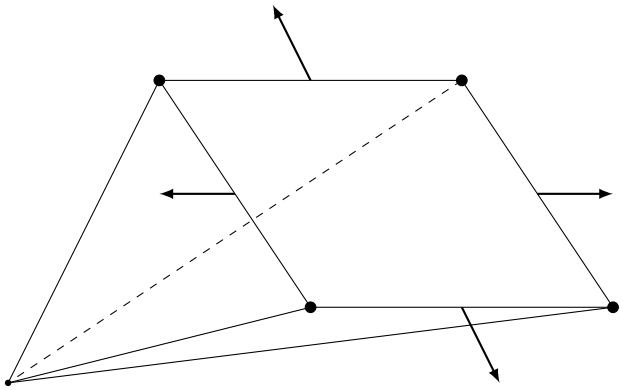


Figure 3: Example of a cone in $\mathbb{R}^3$ whose base is a Delzant polytope. The normal vectors to the facets are represented in the figure by arrows and they are necessarily rational and describe which $U(1)$ subgroup of $\mathbb{T}^3$ is vanishing over the corresponding co-dimension two submanifold of $C\left(Y^{p,q}\right)$.

We then have that the $Y^{p,q}$ manifolds have an effectively acting three-torus $\mathbb{T}^3 \cong U(1)^3$ of isometries (that the torus acts effectively means that it moves at least one point of $C\left(Y^{p,q}\right)$). Such isometries preserve the symplectic structure of the cone $C\left(Y^{p,q}\right)$, which means that, if $\vec{V}$ is the vector field generating the $\mathbb{T}^3$ action with components V^i along the basis of Lie $\left(\mathbb{T}^3\right)$ and ω is the symplectic form of $C\left(Y^{p,q}\right)$ defined in (2.2.20), then:

$$\mathcal{L}_{\vec{V}}\omega = 0, \tag{2.2.21}$$

where $\mathcal{L}_{\vec{V}}$ is the Lie derivative. Using the identity $\mathcal{L}_{\vec{V}} = di_{\vec{V}} + i_{\vec{V}}d$, where $i_{\vec{V}}$ is the interior product with $\vec{V}$, then from equation (2.2.21) and the the fact that ω is closed we can conclude that:

$$d\left(i_{\vec{V}}\omega\right) = 0. \tag{2.2.22}$$

Equation (2.2.22) can be "integrated" if the cohomology class $\left[i_{\vec{V}}\omega\right]$ associated to the one form $i_{\vec{V}}\omega$, is trivial, that is: $\left[i_{\vec{V}}\omega\right] \in H^1\left(C\left(Y^{p,q}\right);\mathbb{R}\right)$. In this case the action is *Hamiltonian* and the resulting function, upon integration of (2.2.22), is called the moment map μ of the toric action:

$$\mu : C\left(Y^{p,q}\right) \to \text{Lie}\left(\mathbb{T}^3\right) \cong \mathbb{R}^3, \tag{2.2.23}$$

subjected to the condition:

$$d\vec{\mu} = i_{\vec{V}}\omega, \tag{2.2.24}$$

where $\vec{\mu}$ has components μ^i along the canonical basis $\{e_1, e_2, e_3\}$ of Lie $\left(\mathbb{T}^3\right)$. The condition (2.2.24) is a direct consequence of μ being the "integral" of (2.2.22), therefore we see that the moment map is defined up to an integration constant.

The set $\mu\left(C\left(Y^{p,q}\right)\right)$ is a convex rational polytope in $\mathbb{R}^3$ called the Delzant polytope [89] (see figure 3). With this in mind, it is possible to think of the toric cone $C(Y^{p,q})$ as a torus fibration over the Delzant polytope. It is sufficient to have the data from the polytope to recover the original symplectic toric manifold $C(Y^{p,q})$. Furthermore, there is a one to one correspondence between Delzant polytopes and compact symplectic manifolds. Crucially, this allows us to interpret $C(Y^{p,q})$ as the vacuum of a linear gauged linear sigma model [90]. The following choice of basis will be sufficient to ensure that the orbits of the vectors acting on $C\left(Y^{p,q}\right)$ do close:

$$e_1 = \frac{\partial}{\partial\phi} + \frac{\partial}{\partial\psi}, \tag{2.2.25}$$

$$e_2 = \frac{\partial}{\partial\phi} - \frac{p-q}{2}\frac{\partial}{\partial\alpha}, \tag{2.2.26}$$

$$e_3 = \frac{\partial}{\partial\alpha}, \tag{2.2.27}$$

in terms of which the moment map can be written as:

$$\vec{\mu} = \{\mu_1, \mu_2, \mu_3\} = \left\{\frac{r^2}{6}(1-y)(\cos\theta - 1), \frac{r^2}{6}(1-y)\cos\theta - \frac{r^2}{2}(p-q)ly, lr^2y\right\}. \tag{2.2.28}$$

We would like to find the image of $\vec{\mu}$, to this end, we note that the edges of the cone can be obtained by selecting a particular value of the coordinate r, say $r = 1$, and then finding the submanifold fixed under the action of $\mathbb{T}^2 \subset \mathbb{T}^3$. There are four submanifolds of $C(Y^{p,q})$ that remain fixed under the $\mathbb{T}^2$ action, and for $r = 1$, they correspond to the north and south poles of the base and fibre two spheres of B_4 (recall that $B_4 \cong S^2 \times S^2$). Specifically, the manifolds in question will be the S^1 fibers over the corresponding point in B_4. Following the notation of [79], we label such submanifolds in the following way: NN $= \{y = y_2,\ \theta = 0\}$, NS $= \{y = y_2,\ \theta = \pi\}$, SN $= \{y = y_1,\ \theta = 0\}$, SS $= \{y = y_1,\ \theta = \pi\}$, which have the following images under the moment map:

$$\begin{aligned}
\vec{\mu}\left(\mathrm{NN}\right) &= \ell y_2\left(0, 0, 1\right), \\
\vec{\mu}\left(\mathrm{NS}\right) &= \ell y_2\left(q-p, q-p, 1\right), \\
\vec{\mu}\left(\mathrm{SN}\right) &= \ell y_1\left(0, -p, 1\right), \\
\vec{\mu}\left(\mathrm{SS}\right) &= \ell y_1\left(p+q, q, 1\right),
\end{aligned} \tag{2.2.29}$$

where the following relations have been used:

$$\begin{aligned}
1 - y_1 &= -3\ell(p+q)y_1, \\
1 - y_2 &= 3\ell(p-q)y_2,
\end{aligned} \tag{2.2.30}$$

which can be easily derived from (2.2.11), (2.2.12) and (2.2.14). Since $y_1 < 0$ and $y_2 > 0$, we see that the points in (2.2.29) are the edges of a polyhedral cone with four facets in $\mathbb{R}^3$ and it is generated by the vectors:

$$u_1 = [0, p, -1], \;\; u_2 = [-(p+q), -q, -1], \;\; u_3 = [0, 0, 1], \;\; u_4 = [q-p, q-p, 1]. \tag{2.2.31}$$

Note that the normal and outward pointing vectors associated to each facet will be given by:

$$n_1 = [1, 0, 0], \;\; n_2 = [1, -2, q-p], \;\; n_3 = [1, -1, -p], \;\; n_4 = [1, -1, 0]. \tag{2.2.32}$$

Gauge linear sigma model

In physics, a gauge linear sigma model is a two dimensional gauge theory [91]. To be concrete, let us analyze a $U(1)^r$ gauge theory with no superpotential and d chiral super fields Φ_I with lower component z_I, we then have the potential energy:

$$\mathcal{U}(z_I) = \sum_{a=1}^{r} \frac{g_a^2}{2} \left(\sum_{I=1}^{d} Q_I^a |z_I|^2 - \xi_a \right)^2 \tag{2.2.33}$$

where Q_I^a is a matrix of $U(1)$ charges acting on $\mathbb{C}^4$ as

$$(z_1, \cdots, z_d) \to \left(\lambda^{Q_1^a} z_1, \cdots, \lambda^{Q_J^a} z_d \right), \;\; a = 1, \cdots, r. \tag{2.2.34}$$

and ξ_a are Fayet-Illiapoulus parameters and g_a are the gauge couplings associated to the gauge fields of each $U(1)$ symmetry. The supersymmetric ground state of this theory is obtained by setting $\mathcal{U}(z_I) = 0$, hence we have the D-terms equations:

$$\sum_{I=1}^{d} Q_I^a |z_I|^2 = \xi_a, \;\; a = 1, \cdots, r. \tag{2.2.35}$$

Therefore, modulo gauge equivalence, the supersymmetric vacuum of the gauged linear sigma model is parametrized by the solutions to the equations (2.2.35).

Let us now try to connect $C(Y^{p,q})$ to the gauge linear sigma model we have just described. To do so, we try to construct $C(Y^{p,q})$ from a Delzant polytope $\mathcal{D}$ (which ultimately will be the image of $C(Y^{p,q})$ under $\vec{\mu}$). If we consider a set of normal vectors like (2.2.32), then, for some $\lambda_I \in \mathbb{R}$ $(I = 1, \cdots, 4)$ we can define $\mathcal{D}$ as :

$$\mathcal{D} = \left\{ x \in \mathbb{R}^3 | \langle x, n_I \rangle \leq \lambda_I, \;\; I = 1, \cdots, 4 \right\}, \tag{2.2.36}$$

where $\langle \cdot, \cdot \rangle$ denotes the inner product of vectors in $\mathbb{R}^3$. Let us consider a map $\pi : \mathbb{R}^4 \to \mathbb{R}^3$ which maps the standard basis of $\mathbb{R}^4$ to n_I, namely: $\pi(e_I) = n_I$ for $I = 1, 2, 3, 4$. We see that $\dim [\mathrm{Ker}(\pi)] = 4 - 3 = 1$ which defines the corresponding torus $\mathbb{T} \subset \mathbb{T}^4$. Consider now $\mathbb{C}^4$ with coordinates z_J, $J = 1, \cdots, 4$ that we think about as lowest components of chiral superfields Φ_J (anticipating the relation with the gauge linear sigma model where $d = 4$). Consider also the usual $\mathbb{T}^4$ action on $\mathbb{C}^4$ which has a moment map associated and requires us to impose the constraints:

$$\sum_{I=1}^{4} Q_I^J |z_I|^2 = \lambda_J, \;\; J = 1, \cdots, 4, \tag{2.2.37}$$

where Q_I^J is a matrix of $U(1)$ charges acting on $\mathbb{C}^4$ as

$$(z_1, \cdots, z_4) \to \left(\lambda^{Q_1^J} z_1, \cdots, \lambda^{Q_4^J} z_4\right), \quad J = 1, \cdots, 4. \tag{2.2.38}$$

The parameters λ_J are the real parameters appearing in (2.2.36) and $\lambda \in U(1)$. From the induced action by $\mathbb{T} \subset \mathbb{T}^4$, it is possible to obtain the induced moment map for the $\mathbb{T}$ action. This makes it possible to implement a *Kähler quotient*, which we denote as $X = \mathbb{C}^4//\mathbb{T}$, and just means to take a fiber at a point fixed by the moment map and quotient it by the action of $\mathbb{T}$. To see explicitly how to perform the Kähler quotient, we define the action of the group $\mathbb{T} \cong U(1)$ on $\mathbb{C}^4$ by specifying the integral charge vector $Q = \{Q_I | I = 1, \cdots, 4\}$ with which the $U(1)$ acts on $\mathbb{C}^4$ as:

$$(z_1, \cdots, z_4) \to \left(\lambda^{Q_1} z_1, \cdots, \lambda^{Q_4} z_4\right). \tag{2.2.39}$$

Note that equation (2.2.39) is a particular case of (2.2.34)

We are then in conditions of explicitly imposing the constraint defining the Kähler quotient as:

$$\sum_{i=1}^{4} Q_I |z_I|^2 = \xi. \tag{2.2.40}$$

Once condition (2.2.40) is imposed we have to quotient out by $U(1)$, which yields a symplectic manifold of complex dimension $4-1=3$. Furthermore, the resulting manifold inherits a $\mathbb{T}^3 = \mathbb{T}^4/\mathbb{T}$ action from the one of $\mathbb{C}^4$ which renders it toric. Precisely the image of $\mathbb{C}^4//\mathbb{T}$ under its moment map associated to $\mathbb{T}^3$ is $\mathcal{D}$. This final remark completes the Delzant construction [89].

Note that (2.2.40) is precisely the D-term equation associated to a gauged linear sigma model with ξ as Fayet-Illiapoulus parameter. The quotient by $U(1)$ removes the gauge degrees of freedom. We then conclude that the Kähler quotient leads to the classical vacuum of the gauged linear sigma model. An important property of X is that its first Chern class vanishes, which is equivalent to the statement that the sum of $U(1)$ charges is zero:

$$\sum_{I=1}^{4} Q_I = 0, \tag{2.2.41}$$

subsequently, the one-loop beta function for the gauge coupling g (particular case of g_a from equation (2.2.33)) associated to the $U(1)$ global symmetry vanishes. The associated gauged linear sigma model is Calabi-Yau even though the metric induced by the Kähler quotient is not Ricci-flat.

Starting then with the set of outward pointing vectors $\{n_I\}$ in (2.2.32) we see that the Kernel of the map π is simply the space generated by $(p, p, q-p, -p-q)$, therefore the Delzant theorem implies the existence of a $U(1)$ gauged linear sigma model on $\mathbb{C}^4$ with vector charge $Q = (p, p, q-p, -p-q)$ which trivially satisfies (2.2.41). We now relate the gauge linear sigma model with charge $Q = (p, p, q-p, -p-q)$ to the a convex polygon in $\mathbb{R}^2$ with vertices having integer coordinates. Such polygon is called toric Gorenstein canonical singularity of complex dimension 2. Let $\{\mathcal{V}_I|, I, \cdots, 4\}$ such that $\mathcal{V}_I \in \mathbb{R}^2$ with integer coordinates and being such that they either lay within or on the boundary of the polygon. Marking such points gives the so called toric diagram. If we now consider the linear relations among the $\mathcal{V}_I$ with coefficients being the $U(1)$ charges Q_I subjected to the constraint (2.2.41), we have:

$$\sum_{I=1}^{4} Q_I \mathcal{V}_I = 0. \tag{2.2.42}$$

We have landed again in the Delzant construction for the $\mathbb{C}^4$ gauge linear sigma model with $U(1)$ gauge group and Fayet-Illiapoulus parameter set to zero, which defines the toric singularity.

Note that by turning on a Fayet-Illiapolous parameter on the right hand side of (2.2.42) we implement a partial resolution of the singularity. Having considered all vectors $\mathcal{V}_I$ in the interior of the polygon ensures that the linear sigma model reproduces all the toric crepant resolutions of the toric singularity. It will be sufficient for us to focus on the minimal presentation, namely considering only the vertices of the polygon.

The toric diagram for $C(Y^{p,q})$

Recalling that $\mu\left(C(Y^{p,q})\right)$ is a four faceted polyhedral with primitive outward pointing normal vectors given by (2.2.32), we see that all $\{n_I\}$ are in the plane e_1 with projection equal to 1, hence we obtain the set of vectors:

$$[0,0],\ \ [-2,p-q],\ \ [-1,-p],\ \ [-1,0]. \tag{2.2.43}$$

One can bring two vertices of the diagram to the points $(0,0)$ and $(0,1)$ of the integer lattice by using and $SL(2,\mathbb{Z})$ transformation on the quadrangle defined by (2.2.43). This permit us to obtain the set of $\mathcal{V}_I$ vectors upon application of the $SL(2,\mathbb{Z})$ transformation:

$$T=\begin{pmatrix} q-p-1 & -1 \\ q-p & -1 \end{pmatrix}, \tag{2.2.44}$$

which yields:

$$\mathcal{V}_1=[q-p-1,q-p],\ \ \mathcal{V}_2=[1,0],\ \ \mathcal{V}_3=[p,p],\ \ \mathcal{V}_4=[0,0], \tag{2.2.45}$$

and provides a minimal presentation of the singularity. Simple examples for $Y^{2,0}$ (the conifold) $Y^{2,1}$ (the complex cone over the first del Pezzo surface $d\mathbf{P}_1$) and $Y^{3,2}$ are represented in figure 4 all embedded into $\mathbb{C}^3/\mathbb{Z}_{p+1}\times\mathbb{Z}_{p+1}$.

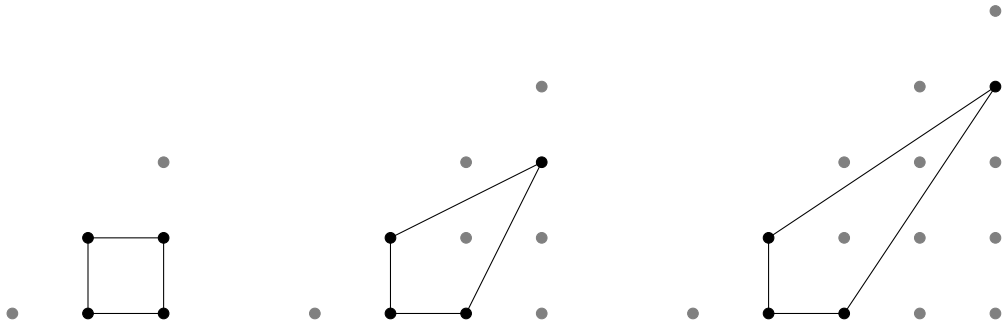


Figure 4: Toric diagrams associated to $Y^{1,0}$ (the conifold), $Y^{2,1}$ and $Y^{3,1}$ respectively. All of them are embedded in the corresponding orbifold $\mathbb{C}^3/\mathbb{Z}_{p+1}\times\mathbb{Z}_{p+1}$.

We emphasize that, given a Gorenstein canonical singularity, an algorithm for reconstructing a quiver gauge theory with a singularity at its Higgs branch was developed in [84, 92] exploiting the fact that any singularity like the ones appearing in the Higgs branch of the quiver gauge theories can be obtained by partial resolution of the orbifold $\mathbb{C}^3/\mathbb{Z}_{p+1}\times\mathbb{Z}_{p+1}$. Intuitively this can be seen in figure 4 by noticing that partial resolution boils down to erasing nodes from the $\mathbb{C}^3/\mathbb{Z}_{p+1}\times\mathbb{Z}_{p+1}$ orbifold.

2.2.2 Field theory dual of $Y^{p,q}$ geometries

The algorithm proposed in [84, 92] becomes quite involved and requires a computer to be implemented already at fairly low values of p, however, the picture presented in [93] simplifies a lot the analysis. A more systematic study was carried in [83] where more precise information about the gauge theory was extracted from the toric diagrams. The 4 steps to follow are:

1) Obtain the number $n_{\rm v}$ of gauge groups on the quiver.

2) Find the number n_χ of bi-fundamental chiral superfields.

3) Find the gauge quantum number associated to each chiral superfield.

4) Find which of the allowed gauge invariant terms do appear in the superpotential.

Step 1) can be done by noticing that $n_{\rm v}$ is strictly controlled by the geometry and remains fixed under dualities of the field theory. Different gauge groups are seen as living on the world-volume of bound states of D-branes which wrap even dimensional cycles in the geometry (fractional branes). Therefore, the number of gauge groups in the quiver corresponds precisely to the number of possible ways in which the wrapping of D-branes on even dimensional cycles can be performed. Specifically we can have 3, 5 and 7-branes wrapping 0,2 and 4-cycles respectively. For the $Y^{p,q}$ manifolds this quantity is captured by the Euler characteristic of the base manifold B_4. In the toric diagram, the Euler characteristic is encoded in the number of simple triangles[7] in any possible triangulation of the diagram. Note that a vertex of the form $(p-q-1, p-q) = (p-q, p-q) + (-1, 0)$ lays on

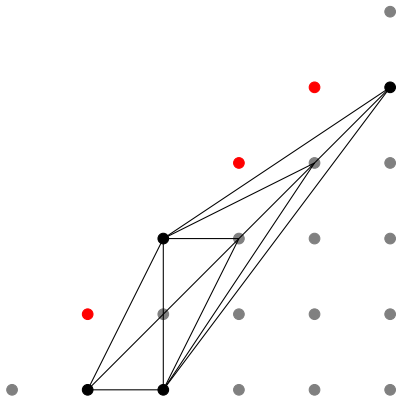


Figure 5: Triangulation of the toric diagram of $Y^{4,2}$ (embedded in the orbifold $\mathbb{C}^3/\mathbb{Z}_5 \times \mathbb{Z}_5$) where the number of simple triangles gives the value of $n_{\rm v} = 8$. Note also that, for a fixed p, as we decrease q, the node at the upper left side of the diagram moves up along the hypotenuse (see red dots) until it reaches $q = 0$ to form a parallelogram.

the line connecting $(0, 0)$ and (p, p) but shifted one lattice unit to the left of such line. A uniform triangulation can be easily done as shown in figure 5 for the specific case of $Y^{4,2}$, which allows us to conclude that:

$$n_{\rm v} = 2p. \tag{2.2.46}$$

[7] by simple triangles we mean those which do not contain smaller triangles

Note also that, for a fixed p, as we decrease q, the node at the upper left side of the diagram moves up along the hypotenuse (see red dots in figure 5) until it reaches $q = 0$ to form a parallelogram.

Each of the toric diagram has an associated (p, q)–web, corresponding to the reciprocal diagram in which lines are replaced by orthogonal lines and nodes are exchanged with faces. The charge of each external leg is fixed by the boundary of the toric diagram as shown in figure 6 for the case of $Y^{4,2}$.

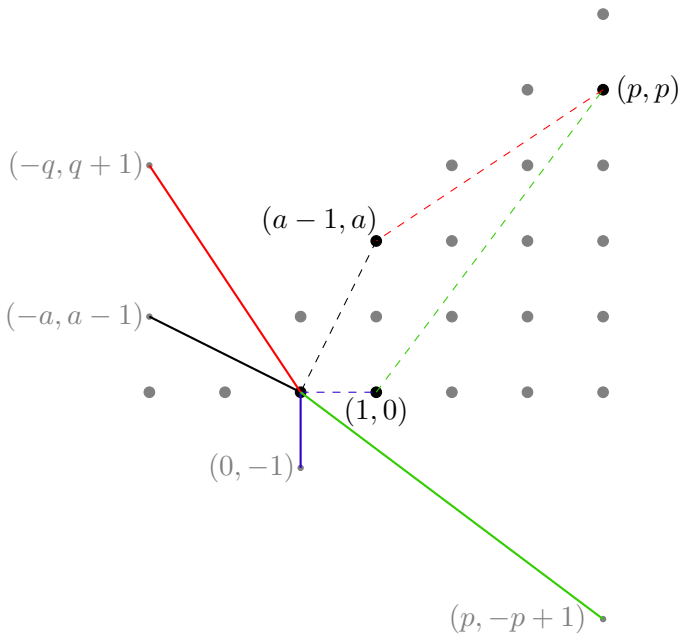


Figure 6: Example of a (p, q)-web for $Y^{4,2}$ and we have defined $a = p - q$. We obtain the reciprocal diagram by simply tracing orthogonal lines to each side of the toric diagram (represented here with dashed lines). We represent with the same color and continuous line the dual to each side. We keep the length of the reciprocal line to be the same as the original, hence the endpoints labeled in gray are easily determined if we make all reciprocal lines meet at the origin of the lattice. We refer to the reciprocal lines as external legs and they serve to fix the number of chiral fields n_χ in the quiver gauge theory.

From the lattice coordinates of the endpoints of the external legs represented in figure 6 it is possible to determine n_χ by means of the following formula:

$$n_\chi = \frac{1}{2} \sum_{I,J \in \text{legs}} \left| \det \begin{pmatrix} p_I & q_I \\ p_J & q_J \end{pmatrix} \right| = 4p + 2q, \tag{2.2.47}$$

where we have denoted as (p_I, q_I), $I = 1, \cdots, 4$ the charges of the external legs encoded in the

toric web 6 which explicitly take the form:

$$\begin{aligned}(p_1, q_1) &= (-p+q, p-q-1),\\ (p_2.q_2) &= (-q, q+1),\\ (p_3, q_3) &= (p, -p+1),\\ (p_4, q_4) &= (0, -1).\end{aligned} \tag{2.2.48}$$

Formula (2.2.47), which essentially finalizes step 2), was carefully discussed in [94] and is obtained by mapping the even dimensional cycles to 3-cycles in the mirror manifold and computing their respective intersection. Steps 3) and 4) are needed to determine the superpotential of the theory. A crucial property of any quiver theory corresponding to an affine toric variety, as the one we are presented with, is that each field in the quiver appears exactly twice in the superpotential (each time with different sign). This, together with the fact that the field theories we are interested in exhibit a $SU(2)$ global symmetry, restricts the possible superpotentials. In fact, it will turn out that, up to an overall rescaling, there will be only one superpotential satisfying all the above mentioned requirements for every toric quiver gauge theory.

2.2.3 The $Y^{p,q}$ quivers generated iteratively from the $Y^{p,p}$ quiver

Once we have the number of fields, it is necessary to specify how do each of them transform under the $n_{\rm v}$ gauge groups $SU(N)$. The method presented in [94] starts with the case of $q = p$ for fixed p and then construct the quiver for lower values of q using an iterative procedure. The quiver for $Y^{p,p}$ was already constructed in [95] and we present it in figure 7 for the specific case of $p = 4$.

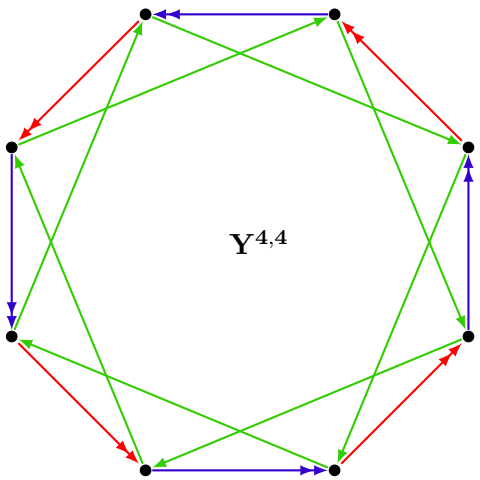


Figure 7: Quiver diagram for $\mathbb{C}/\mathbb{Z}_8$ orbifold corresponding to the $Y^{4,4}$ geometry. Superpotential terms appear in the quiver diagram as triangles combining a green, a blue and a red arrow.

The manifold $Y^{p,p}$ is the base of the orbifold $\mathbb{C}^3/\mathbb{Z}_{2p}$ which has a group action $z_i \to \omega^{a_i} z_i$ on the coordinates of $\mathbb{C}^3$, with $\omega^{2p} = 1$ and $a_1 = 1, a_2 = 1, a_3 = -2$. The fact that $a_1 = a_2$ implies that there is an $SU(2) \times U(1)$ isometry of $\mathbb{C}^3/\mathbb{Z}_{2p}$ which becomes a global symmetry of the quiver gauge theory and every field and their combinations transform in irreducible representations of this group. The fields are divided as follows: from the $6p$ fields there are $4p$ which are organized in $2p$ doublets, denoted as $X^{\alpha}_{i,i+1}$, $i = 1, \cdots, 2p \mod (2p)$, $\alpha = 1, 2$, the remaining $2p$ fields are singlets

and we denote them by $Y_{i,i-2}$ (the index i runs over the nodes of the quiver and addition and subtraction are used modulo $2p$). In figure 7 we represent doublets in blue and red and they are the edges of the polygonal quiver diagram. The singlets are represented in green and join points adjacent to each node in the quiver, thus forming triangles which give rise to superpotential terms. The superpotential can be written as:

$$W_{Y^{p,p}} = \sum_{i=1}^{2p} \epsilon_{\alpha\beta} X^{\alpha}_{i,i+1} X^{\beta}_{i+1,i+2} Y_{i+2,i}, \tag{2.2.49}$$

where $\epsilon_{\alpha\beta}$ is the two dimensional epsilon symbol introduced to properly contract the doublets such that the $SU(2)$ global symmetry is respected. A further refinement of the notation is in order since we would like to capture the fact that the group $\mathbb{Z}_{2p}$ can be reduced as $\mathbb{Z}_2 \times \mathbb{Z}_p$, hence we denote $X_{2i,2i+1} = U_{2i,2i+1}$ ($\mathbb{Z}_2$ even, represented by blue arrows) and $X_{2i+1,2i+2} = V_{2i+1,2i+2}$ ($\mathbb{Z}_2$ odd, represented by red arrows). With this notation, the superpotential can be rewritten as:

$$W_{Y^{p,p}} = \sum_{i=1}^{p} \epsilon_{\alpha\beta} \left(U^{\alpha}_{2i,2i+1} V^{\beta}_{2i+1,2i+2} Y_{2i+2,2i} + V^{\alpha}_{2i+1,2i+2} U^{\beta}_{2i+2,2i+3} Y_{2i+3,2i+1} \right). \tag{2.2.50}$$

Now we are ready to start the iterative procedure presented in [94]. To obtain the $Y^{p,p-1}$ quiver from that of $Y^{p,p}$ we essentially have to remove three fields and add one in the following way:

- Take a blue edge of the polygon, that is a $V_{2i+1,2i+2}$ doublet field joining two consecutive nodes, say $2i+1$ and $2i+2$. Remove one arrow from the edge, which makes it into a singlet and call it $Z_{2i+1,2i+2}$ (color it also differently, say violet, see the top edge in figure 8).
- Remove the two singlets (green arrows) connected to the $2i+1$ and $2i+2$ nodes (which are the endpoints of the new singlet $Z_{2i+1,2i+2}$). The effect of this action on the superpotential is that the cubic terms containing $Y_{2i+2,2i}$ and $Y_{2i+3,2i+1}$ are no longer present in the superopotential.
- Add a singlet $Y_{2i+3,2i}$ joining nodes $2i+3$ and $2i$ such that there is a tetrahedron formed by $Z_{2i+1,2i+2}, U_{2i+2,2i+3}, U_{2i,2i+1}$ and $Y_{2i+3,2i}$ which give rise to a new monomial term to be added to the superpotential.

The superpotential now looks like:

$$\begin{aligned} W_{Y^{p,p-1}} = & \sum_{j\neq i=1}^{p} \epsilon_{\alpha\beta} \left(U^{\alpha}_{2j,2j+1} V^{\beta}_{2j+1,2j+2} Y_{2j+2,2j} + V^{\alpha}_{2j+1,2j+2} U^{\beta}_{2j+2,2j+3} Y_{2j+3,2j+1} \right) \\ & + \epsilon_{\alpha\beta} Z_{2i+1,2i+2} U^{\alpha}_{2i+2,2i+3} Y_{2i+3,2i} U^{\beta}_{2i,2i+1}. \end{aligned} \tag{2.2.51}$$

A similar procedure generates the $Y^{p,p-2}$ quiver and we represent the corresponding diagram for the case of $Y^{4,2}$ in figure 8 on the right.

Repeating this procedure all the way down to $Y^{p,0}$ and we show the last two quivers for $p=4$ in figure 9, hence, any $Y^{p,q}$ quiver can be obtained and the general superpotential is:

$$\begin{aligned} W_{Y^{p,q}} = & \sum_{k=1}^{p} \epsilon_{\alpha\beta} \left(U^{\alpha}_{2k,2k+1} V^{\beta}_{2k+1,2k+2} Y_{2k+2,2k} + V^{\alpha}_{2k+1,2k+2} U^{\beta}_{2k+2,2k+3} Y_{2k+3,2k} \right) \\ & + \epsilon_{\alpha\beta} \sum_{k=1}^{p} Z_{2k+1,2k+2} U^{\alpha}_{2k+2} Y_{2k+3,2k} U^{\beta}_{2k,2k+1}. \end{aligned} \tag{2.2.52}$$

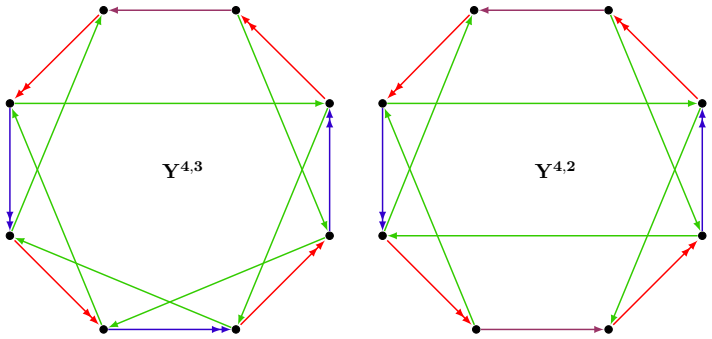


Figure 8: Quiver diagram corresponding to the $Y^{4,3}$ and $Y^{4,2}$ geometries. Superpotential terms appear in the quiver diagram as triangles combining a green, a blue and a red arrow and Z singlets are colored in violet.

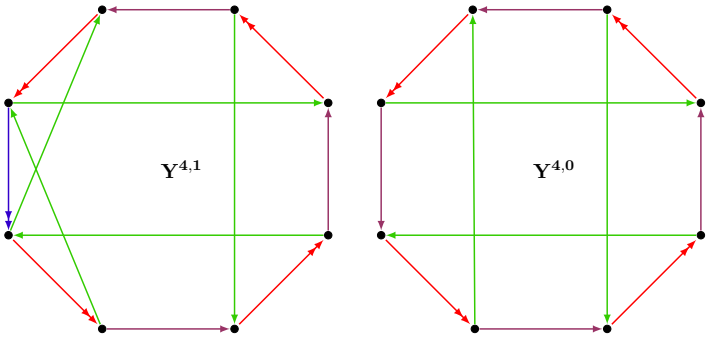


Figure 9: Quiver diagram corresponding to the $Y^{4,1}$ and the $Y^{4,0}$ geometries.

Moreover, the $n_\chi = 4p + 2q$ fields organize as follows; there are p doublets U and q doublets V, $p - q$ singlets Z and $p + q$ diagonal singlets Y. The application of a-maximization [86] permits to compute the R-charges. For the purposes of our later computation it will be sufficient to use R-trial charges assigned even before applying the a-maximization process. We now continue the presentation of other toric quiver gauge theories.

2.2.4 The $X^{p,q}$ theories

The construction presented in the previous section opened a path for new explorations in the context of toric quiver gauge theories. Starting from $Y^{p,q}$ theories one can engineer other theories being also toric by using different tools. A particularly useful way of doing this is by adding flavors to the starting theory, which can be interpreted as an inverse Higgs mechanism for the quiver gauge theory. This allows the construction of a new infinite family of theories called $X^{p,q}$ which were found in [96]. The motivation comes from the following situation: consider the case of the complex cone over the second del Pezzo surface $d\mathbf{P}_2$, which is essentially $\mathbb{P}^2$ blown up at two points (the concept of blowup is in fact a well defined geometrical transformation which replaces a subspace of a given space by the directions going out of that subspace and it intuitively reproduces the notion of zooming in). It is possible to obtain $d\mathbf{P}_1$ by a blow down of an exceptional $\mathbb{P}^1$ (corresponding to the $Y^{2,1}$ manifold). From the point of view of gauge theory this corresponds to give a vacuum expectation value to a certain bi-fundamental field, hence obtaining the $d\mathbf{P}_1$ theory from the $d\mathbf{P}_2$.

A different Higgsing process allows also to obtain the theory associated to $\mathbb{F}_0$ ($Y^{2,0}$). Therefore, $d\mathbf{P}_2$ theory is the example of a field theory from which one can get, via Higgsing, two different $Y^{p,q}$ theories. We illustrate the Higgsing process from the point of view of the toric diagram in figure 10. Vertices of equal color are those which are preserved from $d\mathbf{P}_2$ to either $d\mathbf{P}_1$(we preserve the black vertex and eliminate the blue one) or $\mathbb{F}_0$ (we preserve the blue vertex and eliminate the black one).

The name for a family of theories generalizing the case of $d\mathbf{P}_2$ is $X^{p,q}$ theories, and consequently, from each of them one can arrive to $Y^{p,q}$ and $Y^{p,q-1}$. The $X^{p,q}$ theories have $\mathcal{N}=1$ supersymmetry and $SU(N)^{2p+1}$ gauge theories and the authors of [96] present a generic algorithm to obtain them.

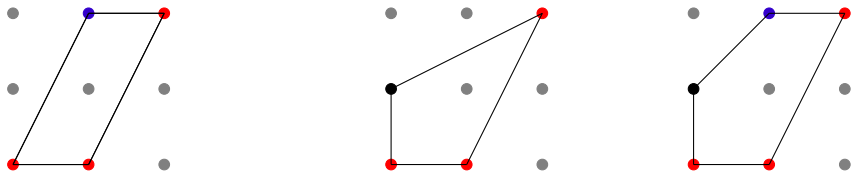


Figure 10: Example of toric diagrams for $\mathbb{F}_0$, $d\mathbf{P}_1$ and $d\mathbf{P}_2$. The figure illustrates the Higgsing process from the point of view of the toric diagram. Vertices of iqual color are hose which are preserved from $d\mathbf{P}_2$ to either $d\mathbf{P}_1$(we preserve the black vertex and eliminate the blue one) or $\mathbb{F}_0$ (we preserve the blue vertex and eliminate the black one).

To be able to generate an $X^{p,q}$ theory form a given $Y^{p,q}$ theory we need to implement the inverse of Higgsing some bi-fundamental fields. Let us consider separately the cases $q=p$ and $q<p$.

The $q<p$ case

Let us now consider the quiver diagram for $Y^{p,q}$, which we are familiar with from the discussion of section 2.2.2. Since we are considering $q<p$ there will be at least one Z singlet in the quiver (a violet arrow in figures 8 and 9). It is possible to argue that we can bring the violet arrow as close as possible to the leg of the $Y^{p,q}$ quiver which we will modify by performing a sequence of Seiberg dualities [96]. In practice, the transformation of the quiver boils down to blowing up a node into two nodes. Let us call k the node which is going to be blown and $k_{(1,2)}$ the two new nodes that appear. Following a counter clock-wise orientation we call $k-1$ to the node before k and $k+1$ the one after. Therefore the steps to construct the $X^{p,q}$ quiver are the following:

- Draw bi-fundamental fields $X_{k-1,k_{1,2}}, X_{k_1,k_2}, X_{k_{1,2},k+1}$.
- For all $Z_{i,k}$ singlets in the $Y^{p,q}$ quiver (violet arrows entering k), draw a bi-fundamental X_{i,k_1}.
- For all $Z_{k,i}$ singlets in the $Y^{p,q}$ quiver (violet arrow exiting k), draw a bi-fundamental $X_{k_2,i}$.
- Leave the remaining bi-fundamentals in the $Y^{p,q}$ quiver as they are.

We see that the number chiral fields is $n_\chi = 4p+2q+1$ and also that $n_{\rm v} = 2p+1$. The superpotential has to be consequently modified since we want to mke sure we can reproduce the $Y^{p,q}$ superpotential

(2.2.51) by Higgsing. We then conclude that the superpotential looks like:

$$\begin{aligned} W_{X^{p,q}} = & U^{(1)}_{k+2,k+3} Y_{k+3,k_1} Z_{k_1,k_2} Z_{k_2,k+1} Z_{k+1,k+2} + Z_{k-1,k_1} Y_{k_1,k+1} Y_{k+1,k-1} \\ & + U^{(2)}_{k+4,k-1} Y_{k-1,k_2} Y_{k_2,k+4} - Y_{k+3,k_1} Y_{k_1,k+1} Z_{k+1,k+2} U^{(1)}_{k+2,k+3} - Y_{k-1,k_2} Z_{k_2,k+1} Y_{k+1,k-1} \\ & - U^{(1)}_{k+4,k-1} Z_{k-1,k_1} Z_{k_1,k_2} Y_{k_2,k+4} + \text{unchanged}, \end{aligned} \tag{2.2.53}$$

where by "unchanged" we mean that the remaining terms in the superpotential are the same as in the $Y^{p,q}$ theory. A visualization of the whole process can be seeing in figure 11 where we show a portion of the $X^{p,q}$ quiver where all closed cycles shown account for a term in (2.2.53).

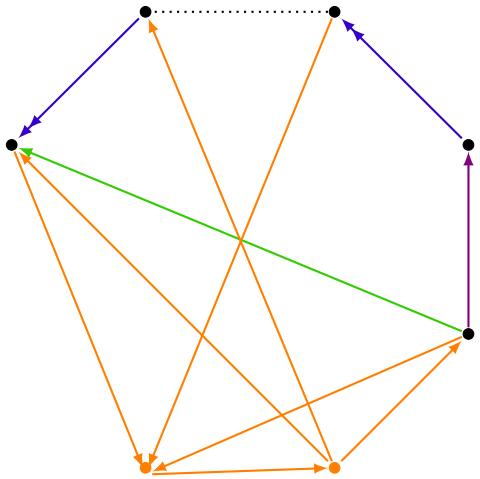


Figure 11: Relevant portion of quiver diagram for $X^{p,q}$ theory. The remaining part of the quiver is represented by a dotted line. New nodes k_1 and k_2 and fields $X_{k_{(1,2)},j}$, $X_{j,k_{(1,2)}}$ are drawn in orange. New superpotential terms appear in the quiver diagram as parallelograms. The labeling follows a counter-clockwise order.

The $p = q$ case

When $p = q$ the superpotential has no quintic term since such term cannot produce any consistent contribution to the $Y^{p,p}$ superpotential upon Higgsing. The procedure explained before has to be modified only as follows. Instead of drawing a bi-fundamental between nodes $k+3$ and k_1, we draw one connecting $k+2$ and k_1, which modifies figure 11 as shown in figure 12 and the superpotential can be written as:

$$\begin{aligned} W_{X^{p,p}} = & Z_{k_2,k+1} Y_{k+1,k-1} Y_{k-1,k_2} + U^{(2)}_{k+1,k+2} Y_{k+2,k_1} Y_{k_1,k+1} - Y_{k_1,k+1} Y_{k+1,k-1} Z_{k-1,k_1} \\ & - Y_{k-1,k_2} Y_{k-1,k_2} Y_{k_2,k+4} U^{(2)}_{k+4,k-1} - Z_{k_2,k+1} U^{(1)}_{k+1,k+2} Y_{k+2,k_1} Z_{k_1,k_2} \\ & + Z_{k_1,k_2} Y_{k_2,k+4} U^{(1)}_{k+4,k-1} Z_{k-1,k_1} + \text{unchanged}. \end{aligned} \tag{2.2.54}$$

It is simple to obtain now the toric diagram associated to the $X^{p,q}$ theory by reproducing the process illustrated in figure 10, we then have the generic toric diagram of figure 13. We can isolate the toric diagram of the generic $X^{p,q}$ theory and find the (p, q) web as shown in figure 14. We

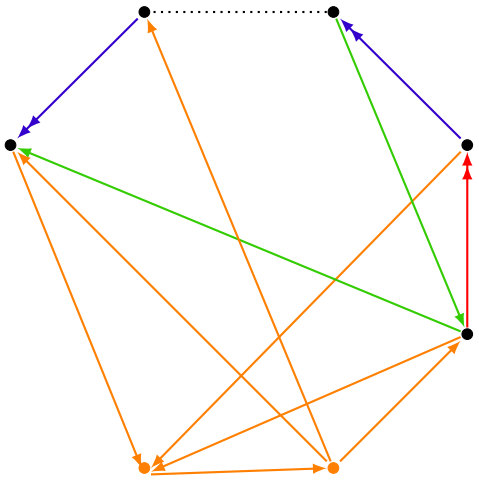


Figure 12: Relevant portion of quiver diagram for $X^{p,p}$ theory. The remaining part of the quiver is represented by a dotted line. New nodes and fields are drawn in orange and new superpotential terms appear in the quiver diagram as parallelograms contaning at least one orange line.

denote the coordinates of the endpoints of the (p,q)-web as (p_I, q_I), $I = 1, \cdots, 5$ as in the $Y^{p,q}$, thus, we have:

$$\begin{aligned}(p_1, q_1) &= (p, -p+1),\\ (p_2, q_2) &= (-q, q+1),\\ (p_3, q_3) &= (-1, 1),\\ (p_4, q_4) &= (-a, a-1),\\ (p_5, q_5) &= (0, -1).\end{aligned} \tag{2.2.55}$$

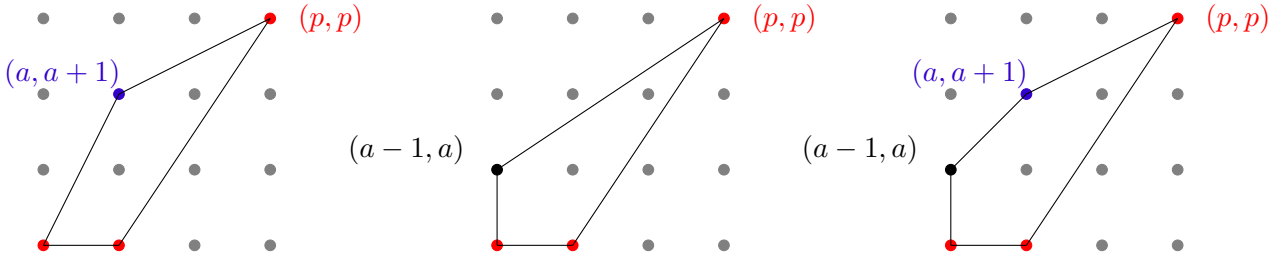


Figure 13: Generic toric diagram for $X^{p,q}$ theory on the right as a simple generalization of the case of $d\mathbf{P}_2$ shown in figure 10. Here $a = p - q$ and we show the $Y^{p,q-1}$ toric diagram on the left and the $Y^{p,q}$ toric diagram on the center.

2.2.5 The $L^{a,b,c}$ geometries

The work [97] showed that it is possible to obtain a family of local toric Kähler–Einstein metrics by taking a certain scaling limit of a Euclideanised form of the Plebanski–Demianski metrics studied in [98]. Furthermore the authors showed that the metrics they found were exactly the ones used in e generalization of $Y^{p,q}$ geometries in [99]. This generalized family of geometries is denoted as

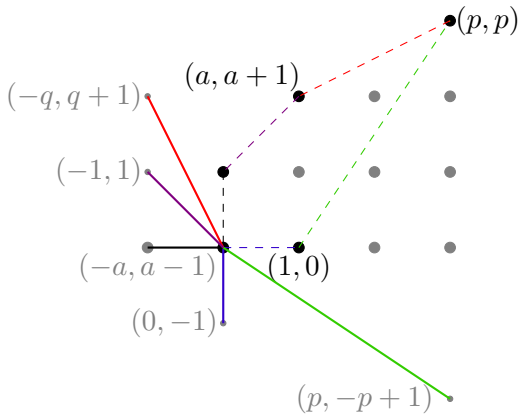


Figure 14: Example of a (p,q)-web for $X^{p,q}$ and we have defined $a=p-q$. We obtain the reciprocal diagram by simply tracing orthogonal lines to each side of the toric diagram (represented here with dashed lines). We represent with the same color and continuous line the dual to each side. We keep the length of the reciprocal line to be the same as the original, hence the endpoints labeled in gray are easily determined if we make all reciprocal lines meet at the origin of the lattice.

$L^{a,b,c}$ and it is completely specified by the integer numbers a,b,c. The $Y^{p,q}$ metric is recovered from that of $L^{a,b,c}$ for $a=p-q$, $b=p+q$ and $c=p$.

Moreover, in a similar fashion to the $Y^{p,q}$ case discussed in section 2.2.1, there are precisely four Killing vector fields $K_{I=1,2,3,4}$, that vanish on co-dimension 2 submanifolds. This means that the image of the Calabi–Yau cone $C(L^{a,b,c})$ under the moment map $\vec{\mu}$ for the $\mathbb{T}^3$ action is a four faceted polyhedral cone in $\mathbb{R}^3$. The following relation has to be satisfied by the set of vectors $\mathcal{V}_I$:

$$a\mathcal{V}_1+b\mathcal{V}_2-c\mathcal{V}_3+(a+b-c)\mathcal{V}_4=0, \tag{2.2.56}$$

where the vectors $\mathcal{V}_i$ are obtained via an appropriate $SL(2,\mathbb{Z})$ transformation on the vectors normal to the facets of the polyhedral $\vec{\mu}\left(C(L^{a,b,c})\right)$. It is then possible to follow a Delzant construction to associate the toric diagram to a gauged linear sigma model by defining a Kähler quotient $\mathbb{C}^4/\mathbb{T}$, with $\mathbb{T}\cong U(1)$ and $U(1)$ acts on the coordinates of $\mathbb{C}^4$ with the vector charge $Q=(a,b,-c,-a-b+c)$.

2.2.6 The field theory dual to $L^{a,b,c}$

Exploiting the relations between the (p,q)-web for five branes and toric diagrams it possible to construct the quivers associated to the $L^{a,b,c}$ theories. In this process a major role is played by the mesonic BPS operators which was related in [100] to BPS geodesics. Specifically, a non-trivial match was established between the $U(1)_F\times U(1)_F$, $U(1)_R$ conserved charges of BPS geodesics and those of BPS mesons however we shall not go deeper into this discussion since, as we will see below, all our relevant information can be extracted directly from toric data. The toric diagram associated to the $L^{a,b,c}$ geometry will have four edges and is represented in figure 15. Once again, we can bring two vertices of the diagram to the points $(0,0)$ and $(0,1)$ of the integer lattice by using and $SL(2,\mathbb{Z})$ transformation on the toric diagram. We list the coordinates of the endpoints of the (p,q)-web:

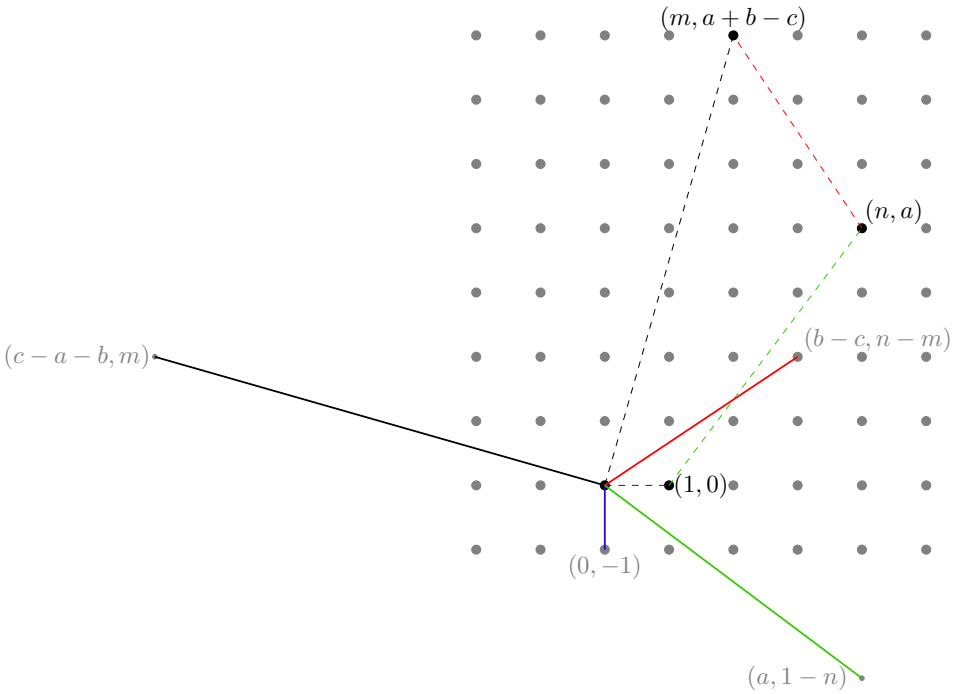


Figure 15: A generic four sided toric diagram of $L^{a,b,c}$ with the (p, q)-web included following the same color code used in section 2.2.2. The values of m and n have to satisfy the Diophantine equation $b = n(a + b - c) - am$. To this diagram corresponds one baryonic symmetry, however, generically, one has that $\#-$ of baryonic symmetries $+3 = \#$-of external legs of (p, q)-web. From this data we extract $n_{\rm v} = a + b$ and $n_\chi = a + 3b$.

$$\begin{aligned}(p_1, q_1) &= (a, 1-n),\\ (p_2, q_2) &= (b-c, n-m),\\ (p_3, q_3) &= (c-a-b, m),\\ (p_4, q_4) &= (0, -1).\end{aligned} \tag{2.2.57}$$

2.2.7 Generic properties of toric quiver gauge theories

In what follows we gather generic information and properties which are common to all the previously discussed toric quiver gauge theories. An important property which we shall use later in our developments is the fact that, given the number of gauge groups $n_{\rm v}$ of a toric quiver gauge theory, the number n_χ of chiral fields and the number n_W of terms in the superpotential, they satisfy the relation:

$$n_{\rm v} + n_\chi - n_W = 0. \tag{2.2.58}$$

The reason is that the gauge theory living on a brane at the tip of a toric Calabi-Yau cone, the quiver can be extended and drawn on a torus [101, 102], hence (2.2.58) is a consequence of the Euler relation on a torus. We will follow the prescription of [103] to provide an R-charge and global non-anomalous flavor charges purely using the toric data. To this end, let us define as d

the number of vertices in the toric diagram (recall that this number corresponds to the number of gauge vector fields $A_{I=1,\cdots,d}$ in the five dimensional bulk theory [54]).

The number of global non-R-symmetries is $d-1$, since we have always two global symmetries associated to the toric action and baryonic symmetries associated to the $d-3$ three-cycles of the SE_5 at hand. This total number of $U(1)$ symmetries determines the number of independent parameters $r_{I=1,\cdots,d}$ which are used in the process of a-maximization (or volume minimization) presented in [103]. The prescription to assign R-charges and $U(1)$ flavor charges is the following:

- To each (p_I, q_I) vector in the (p,q) web, associate chiral field $\Phi_{ab}^{(I)}$ with trial R-charge $r_{ab}^{(I)} \equiv r_I$ and satisfying the following constraint:

$$\sum_{I=1}^{d} r_I = 2. \tag{2.2.59}$$

- For a type of chiral field with multiplicity $\left|\det \begin{pmatrix} p_I & q_I \\ p_J & q_J \end{pmatrix}\right|$ the R-charge assigned is $r_{I+1} + \cdots + r_J$ (here the indices I, J are understood to be modulo d). Moreover, we have adopted the convention used in [103] to assign ordered indices I, J to the edges of the (p,q)-web. The convention is that, given two vectors in the (p,q)-web, we label them with the indices I, J, that is (p_I, q_I) and (p_J, q_J) if we can rotate (p_I, q_I) counter-clockwise towards (p_J, q_J) with an angle less or equal than 180°.

The assignment for global $U(1)$ flavor symmetries is very similar to the R-charge case, namely:

- Assign a global $U(1)_{k=1,\cdots,d-1}$ charge $F_I^{(k)}$ to the chiral field associated to the web vector (p_I, q_I) but now the constraint the parameters must satisfy is:

$$\sum_{I=1}^{d} F_I^{(k)} = 0, \quad k = 1, \cdots, d-1. \tag{2.2.60}$$

- The global charge assigned to chiral field of multiplicity $\left|\det \begin{pmatrix} p_I & q_I \\ p_J & q_J \end{pmatrix}\right|$ is $F_{I+1} + \cdots + F_J$ (same convention for assigning I, J labels).

We can summarize the output of performing the assignment in tables for each theory discussed in the previous section. We therefore have for the $Y^{p,q}$ theory the charge assignment and multiplicities shown in table 1, for the $X^{p,q}$ theory we have the charge assignment and multiplicities reported in table 2 whereas for $L^{a,b,c}$ theories, the charge assignment and multiplicities is presented in table 3.

A way of generically encode the data associated to the symmetries of the theories summarized in the previous tables is to define Q_I^{ab} for every chiral field Φ_{ab} connecting the nodes a and b of the quiver such that:

$$r_{ab} = \sum_{I=1}^{d} Q_I^{ab} r_I, \tag{2.2.61}$$

$$F_{ab}^{(k)} = \sum_{I=1}^{d} Q_I^{ab} F_I^{(k)}, \quad k = 1, \cdots, d-1. \tag{2.2.62}$$

Multiplicity	$U(1)_k$	$U(1)_R$
$p+q$	$F_1^{(k)}$	r_1
p	$F_2^{(k)}$	r_2
$p-q$	$F_3^{(k)}$	r_3
p	$F_4^{(k)}$	r_4
q	$F_2^{(k)}+F_3^{(k)}$	r_2+r_3
q	$F_3^{(k)}+F_4^{(k)}$	r_3+r_4

Table 1: Charge assignment and multiplicities of fields for $Y^{p,q}$ theory where $k=1,2,3$ and two of the global charges are really enhanced to $SU(2)$ as we discussed in section 2.2.2.

Multiplicity	$U(1)_k$	$U(1)_R$
$p+q-1$	$F_1^{(k)}$	r_1
1	$F_2^{(k)}$	r_2
1	$F_3^{(k)}$	r_3
$p-q$	$F_4^{(k)}$	r_4
p	$F_5^{(k)}$	r_5
$p-1$	$F_2^{(k)}+F_3^{(k)}$	r_2+r_3
1	$F_3^{(k)}+F_4^{(k)}$	r_3+r_4
$q-1$	$F_2^{(k)}+F_3^{(k)}+F_4^{(k)}$	$r_2+r_3+r_4$
1	$F_1^{(k)}+F_2^{(k)}$	r_1+r_2
q	$F_4^{(k)}+F_5^{(k)}$	r_4+r_5

Table 2: Charge assignment and multiplicities for $X^{p,q}$ theory where $k=1,2,3,4$.

Multiplicity	$U(1)_k$	$U(1)_R$
b	$F_1^{(k)}$	r_1
$a+b-c$	$F_2^{(k)}$	r_2
a	$F_3^{(k)}$	r_3
c	$F_4^{(k)}$	r_4
$c-a$	$F_2^{(k)}+F_3^{(k)}$	r_2+r_3
$b-c$	$F_3^{(k)}+F_4^{(k)}$	r_3+r_4

Table 3: Charge assignment and multiplicities of fields for $L^{a,b,c}$ theory where $k=1,2,3$.

Using the R-symmetry fugacity $\widetilde{\nu}_R$ and denoting the flavor symmetries fugacities as ξ_k, then we can define the quantity:

$$\Delta_{ab}=\widetilde{\nu}_R r_{ab}+\sum_{k=1}^{d-1}\xi_k F_{ab}^{(k)}=\sum_{I=1}^{d}Q_I^{ab}\left(\widetilde{\nu}_R r_I+\sum_{k=1}^{d-1}\xi_k F_I^{(k)}\right), \tag{2.2.63}$$

which enter in the argument of the Elliptic gamma function in the SCI and was generically denoted as Δ_a in (2.1.11). Defining a redundant fugacity we can rewrite (2.2.63) as:

$$\Delta_{ab} = \sum_{I=1}^{d} Q_I^{ab} \Delta_I. \tag{2.2.64}$$

Note that, from the definition of Δ_I and from relations (2.2.59) and (2.2.60) we see they have to obey the following constraint:

$$\sum_{I=1}^{d} \Delta_I = \sum_{I=1}^{d} \left(\widetilde{\nu}_R r_I + \sum_{k=1}^{d-1} \xi_k F_I^{(k)} \right) = 2\widetilde{\nu}_R \tag{2.2.65}$$

Using (2.1.10), we can rewrite $\widetilde{\nu}_R = \nu_R \pm \frac{1}{2}$ to obtain the constraint:

$$\sum_{I=1}^{d} \Delta_I = \tau + \sigma \pm 1. \tag{2.2.66}$$

We can think of Δ_I as chemical potentials for d $U(1)$ flavor symmetries, one of them being redundant (since there are only $d-1$). In the next chapter we will use an assignment of charges based on this data, which boils down to specify values of r_I and $F_I^{(k)}$.

2.3 The entropy function of $\mathcal{N} = 1$ SCFT's

We would now like to move a further step towards finding the entropy of black holes dual to a large class of $\mathcal{N} = 1$ toric quiver gauge theories. It was put forward in [104] that a certain class of asymptotic to $\mathrm{AdS}_5 \times S^5$ black holes with three electric charges $Q_I (I = 1, 2, 3)$, associated with rotations in S^5, and two angular momenta J_ϕ, J_ψ in $\mathrm{Ad}S_5$ have a Bekenstein-Hawking entropy which can be obtained as the Legendre transform of the so called entropy function:

$$S_{\mathrm{E}} = -i\pi \frac{N^2 \Delta_1 \Delta_2 \Delta_3}{6\tau\sigma}, \tag{2.3.1}$$

where Δ_I are chemical potentials conjugated to the electric charges Q_I and τ, σ are chemical potentials conjugated to the angular momenta J_ϕ, J_ψ which satisfy the constraint:

$$\Delta_1 + \Delta_2 + \Delta_3 - \tau - \sigma = \pm 1. \tag{2.3.2}$$

The statement was further generalized in [53] where the authors conjectured that supersymmetric black hole solutions asymptotic to $\mathrm{AdS}_5 \times \mathrm{SE}_5$, where the internal space SE_5 is a Sasaki-Einstein manifold. The five dimensional theory contains d massless vector multiplets corresponding to the R-symmetry and global symmetries of the dual field theory. Concretely, the entropy function whose Legendre transform should yield the Bekenstein-Hawking black hole entropy was:

$$S_E = -i\pi \frac{N^2}{6\tau\sigma} C_{IJK} \Delta_I \Delta_J \Delta_K, \tag{2.3.3}$$

where the coefficients C_{IJK} with $I = 1, \cdots, d$, in a compactification on $\mathrm{Ad}S^5 \times \mathrm{SE}_5$ are proportional to the anomaly coefficients $\mathrm{Tr}\,(Q_I Q_J Q_K)$ for the d symmetries Q_I associated with the gauge fields A_I in the bulk five-dimensional theory [54]. In terms of the toric data we have that:

$$\frac{N^2}{2} \left|\det\left(V_I, V_J, V_K\right)\right| = N^2 C_{IJK}, \tag{2.3.4}$$

where V_I are the vectors defining the toric diagram in $\mathbb{R}^3$ (for example, take the $\mathbb{R}^2$ vectors $\mathcal{V}_I$ defined in (2.2.45) and a third component equal to 1). Initially the entropy function S_E was associated to the supersymmetric Casimir energy [105–108] but there was lack of proper understanding as to how and why such quantity should be related to the entropy of the black holes under consideration. There was some light shed on this question for the case of $\mathcal{N} = 4$ SYM theory since the entropy function was successfully connected to $\log \mathcal{I}$, hence the entropy function was given a concrete interpretation in terms of a counting problem.

Further developments in [42–45] showed that in the large rank limit and also Cardy-like limit of the SCI of 4d $\mathcal{N} = 4$ SYM and other $\mathcal{N} = 1$ superconformal field theries accounts for the entropy function, namely $\log \mathcal{I} = S_E$. In fact, for a large class of $\mathcal{N} = 1$ toric quiver gauge theories discussed in section 2.2, the authors of [46] gathered more evidence in favor of the conjecture of [53] by proving that $\log \mathcal{I}$ captures S_E in the large N limit and Cardy-like expansion. In the next chapter we will explicitly show the validity of $\log \mathcal{I}$ capturing the behavior of S_E beyond the Cardy-like limit for the large class of toric quiver gauge theories we have discussed.

CHAPTER 3
The SCI and the entropy function at leading N^2 order

3.1 Bethe Ansatz solutions for $\mathcal{N}=1$ toric quiver gauge theories

The goal of this chapter is to estimate the SCI in the large N limit for a large class of $\mathcal{N}=1$ toric quiver gauge theories reviewed in chapter 2. We proceed using the BA approach in such a way that we generalize the solutions to the BAEs used in [38].

The result we reviewed in section 2.1 (which was developed in [39] and [38], based on [40]), allows us to rewrite the SCI in terms of solutions to the BA system of equations (2.1.27), which we reproduce here for the reader's convenience:

$$Q_i\left(u;\xi,\nu_R,\omega\right)=1\ \ \forall\ \ i=1,...,\mathrm{rk}\left(G\right), \tag{3.1.1}$$

where ω is such that $r\tau=s\sigma$ with r and s coprime integer numbers (in practice we will evaluate the equations for $r=s$). It will be convenient to write the explicit form of the BA operator as follows:

$$Q_i\left(u;\xi,\nu_R,\omega\right)=\prod_{a=1}^{n_\chi}\prod_{\rho_a\in\mathfrak{R}_a}P\left(\rho_a\left(u\right)+\omega_a\left(\xi\right)+r_a\nu_R;\ \omega\right)^{\rho_a^i}, \tag{3.1.2}$$

where

$$P\left(u;\omega\right)=\frac{e^{-\pi i\frac{u^2}{\omega}+\pi iu}}{\theta_0\left(u;\omega\right)}. \tag{3.1.3}$$

Thus,

$$P\left(\rho_a\left(u\right)+\omega_a\left(\xi\right)+r_a\nu_R;\ \omega\right)=\frac{e^{-\pi i\frac{1}{\omega}\left(\rho_a(u)+\omega_a(\xi)+r_a\nu_R\right)^2+\pi i\left(\rho_a(u)+\omega_a(\xi)+r_a\nu_R\right)}}{\theta_0\left(\rho_a\left(u\right)+\omega_a\left(\xi\right)+r_a\nu_R;\omega\right)}, \tag{3.1.4}$$

where:

$$\theta_0\left(u;\omega\right)=\left(e^{2\pi iu};e^{2\pi i\omega}\right)_\infty\left(e^{2\pi i(\omega-u)};e^{2\pi i\omega}\right)_\infty. \tag{3.1.5}$$

Now we would like to evaluate the BAEs for the case of a toric quiver gauge theory. Toric quiver gauge theories, as we have reviewed in the previous chapter, describe the low energy dynamics of a stack of N D3 branes probing the tip of a toric Calabi-Yau singularity; there is by now a vast literature detailing how to construct a supersymmetric field theory given toric data. Consider a toric quiver gauge theory whose gauge group G has n_{v} simple factors (in all the $\mathcal{N}=1$ quiver gauge theories we will deal with, the number of simple factors coincides with the number of vector multiplets). We focus, for concreteness, on the case in which all the gauge group factors are $SU(N_a)$, a goes from 1 to n_{v}, with $N_a=N\ \forall\, a$, the same numerical value for all nodes. In these theories the weight vectors ρ are such that for any bi-fundamental field Φ_{ab} (notice that in the more generic notation used in section 2.1, the index a of Φ_a would now split into ab):

$$\rho_{ij}^{\Phi_{ab}}\left(u\right)\equiv u_{ij}^{ab}\equiv u_i^a-u_j^b. \tag{3.1.6}$$

Let us now evaluate the BA operator for a generic field Φ_{ab} (when Φ_{ab} transforms in the adjoint representation of G then, in this notation, $a=b$):

$$Q_{i_a}\left(u;\xi,\tau,\sigma,\omega\right)=\prod_{(a,b)}\prod_{j_b}\prod_{\rho_{ij}^{(a,b)}}P\left(u_{i_a}-u_{j_b}+\Delta_{ab}\right)^{\rho_{ij}^{(a,b)}}, \tag{3.1.7}$$

where (a,b) run over all the fields Φ_{ab} for a fixed a and r_{ab} are the R-charges of the fields Φ_{ab}. The $d-1$ fugacities correspond to the flavor symmetries appearing in the generic toric gauge theories that we will study, d is the number of external points of the toric diagram that are related to the quivers defining the theory [46]. If we denote $\langle a,b\rangle \equiv (a,b)|_{\rho_{ij}^{(a,b)}>0}$, which implies:

$$\begin{aligned} Q_{i_a}\left(u;\xi,\tau,\sigma,\omega\right) &= \prod_{\langle a,b\rangle}\prod_{j_b}\prod_{\rho_{ij}^{\langle a,b\rangle}}\left[\frac{P\left(u_{i_a}-u_{j_b}+\Delta_{ab}\right)}{P\left(u_{j_b}-u_{i_a}+\Delta_{ba}\right)}\right]^{\rho_{ij}^{\langle a,b\rangle}} \\ &= \prod_{\langle a,b\rangle}\prod_{j_b}\prod_{\rho_{ij}^{\langle a,b\rangle}}\left[\frac{e^{-2\pi i\left(-u_{i_a}+u_{j_b}\right)}\theta_0\left(-u_{j_b}+u_{i_a}+\Delta_{ab};\omega\right)}{\theta_0\left(u_{i_a}-u_{j_b}+\Delta_{ba};\omega\right)}\right]^{\rho_{ij}^{\langle a,b\rangle}} \\ &= e^{-2\pi i\sum_{j_b}\left(u_{i_a}-u_{j_b}\right)}\prod_{\langle a,b\rangle}\prod_{j_b}\frac{\theta_0\left(-u_{i_a}+u_{j_b}+\Delta_{ab};\omega\right)}{\theta_0\left(-u_{j_b}+u_{i_a}+\Delta_{ba};\omega\right)}. \end{aligned} \tag{3.1.8}$$

Let us now introduce a Lagrange multiplier λ_a that accounts for the constraint ensuring the $SU(N)$ condition $\sum_i u_i^a = 0$ [38], with its help, equation (3.1.8) can be written as:

$$Q_{i_a}\left(u;\xi,\tau,\sigma,\omega\right) = e^{2\pi i\left(\sum_b \lambda_b - \sum_{j_b} u_{ij}^{ab}\right)}\prod_{\langle a,b\rangle}\prod_{j_b}\frac{\theta_0\left(-u_{ij}^{ab}+\Delta_{ab};\omega\right)}{\theta_0\left(-u_{ji}^{ba}+\Delta_{ba};\omega\right)}, \tag{3.1.9}$$

where we have denoted $u_{i_a}-u_{j_b}\equiv u_{ij}^{ab}$. Restricting ourselves to the case with $\tau=\sigma$, we would like to propose a set of u_{ij}^{ab} that makes (3.1.9) equal to 1, thus solving the BA equation (3.1.1). It is natural to make an attempt with a direct generalization of the type of solution encountered in [38], namely: $u_{ij}^{ab}=\frac{\tau}{N}\left(i_a-j_b\right)$. These solutions appeared first in [52] while evaluating the topologically twisted of 4d $\mathcal{N}=1$ theories on $T^2\times S^2$ in the high temperature limit; it was later shown in [68] that such configuration provides an exact solution to the BAEs.

Consider one generic factor entering in (3.1.9) for a fixed value of b:

$$\prod_{j_b}\frac{\theta_0\left(u_{ij}^{ab}+\Delta_{ab};\omega\right)}{\theta_0\left(-u_{ij}^{ab}+\Delta_{ba};\omega\right)}\Big|_{u_{ij}^{ab}=\frac{\tau}{N}(i_a-i_b)} = \frac{\prod_{k=0}^{i_a-1}\theta_0\left(\frac{\tau}{N}k+\Delta_{ab}\right)\times\prod_{k=i_a-N}^{-1}\theta_0\left(\frac{\tau}{N}k+\Delta_{ab}\right)}{\prod_{k=0}^{N-i_a}\theta_0\left(\frac{\tau}{N}k+\Delta_{ba}\right)\times\prod_{k=i_a-1}^{-1}\theta_0\left(\frac{\tau}{N}k+\Delta_{ba}\right)} \tag{3.1.10}$$

$$\begin{aligned} \prod_{j_b}\frac{\theta_0\left(u_{ij}^{ab}+\Delta_{ab};\omega\right)}{\theta_0\left(-u_{ij}^{ab}+\Delta_{ba};\omega\right)} &= \frac{\prod_{k=0}^{N-1}\theta_0\left(\frac{\tau}{N}k+\Delta_{ab}\right)\times\prod_{k=i_a-N}^{-1}\left(-e^{2\pi i\tau\frac{k}{N}}e^{2\pi i\Delta_{ab}}\right)}{\prod_{k=0}^{N-1}\theta_0\left(\frac{\tau}{N}k+\Delta_{ba}\right)\times\prod_{k=1-i_a}^{-1}\left(-e^{2\pi i\tau\frac{k}{N}}e^{2\pi i\Delta_{ba}}\right)} \\ &= \frac{\prod_{k=0}^{N-1}\theta_0\left(\frac{\tau}{N}k+\Delta_{ab}\right)}{\prod_{k=0}^{N-1}\theta_0\left(\frac{\tau}{N}k+\Delta_{ba}\right)}\times\left(e^{\pi i(-1+\tau)}\right)^{(2i_a-N-1)}\times \\ &\times e^{-2\pi i[i_a(\Delta_{ab}+\Delta_{ba})-N\Delta_{ab}-\Delta_{ba}]} \\ &= \frac{\prod_{k=0}^{N-1}\theta_0\left(\frac{\tau}{N}k+\Delta_{ab}\right)}{\prod_{k=0}^{N-1}\theta_0\left(\frac{\tau}{N}k+\Delta_{ba}\right)}\times e^{2\pi i_a(\tau-1-\Delta_{ba}-\Delta_{ab})}\times \\ &\times e^{\pi i[(1-\tau)(1+N)+2(\Delta_{ba}+N\Delta_{ab})]} \\ &\equiv F(\Delta_{ab},\Delta_{ba},\tau)e^{2\pi i_a(\tau-1-\Delta_{ba}-\Delta_{ab})}. \end{aligned}$$

In (3.1.10) we have used the following properties of the θ_0 function:

$$\begin{aligned}\theta_0\left(u+n+m\tau;\tau\right) &= -e^{-2\pi miu-\pi im\tau(m-1)}\theta_0\left(u;\tau\right)\\ \theta_0\left(u;\tau\right) &= \theta_0\left(\tau-u;\tau\right) = -e^{2\pi iu}\theta_0\left(-u;\tau\right),\end{aligned} \tag{3.1.11}$$

and for the sake of compactness we have absorbed all the factors independent of i_a in the function $F(\Delta_{ab},\Delta_{ba},\tau)$. Inserting (3.1.10) back into (3.1.9) leads to multiplying all the results obtained in (3.1.10) for all n_a values of b connected with a via some field Φ_{ab} :

$$\begin{aligned}Q_{i_a}\left(u;\xi,\tau\right) &= e^{2\pi i\left(\sum_b \lambda_b-\sum_{j_b}\frac{\tau}{N}(i_a-j_b)\right)}F_a(\tau)e^{2\pi i_a\left[n_a(\tau-1)-\sum_{b=1}^{n_a}(\Delta_{ba}+\Delta_{ab})\right]}\\ \text{where } F_a(\tau) &\equiv \prod_{b=1}^{n_a}F(\Delta_{ab},\Delta_{ba},\tau)\\ \sum_{b=1}^{n_a}\left(\Delta_{ab}+\Delta_{ba}\right) &= \sum_{b=1}^{n_a}r_{ab}\tau\\ &\Downarrow\\ Q_{i_a}\left(u;\xi,\tau\right) &= e^{2\pi i\left(\sum_b \lambda_b-n_a\frac{\tau}{N}\left(Ni_a-\frac{N(N-1)}{2}\right)\right)}F_a(\tau)e^{2\pi i_a n_a(\tau-1)}\\ &= e^{2\pi i\left(\sum_b \lambda_b-n_a\tau\frac{N-1}{2}\right)}F_a(\tau)e^{-2\pi i_a n_a}.\end{aligned} \tag{3.1.12}$$

Upon a proper choice for the Lagrange multipliers we can ensure that:

$$Q_{i_a}\left(u;\xi,\tau\right) = e^{-2\pi i_a n_a} = 1\ \blacksquare. \tag{3.1.13}$$

3.1.1 Evaluation of the index

The formula for the SCI in terms of solutions to the BAEs (2.1.28) written in a notation suitable for $\mathcal{N}=1$ toric quiver gauge theories have the form:

$$\begin{aligned}\mathcal{I}\left(p,q;v\right) &= \kappa_G\sum_{\hat{u}\in\mathfrak{M}_{BAE}}\mathcal{Z}_{tot}\left(\hat{u};\xi,\nu_R,r\omega,s\omega\right)H\left(\hat{u};,\xi,\nu_R,\omega\right)^{-1}\\ \kappa_G &= \frac{(p;p)_\infty^{\mathrm{rk}(G)}\,(q;q)_\infty^{\mathrm{rk}(G)}}{|\mathcal{W}_G|}\\ \mathcal{Z}_{tot}\left(u;\xi,\nu_R,r\omega,s\omega\right) &= \sum_{\{m_{i_a}\}=1}^{rs}\mathcal{Z}\left(u-m\omega;\xi,\nu_R,r\omega,s\omega\right)\\ \mathcal{Z}\left(u;\xi,\nu_R,r\omega,s\omega\right) &= \frac{\prod_{\Phi_{ab}}\prod_{i_a\neq j_b}\widetilde{\Gamma}\left(u_{i_a}-u_{j_b}+\Delta_{ab};\tau,\sigma\right)}{\prod_{\alpha\in D}\widetilde{\Gamma}\left(\alpha\left(u\right);\tau,\sigma\right)}\\ H\left(u;\xi,\nu_R,\omega\right) &= \det\left[\frac{1}{2\pi i}\frac{\partial Q_{i_a}\left(u;,\xi,\nu_R,\omega\right)}{\partial u_{j_b}}\right]_{i_a j_b}.\end{aligned} \tag{3.1.14}$$

Dominant contributions to the index in the large N limit will come from terms analogous to those dominating the expression obtained in [38] for the $\mathcal{N}=4$ SYM theory. This implies that in order

to investigate the large N limit of (3.1.14), we only need to consider the following term:

$$\widetilde{\Gamma}\left(u_{ij}^{ab}+\Delta_{ab};\tau\right)=\frac{e^{-\pi i\mathcal{Q}\left(u_{ij}^{ab}+\Delta_{ab};\tau,\tau\right)}}{\theta_0\left(\frac{u_{ij}^{ab}+\Delta_{ab}}{\tau};-\frac{1}{\tau}\right)}\times\prod_{k=0}^{\infty}\frac{\psi\left(\frac{k+1+u_{ij}^{ab}}{\tau}\right)}{\psi\left(\frac{k-u_{ij}^{ab}-\Delta_{ab}}{\tau}\right)} \tag{3.1.15}$$

$$\begin{aligned}\mathcal{Q}\left(u;\tau,\sigma\right)&=\frac{u^3}{3\tau\sigma}-\frac{\tau+\sigma-1}{2\tau\sigma}u^2+\frac{\left(\tau+\sigma\right)^2+\tau\sigma-3\left(\tau+\sigma\right)+1}{6\tau\sigma}u+\frac{\left(\tau+\sigma-1\right)\left(\tau+\sigma-\tau\sigma\right)}{12\tau\sigma}\\ \mathcal{Q}\left(u+\Delta;\tau\right)&=\frac{u^3}{3\tau^2}+u^2\left(\frac{\Delta}{\tau^2}-\frac{2\tau-1}{2\tau^2}\right)+u\left(\frac{1-6\tau+5\tau^2}{6\tau^2}+\frac{\Delta^2}{\tau^2}-\frac{2\tau-1}{\tau^2}\Delta\right)-\\&-\frac{\Delta^2}{2\tau^2}\left(2\tau-1\right)+\frac{\Delta}{6\tau^2}\left(5\tau^2-6\tau+1\right)+\frac{1}{12\tau^2}\left(2\tau-1\right)\left(2\tau-\tau^2\right)+\frac{\Delta^3}{\tau^2}.\end{aligned}$$

We have set $p=q$, hence $\sigma=\tau$. Note that, the leading contribution coming from the vector multiplets can be obtained from (4.2.41) by setting $\Delta_{ab}=0$. In the large N limit we can write:

$$\log\mathcal{I}\big|_{\text{large }N}=\sum_{\Phi_{ab}}\sum_{i_a,j_b}\log\widetilde{\Gamma}\left(u_{ij}^{ab}+\Delta_{ab};\tau,\tau\right)\big|_{\text{large }N}-\sum_{\alpha\in D}\widetilde{\Gamma}\left(\alpha\cdot u,\tau,\tau\right)\big|_{\text{large }N}. \tag{3.1.16}$$

As a clarifying example, let us now analyze the case of $\mathcal{N}=4$ SYM theory, originally studied in [38] and perform the same calculation using toric data (recall that S^5 is a particular case of SE_5). The corresponding Φ_{ab} are the three chiral fields $\Phi_{1,2,3}$ appearing in the superpotential :

$$W=\text{Tr}\left(\Phi_1\left[\Phi_2,\Phi_3\right]\right), \tag{3.1.17}$$

with the associated chemical potentials being $\Delta_{1,2,3}$. According to our definition of the chemical potentials we have that, for the R-charge assignment used in [38]:

$$\begin{aligned}\Delta_{\Phi_1}&=\Delta_1,\\ \Delta_{\Phi_2}&=\Delta_2,\\ \Delta_{\Phi_3}&=2\tau-\Delta_1-\Delta_2.\end{aligned} \tag{3.1.18}$$

Using the identity:

$$\widetilde{\Gamma}\left(\Delta+2\tau;\tau\right)=\frac{1}{\widetilde{\Gamma}\left(-\Delta;\tau\right)}, \tag{3.1.19}$$

reduces (3.1.16) to the following expression:

$$\begin{aligned}\log\mathcal{I}(\tau;\Delta)\big|_{\text{Large }N}&=\sum_{i,j}\log\widetilde{\Gamma}\left(u_{ij}^1+\Delta_1;\tau\right)\big|_{\text{Large }N}+\log\widetilde{\Gamma}\left(u_{ij}^2+\Delta_2;\tau\right)\big|_{\text{Large }N}+\\&-\log\widetilde{\Gamma}\left(u_{ij}^3+\Delta_1+\Delta_2;\tau\right)\big|_{\text{Large }N}-\frac{i\pi N^2}{3\tau^2}\tau\left(\tau-\frac{1}{2}\right)\left(\tau-1\right)\\&=-\frac{i\pi N^2}{3\tau^2}\left(\left[\Delta_1\right]_\tau-\tau\right)\left(\left[\Delta_1\right]_\tau-\tau+\frac{1}{2}\right)\left(\left[\Delta_1\right]_\tau-\tau+1\right)-\\&-\frac{i\pi N^2}{3\tau^2}\left(\left[\Delta_2\right]_\tau-\tau\right)\left(\left[\Delta_2\right]_\tau-\tau+\frac{1}{2}\right)\left(\left[\Delta_2\right]_\tau-\tau+1\right)+\\&+\frac{i\pi N^2}{3\tau^2}\left(\left[\Delta_1+\Delta_2\right]_\tau-\tau\right)\left(\left[\Delta_1+\Delta_2\right]_\tau-\tau+\frac{1}{2}\right)\left(\left[\Delta_1+\Delta_2\right]_\tau-\tau+1\right)-\\&-\frac{i\pi N^2}{3\tau^2}\tau\left(\tau-\frac{1}{2}\right)\left(\tau-1\right).\end{aligned} \tag{3.1.20}$$

where $[\Delta_{ab}]_\tau$ is defined such that $[\Delta]_\tau = \Delta \mod 1$ [38] and depends on the region withing the domain of complex chemical potentials one is evaluating (this function can be precisely defined as $[\cdot]_\tau = \{\cdot\}_\tau - 1$ where $\{\cdot\}_\tau$ is defined in (A.13)). If $|\Delta_{ab}| < 1$, then :

$$\log \mathcal{I}(\tau;\Delta)\big|_{\text{Large } N} = -\frac{i\pi N^2}{\tau^2}\Delta_1\Delta_2\left(2\tau - \Delta_1 - \Delta_2 - 1\right), \tag{3.1.21}$$

which is indeed the necessary structure in order for the superconformal index of $\mathcal{N} = 4$ SYM to account for the entropy of the dual AdS_5 black hole [38].

Before proceeding to generic toric quiver gauge theories, let us comment on the choice of R-charge assignment, since one might expect a more symmetric one based on a-maximization. We notice that, if one chooses a set of chemical potentials and R-charges as the one used in [46], namely where $r_1 = r_2 = r_3 = \frac{2}{3}$, in contrast with the choice $r_1 = r_2 = 0,\ r_3 = 2$, then the use of identity (3.1.19) is not directly possible. This means that, if one starts with the data suggested by $a-$maximization [46] ($r_1 = r_2 = r_3 = \frac{2}{3}$), then (3.1.21) should be understood in terms of shifted chemical potentials that would permit some of the arguments of the elliptic gamma functions in (3.1.16) to have the structure $\Delta + 2\tau$ as needed in (3.1.19). Specifically , we have:

$$\begin{aligned}
\Delta_{\Phi_1} + \frac{2}{3}\tau &= \Delta_1 + \frac{2}{3}\tau = \left(\Delta_1 + \frac{2}{3}\tau\right) + \frac{2}{3}\tau - \frac{2}{3}\tau \to \Delta_1 \\
\Delta_{\Phi_2} + \frac{2}{3}\tau &= \Delta_2 + \frac{2}{3}\tau = \left(\Delta_2 + \frac{2}{3}\tau\right) + \frac{2}{3}\tau - \frac{2}{3}\tau \to \Delta_2 \\
\Delta_{\Phi_3} + \frac{2}{3}\tau &= -\Delta_1 - \Delta_2 + \frac{2}{3}\tau \to -\Delta_1 - \Delta_2 + 2\tau,
\end{aligned} \tag{3.1.22}$$

We can either interpret this as a suitable redefinition of the chemical potentials which does not affect the physical R-charge obtained via $a-$maximization or rather as a computation done directly with the more naive R-charge assignment used in [38]. Let us now explore more generically the consequences of shifting Δ_{ab} in such a way that the arguments of the elliptic gamma functions in (3.1.16) look either like Δ or $\Delta + 2\tau$. Suppose we do such a shift obtaining that a certain number, let us call this number n_s, of the total of n_χ chiral fields contributions to (3.1.16) are of the form $\Delta + 2\tau$. Thus, the leading contribution in N to $\log \mathcal{I}(\tau;\Delta)$ takes the form:

$$\begin{aligned}
\log \mathcal{I}(\tau;\Delta) &= -\frac{i\pi N^2}{3\tau^2}\sum_{\Phi_{ab}} s_{ab}\left([s_{ab}\Delta_{ab}]_\tau - \tau\right)\left([s_{ab}\Delta_{ab}]_\tau - \tau + \frac{1}{2}\right)\left([s_{ab}\Delta_{ab}]_\tau - \tau + 1\right) - \\
&- \frac{i\pi N^2}{3\tau^2}\sum_{\text{v}} \tau\left(\tau - \frac{1}{2}\right)(\tau - 1) \\
&= -\frac{i\pi N^2}{3\tau^2}\sum_{\Phi_{ab}} s_{ab}\left[[s_{ab}\Delta_{ab}]_\tau\left([s_{ab}\Delta_{ab}]_\tau + \frac{1}{2}\right)\left([s_{ab}\Delta_{ab}]_\tau + 1\right) - 3\tau\left[s_{ab}\Delta_{ab}\right]_\tau^2\right] - \\
&- \frac{i\pi N^2}{3\tau^2}\sum_{\Phi_{ab}} s_{ab}\left[3\tau^2\left[s_{ab}\Delta_{ab}\right]_\tau - 3\tau\left[s_{ab}\Delta_{ab}\right]_\tau\right] + \\
&+ \frac{i\pi N^2}{3\tau^2}\left(n_\chi - 2n_s - n_{\text{v}}\right)\tau\left(\tau - \frac{1}{2}\right)(\tau - 1).
\end{aligned} \tag{3.1.23}$$

The sum $\sum_{\rm v}$ is carried over the $n_{\rm v}$ vector multiplets and n_χ is the number of chiral fields , s_{ab} is 1 if Φ_{ab} effectively has R-charge 0 and -1 if it has R-charge 2 with a new set of chemical potentials. Conservation of $U(1)$ charges implies $\sum_{\Phi_{ab}} [\Delta_{ab}]_\tau = 0$, which allows us to eliminate every linear term in $[\Delta_{ab}]_\tau$ appearing in (3.1.23), therefore we can write:

$$\begin{aligned}\log \mathcal{I}(\tau;\Delta) = &-\frac{i\pi N^2}{3\tau^2}\sum_{\Phi_{ab}} s_{ab} K\left(s_{ab}\left[\Delta_{ab}\right]_\tau,\tau\right)+ \\ &+\frac{i\pi N^2}{3\tau^2}\left(n_\chi-2n_s-n_{\rm v}\right)\tau\left(\tau-\frac{1}{2}\right)(\tau-1)\,,\end{aligned} \tag{3.1.24}$$

where we have defined

$$\begin{aligned}K(\Delta,\tau) &\equiv [\Delta]_\tau\left([\Delta]_\tau+\frac{1}{2}\right)\left([\Delta]_\tau+1\right)-3\tau\,[\Delta]_\tau^2 \\ &= \frac{1}{2}\left(2\Delta^3-3|\Delta|\Delta+\Delta-6\tau|\Delta|\Delta\right)\end{aligned} \tag{3.1.25}$$

Recalling that:

$$\begin{aligned}[\Delta+1]_\tau &= [\Delta]_\tau\,,\\ [-\Delta]_\tau &= -[\Delta]_\tau-1,\\ [\Delta+\tau]_\tau &= [\Delta]_\tau+\tau,\end{aligned} \tag{3.1.26}$$

then (3.1.25) holds when $|\Delta|<1$.

Let us now analyze the properties of the function we have obtained. Equation (3.1.24) is very similar to the one obtained in [46] when analyzed in the Cardy-like limit of the index, however, there is an extra contribution of the form $\frac{i\pi N^2}{3\tau^2}\left(n_\chi-2n_s-n_{\rm v}\right)\tau\left(\tau-\frac{1}{2}\right)(\tau-1)$ which is still of order $\mathcal{O}(N^2)$ but sub-leading when $\tau\to 0$. Notice that at this point there is no dependence on the holonomies of the gauge groups since we have already evaluated in the solutions of the BAEs. We still need to determine if we can find a consistent way of redefining the chemical potentials, thus fixing the value of n_s and s_{ab}. The shifting has to preserve the R- charge of the superpotential which is ensured by the constrain:

$$\sum_{(ab)\in A}\Delta_{ab}=2\tau, \tag{3.1.27}$$

where A denotes monomial terms of the superpotential W. Let us call n_W the number of elements in A. Using the fact that for these toric quiver gauge theories each chiral field appears only once in exactly two terms in the superpotential, then (3.1.27) implies that $2n_s=n_W$.

To gain a better understanding of the implications that shifting the chemical potentials has on the SCI of a toric quiver gauge theory let us consider:

$$\mathcal{I}(\tau;\Delta) = \mathrm{Tr}_{\mathcal{H}(S^1\times S^3)}\,(-1)^F\,e^{-\beta H}e^{2\pi i 2\tau\left(J+\frac{1}{d}\sum_{I=1}^{d}Q_d\right)}e^{2\pi i\sum_{k=1}^{d-1}\Delta_k(Q_k-Q_d)}, \tag{3.1.28}$$

where we have used the same basis for the non R-global symmetries defined in section 2.2.7. Shifting the chemical potentials as

$$\Delta_k\to\Delta_k-\frac{2\tau}{d}\quad\text{with } k=1,\cdots,d-1, \tag{3.1.29}$$

allows us to rewrite the index as

$$\mathcal{I}(\tau;\Delta) = \mathrm{Tr}_{\mathcal{H}(S^1\times S^3)}\,(-1)^F\, e^{2\pi i(\sum_{I=1}^{d}\Delta_I - 2\tau)Q_d} e^{-\beta H} e^{2\pi i 2\tau J} e^{2\pi i\sum_{k=1}^{d-1}\Delta_k Q_k}. \tag{3.1.30}$$

Exploiting the constraint

$$\sum_{I=1}^{d}\Delta_I - 2\tau = \pm 1, \tag{3.1.31}$$

and identifying $e^{2\pi i Q_d} = (-1)^F$ allows us to express the SCI in such a way that bosonic-fermionic cancellations are optimally obstructed:

$$\mathcal{I}(\tau;\Delta) = \mathrm{Tr}_{\mathcal{H}(S^1\times S^3)} e^{-\beta H} e^{2\pi i 2\tau J} e^{2\pi i\sum_{k=1}^{d-1}\Delta_k Q_k}. \tag{3.1.32}$$

Therefore, the shifting (3.1.29) which is dictated by the geometry of the toric diagram, in particular by its number of vertices, turns out to be the adequate one in order to reproduce the dual black hole entropy. Upon implementation of the shifting (3.1.29), we obtain:

$$\Delta_{ab} \to \bar{\xi}_{ab} + 2\tau d_{ab}, \qquad \bar{\xi}_{ab} \equiv \sum_{k=1}^{d-1} Q_k^{ab}\Delta_k, \tag{3.1.33}$$

where

$$d_{ab} = \begin{cases} 1 & \text{for } \sum_{k=1}^{d-1} Q_k^{ab} < 0 \\ 0 & \text{for } \sum_{k=1}^{d-1} Q_k^{ab} \geq 0. \end{cases} \tag{3.1.34}$$

To define d_{ab} we are using the fact that, for a given chiral multiplet Φ_{ab}, $\mathrm{sign}(Q_k^{ab}) = \mathrm{sign}(Q_l^{ab})$, $\forall\ k,l = 1,\cdots,d-1$ which is the main property of the global charges that we will need during our calculations. In this way, we can define $s_{ab} \equiv (-1)^{d_{ab}}$.

Finally, recalling that we are dealing with toric quivers, which can be drawn on a torus providing a polygonalization of the torus as we discussed in chapter 2, we can sue Euler's relation (2.2.58) to argue that the term purely depending on τ vanishes:

$$\begin{aligned} \log\mathcal{I}(\tau;\Delta) &= -\frac{i\pi N^2}{3\tau^2}\sum_{\Phi_{ab}}(-1)^{d_{ab}}\,K\left((-1)^{d_{ab}}\,\Delta_{ab},\tau\right) \\ &+ \frac{i\pi N^2}{3\tau^2}\,(n_\chi - n_W - n_{\mathrm{v}})\,\tau\left(\tau-\frac{1}{2}\right)(\tau-1) \\ &= -\frac{i\pi N^2}{3\tau^2}\sum_{\Phi_{ab}}(-1)^{d_{ab}}\,K\left((-1)^{d_{ab}}\,\Delta_{ab},\tau\right). \end{aligned} \tag{3.1.35}$$

Defining Δ_d such that: $\sum_{I=1}^{d}\Delta_I - 2\tau = -1$ [38], it can be shown that $\log\mathcal{I}(\tau;\Delta)$ can be written as:

$$\log\mathcal{I}(\tau;\Delta) = -\frac{i\pi N^2}{6\tau^2} C_{IJK}\Delta_I\Delta_J\Delta_K. \tag{3.1.36}$$

The coefficients C_{IJK} in (3.1.36) correspond, as pointed out originally in [53] and later in [46], to the Chern-Simons couplings of the holographic dual gravitational description as elucidated in [54] (see equation (2.3.4)). In the following section we proceed to evaluate the superconformal index for various models, some of them recently discussed in a similar context in [46], and compare our results with (3.1.36).

3.2 The superconformal index of various $\mathcal{N}=1$ toric quiver gauge theories

We will apply our general result (3.1.36) in various cases in each of which we follow the prescription of charge assignment used in [46]. Indeed, below we will see that in order to obtain (3.1.36) all the chemical potentials have to be shifted by $-\frac{2\tau}{d}$, exactly like [46]. We will restrict ourselves to the regime of chemical potentials Δ_i of the $d-1$ $U(1)$ global symmetries such that:

$$0 \leq |\Delta_k| \leq \frac{1}{2} \ \forall k, \ \ 0 \leq \sum_{k=1}^{d-1} |\Delta_k| \leq 1, \tag{3.2.1}$$

which is inside the fundamental domain:

$$\text{Im}\left(-\frac{1}{\tau}\right) > \text{Im}\left(\frac{\sum_{k=1}^{d-1}[\Delta_k]_\tau}{\tau}\right) > 0, \tag{3.2.2}$$

which in our case will be useful to evaluate the function $K(\Delta,\tau)$ using equation (4.1.46). The region (3.2.2) has been highlighted in figure 16 in gray. This regime also coincides with the one in which the existence of a universal saddle point in which all the holonomies vanish according to the analysis carried in [46], can be ensured.

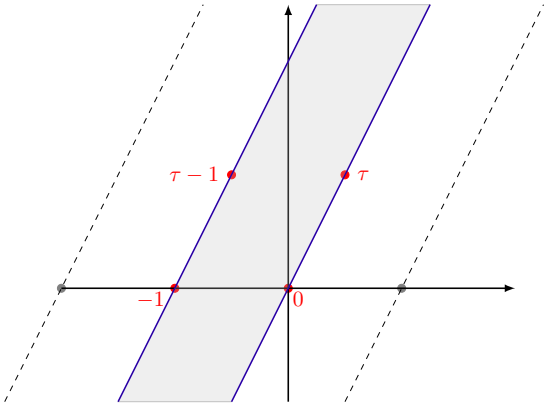
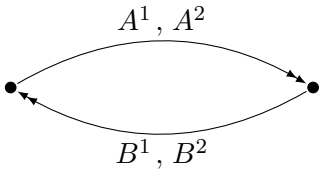


Figure 16: The figure shows the complex plane of chemical potentials for a generic Δ where the region specified by (3.2.2) is shown in gray.

Let us first warm up by studying simple cases and then we move on to generic toric quiver gauge theories, namely $Y^{p,q}$, $X^{p,q}$ and $L^{a,b,c}$. At the risk of some abuse of terminology, we will label the toric quiver gauge theory with the name of the SE_5 manifold associated to the dual description.

3.2.1 The conifold theory

We would like to study the index in the large N limit and thus investigate it beyond the Cardy-like limit. To do so we start with one of the simplest examples of toric quiver gauge theories - the conifold theory [81] which corresponds to $Y^{1,0}$- whose quiver diagram is given below.



The superpotential is

$$W \propto \epsilon_{ij}\epsilon_{kl}\mathrm{Tr}\left[A^i B^k A^j B^l\right]. \tag{3.2.3}$$

The global charges of the conformal field theory are: a $U(1)_R$ factor, two $SU(2)$ factors and finally there is a $U(1)_B$ baryonic symmetry. A fascinating fact about this theory is that it admits a gravity dual in terms of strings in $\mathrm{AdS}_5 \times T^{1,1}$. The isometries of $T^{1,1}$ realize the mesonic symmetries of the field theory in terms of the isometries of $\mathbb{CP}^1 \times \mathbb{CP}^1$; the $U(1)_B$ baryonic symmetry is associated to the unique non-trivial three-cycle of the geometry. It is worth pointing out that the rotating electrically charged black holes dual to the superconformal index have not yet been constructed on the supergravity side, and that remains an outstanding problem.

We use the basis for the charges suggested by the toric diagram discussed in chapter 2 and we summarize them in the following table:

Field	$U(1)_R$	$U(1)_1$	$U(1)_2$	$U(1)_3$
A_1	1/2	1	0	0
A_2	1/2	0	0	1
B_1	1/2	0	1	0
B_2	1/2	-1	-1	- 1

Table 4: Charge assignment and fields for the conifold theory.

Table 4 is a particular case of table 1 where we have assigned symmetric values to r_I and $F_I^{(k)}$ such that they satisfy the constraints (2.2.59) and (2.2.60) respectively. We will follow the same criteria to assign charges in the remainder of this manuscript.

After performing the shifting $\Delta_{1,2,3} \to \Delta_{1,2,3} - \frac{\tau}{2}$, we are ready to evaluate equation (3.1.36):

$$\begin{aligned}\log \mathcal{I}(\tau;\Delta) &= -\frac{i\pi N^2}{3\tau^2}\left[K\left(\Delta_1,\tau\right)+K(\Delta_2,\tau)+K(\Delta_3,\tau)-K\left(-(-\Delta_1-\Delta_2-\Delta_3),\tau\right)\right] \\ &= -\frac{i\pi N^2}{\tau^2}\left[-\Delta_1^2\left(\Delta_2+\Delta_3\right)-\Delta_2\Delta_3\left(1-2\tau+\Delta_2+\Delta_3\right)-\Delta_1\left(\Delta_2+\Delta_3\right)\left(1-2\tau+\Delta_2+\Delta_3\right)\right].\end{aligned} \tag{3.2.4}$$

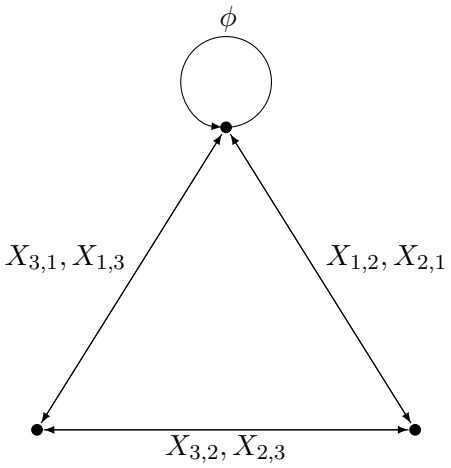
After imposing the condition $\sum_{I=1}^{d}\Delta_I - 2\tau = -1$ yields :

$$\log \mathcal{I}(\tau;\Delta) = -\frac{i\pi N^2}{\tau^2}\left[\Delta_2\Delta_3\Delta_4+\Delta_1\Delta_3\Delta_4+\Delta_1\Delta_2\Delta_3+\Delta_1\Delta_2\Delta_4\right]. \tag{3.2.5}$$

We see that $\log \mathcal{I}(\tau;\Delta)$ presents the behavior proposed in (3.1.36).

3.2.2 The Suspended Pinch Point

The suspended pinch point (SPP) gauge theory corresponds to the near horizon limit of a stack of N $D3$ branes probing the tip of the conical singularity , $x^2y = wz$. The SPP gauge theory is an example of a $X^{p,p}$ theory, specifically $X^{1,1}$, since it can be Higgsed either to obtain the conifold theory discussed before ($Y^{1,0}$) or $\mathbb{C}^3/\mathbb{Z}_2$ (which corresponds to $Y^{1,1}$). The associated quiver is the following:



The superpotential is

$$W_{\text{SPP}} = X_{1,2}X_{2,3}X_{3,2}X_{2,1} - X_{2,3}X_{3,1}X_{1,31}X_{3,2} + X_{1,3}X_{3,1}\phi - X_{1,2}X_{2,1}\phi. \tag{3.2.6}$$

Each $X_{i,j}$ transforms in the $\mathbf{N}$ representation of the index i-th node and in the $\overline{\mathbf{N}}$ of the j-th node. The field ϕ transforms in the adjoint representation of the corresponding gauge group. The charge assignment for the $U(1)_R$ and the extra $U(1)_k$ global symmetries can be taken as:

Field	$U(1)_R$	$U(1)_1$	$U(1)_2$	$U(1)_3$	$U(1)_4$
ϕ	4/5	1	1	0	0
$X_{1,2}$	2/5	0	0	0	1
$X_{2,1}$	4/5	-1	-1	0	-1
$X_{2,3}$	2/5	0	1	0	0
$X_{3,2}$	2/5	1	0	0	0
$X_{3,1}$	4/5	- 1	-1	-1	0
$X_{1,3}$	2/5	0	0	1	0

Table 5: Charge assignment and fields associated to the Suspended Pinched Point theory.

We shift now the chemical potentials $\Delta_{1,2,3,4} \to \Delta_{1,2,3,4} - \frac{2\tau}{5}$. The next step is to use this

information and perform the evaluation (3.1.36).

$$\begin{aligned}\log\mathcal{I}(\tau;\Delta) &= -\frac{i\pi N^2}{3\tau^2}[K\left(\Delta_1+\Delta_2,\tau\right)+K(\Delta_4,\tau)-K(-(-\Delta_1-\Delta_2-\Delta_4),\tau) \qquad (3.2.7)\\ &+ K\left(\Delta_2,\tau\right)+K(\Delta_1,\tau)-K(-(-\Delta_1-\Delta_2-\Delta_3),\tau)+K(\Delta_4,\tau)]\\ &= -\frac{i\pi N^2}{\tau^2}[-\Delta_1^2\left(\Delta_2+\Delta_3+\Delta_4\right)\\ &+ \Delta_1\left((1-2\tau+\Delta_2+\Delta_3)(-\Delta_2-\Delta_3)+(2\tau-1-2\Delta_2)\Delta_4-\Delta_4^2\right)+ \qquad (3.2.8)\\ &+ \Delta_2\left((1-2\tau+\Delta_2)\Delta_3+\Delta_3^2+\Delta_4(1-2\tau+\Delta_2+\Delta_4)\right)].\end{aligned}$$

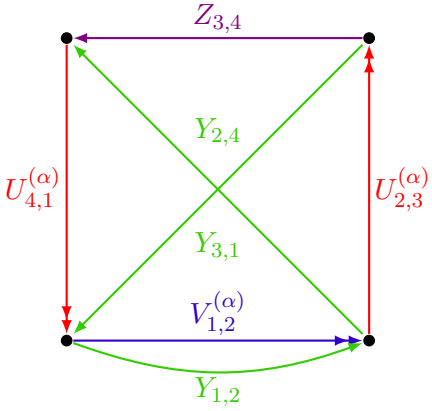
Now we use: $\sum_{I=1}^{5}\Delta_I-2\tau=-1$ we introduce a fifth fugacity Δ_5 that permits us to rewrite (3.2.7) in the following, more symmetric, way:

$$\begin{aligned}\log\mathcal{I}(\tau;\Delta) &= -\frac{i\pi N^2}{\tau^2}[2\Delta_2\Delta_3\Delta_4+\Delta_2\Delta_3\Delta_5+\Delta_2\Delta_4\Delta_5+2\Delta_1\Delta_3\Delta_4+\Delta_5\Delta_3\Delta_2 \qquad (3.2.9)\\ &+ \Delta_1\Delta_4\Delta_5+\Delta_1\Delta_2\Delta_3+\Delta_1\Delta_2\Delta_4+\Delta_1\Delta_2\Delta_5].\end{aligned}$$

This result is in agreement with equation (3.1.36) which is what is expected from toric geometry and reinforces the validity of the analysis of [46] which was limited to the Cardy-Like limit.

3.2.3 The dP$_1$ theory

We consider now the theory arising from a stack of N $D3$ branes at the tip of the complex Calabi-Yau cone whose base is the first del Pezzo surface. The quiver associated to this theory is :



and the superpotential is given by:

$$W_{d\mathbf{P}_1} = \epsilon_{\alpha\beta}\left(U_{2,3}^{(\alpha)}Y_{3,1}V_{2,1}^{(\beta)}-U_{4,1}^{(\alpha)}V_{1,2}^{(\beta)}Y_{2,4}+Y_{1,2}U_{2,3}^{(\alpha)}Z_{3,4}U_{4,1}^{(\beta)}\right). \qquad (3.2.10)$$

The charge assignment specified by the toric data is presented in table 6.

Let us perform the following transformation of the chemical potentials $\Delta_{1,2,3}\to\Delta_{1,2,3}-\frac{\tau}{2}$. Evaluating to leading order in N part of the SCI according to (3.1.36) :

$$\begin{aligned}\log\mathcal{I}(\tau;\Delta) &= -\frac{i\pi N^2}{3\tau^2}[2K(\Delta_1,\tau)+K\left(\Delta_3,\tau\right)+2K(\Delta_2,\tau) \qquad (3.2.11)\\ &- 2K\left(-(-\Delta_1-\Delta_2-\Delta_3),\tau\right)+K(\Delta_2+\Delta_3,\tau)-K(-(-\Delta_1-\Delta_2),\tau)]\\ &= -\frac{i\pi N^2}{\tau^2}[-(2\Delta_1+\Delta_2)\Delta_3^2-3\Delta_1\Delta_2(\Delta_1+\Delta_2+1)\\ &- \left(\Delta_2^2+4\Delta_1\Delta_2+\Delta_2+2\Delta_1(\Delta_1+1)\right)\Delta_3+\tau(6\Delta_1\Delta_2+2(2\Delta_1+\Delta_2)\Delta_3].\end{aligned}$$

Field	$U(1)_R$	$U(1)_1$	$U(1)_2$	$U(1)_3$
$Y_{1,2}$	1/2	0	0	1
$U^{(1)}_{2,3}$	1/2	0	1	0
$U^{(2)}_{2,3}$	1/2	-1	- 1	-1
$X^{(1)}_{4,1}$	1	0	1	1
$X^{(2)}_{4,1}$	1	-1	-1	0
$Z_{3,4}$	1/2	1	0	0
$V^{(1)}_{1,2}$	1/2	0	1	0
$V^{(2)}_{1,2}$	1/2	-1	- 1	- 1
$Y_{3,1}$	1/2	1	0	0
$Y_{2,41}$	1/2	1	0	0

Table 6: Charge assignment and fields of the $d\mathbf{P}_1$ theory, which corresponds to $Y^{2,1}$.

Introducing now Δ_4 via the constraint $\Delta_1+\Delta_2+\Delta_3+\Delta_4-2\tau=-1$ we obtain:

$$\log\mathcal{I}(\tau;\Delta)=-\frac{i\pi N^2}{\tau^2}[2\Delta_1\Delta_2\Delta_3+3\Delta_1\Delta_2\Delta_4+2\Delta_1\Delta_3\Delta_4+2\Delta_2\Delta_3\Delta_4], \tag{3.2.12}$$

which coincides with the expectation (3.1.36).

3.2.4 $Y^{p,q}$ quiver gauge theories

The $Y^{p,q}$ model, as discussed in chapter 2, corresponds to quiver gauge theories with $2p$ gauge groups and a chiral field content of bi-fundamental fields. The charge assignment and the corresponding multiplicity of the fields are shown below:

Multiplicity	$U(1)_1$	$U(1)_2$	$U(1)_3$	$U(1)_R$
$p+q$	1	0	0	1/2
p	0	1	0	1/2
$p-q$	0	0	1	1/2
p	-1	-1	-1	1/2
q	0	1	1	1
q	-1	-1	0	1

Table 7: Charge assignment and multiplicities for $Y^{p,q}$ theory.

We proceed to perform the shifting of chemical potentials as follows: $\Delta_{1,2,3}\to\Delta_{1,2,3}-\frac{\tau}{2}$. Now we evaluate the leading, order $\mathcal{O}(N^2)$, part of the SCI (3.1.36):

$$\begin{aligned}\log\mathcal{I}(\tau;\Delta)=&-\frac{i\pi N^2}{3\tau^2}[(p+q)K\left(\Delta_1,\tau\right)+pK\left(\Delta_2,\tau\right)+(p-q)K\left(\Delta_3,\tau\right)\\&-pK\left(-(-\Delta_1-\Delta_2-\Delta_3),\tau\right)+qK\left(\Delta_2+\Delta_3,\tau\right)-qK\left(-(-\Delta_1-\Delta_2),\tau\right)]\\=&-\frac{i\pi N^2}{3\tau^2}[\Delta_2(\Delta_1-\Delta_3)(-q)(\Delta_1+\Delta_2+\Delta_3-2\tau+1)\\&-p\left((\Delta_2+\Delta_3\Delta_1^2+(\Delta_2+\Delta_3\Delta_1(\Delta_2+\Delta_3-2\tau+1)+\Delta_2\Delta_3(\Delta_2+\Delta_3-2\tau+1)\right)].\end{aligned} \tag{3.2.13}$$

Finally we eliminate τ from (3.2.15) using $\sum_{I=1}^{4}\Delta_I - 2\tau = -1$, which successfully reproduce the structure of (3.1.36):

$$\log\mathcal{I}(\tau;\Delta) = -\frac{i\pi N^2}{3\tau^2}[p\Delta_1\Delta_2\Delta_3 + (p+q)\Delta_1\Delta_2\Delta_4 + p\Delta_1\Delta_3\Delta_4 + (p-q)\Delta_2\Delta_3\Delta_4]. \quad (3.2.14)$$

3.2.5 The $X^{p,q}$ theories

As we saw in section 2.2 the $X^{p,q}$ theories have $2p+1$ gauge groups and has the following charge assignment:

Multiplicity	$U(1)_1$	$U(1)_2$	$U(1)_3$	$U(1)_4$	$U(1)_R$
$p+q-1$	1	0	0	0	2/5
1	0	1	0	0	2/5
1	0	0	1	0	2/5
$p-q$	0	0	0	1	2/5
p	-1	-1	-1	-1	2/5
$p-1$	0	1	1	0	4/5
1	0	0	1	1	4/5
$q-1$	0	1	1	1	6/5
1	1	1	0	0	4/5
q	-1	-1	-1	0	4/5

Table 8: Charge assignment and multiplicities for $X^{p,q}$ theory.

We now implement the shifting of chemical potentials as follows: $\Delta_{1,2,3,4} \to \Delta_{1,2,3,4} - \frac{2\tau}{5}$. Now we evaluate the leading, order $\mathcal{O}(N^2)$, part of the SCI (3.1.36):

$$\begin{aligned}\log\mathcal{I}(\tau;\Delta) = -\frac{i\pi N^2}{3\tau^2}[&(p+q-1)K(\Delta_1,\tau) + K(\Delta_2,\tau) + K(\Delta_3,\tau) \\ &+ (p-q)K(\Delta_4,\tau) - pK(-(-\Delta_1-\Delta_2-\Delta_3-\Delta_4),\tau) \\ &+ (p-1)K(\Delta_2+\Delta_3,\tau) + K(\Delta_3+\Delta_4,\tau) \\ &+ (q-1)K(\Delta_2+\Delta_3+\Delta_4,\tau) + K(\Delta_1+\Delta_2,\tau) - qK(-(-\Delta_1-\Delta_2-\Delta_3),\tau)],\end{aligned} \quad (3.2.15)$$

which yields:

$$\begin{aligned}\log\mathcal{I}(\tau;\Delta) = -\frac{i\pi N^2}{3\tau^2}\,&[(p+q)\Delta_1\Delta_3\Delta_5 + (p-q)\Delta_3\Delta_4\Delta_5 + (p+q-1)\Delta_1\Delta_2\Delta_5 + (p-q+1)\Delta_2\Delta_4\Delta_5 \\ &+p\Delta_1\Delta_4\Delta_5 + p\Delta_1\Delta_3\Delta_4 + p\Delta_1\Delta_2\Delta_4 + \Delta_1\Delta_2\Delta_3 + \Delta_2\Delta_3\Delta_4 + 2\Delta_2\Delta_3\Delta_5]\,.\end{aligned} \quad (3.2.16)$$

Again we have defined $\Delta_5 = -1 + 2\tau - \sum_{I=1}^{4}\Delta_I$.

3.2.6 The $L^{a,b,c}$ theories

The relevant data for this theory, which we discussed in section 2.2, can be summarized in the following table:

Multiplicity	$U(1)_1$	$U(1)_2$	$U(1)_3$	$U(1)_R$
b	1	0	0	1/2
$a+b-c$	0	1	0	1/2
a	0	0	1	1/2
c	-1	-1	-1	1/2
$c-a$	0	1	1	1
$b-c$	-1	-1	0	1

Table 9: Charge assignment and multiplicities for $L^{a,b,c}$ theory.

Similarly to the case of $Y^{p,q}$, upon shifting $\Delta_{1,2,3} \to \Delta_{1,2,3} - \frac{\tau}{2}$ we have:

$$\begin{aligned}\log \mathcal{I}(\tau;\Delta) = -\frac{i\pi N^2}{3\tau^2}\left[bK\left(\Delta_1,\tau\right) + (a+b-c)K\left(\Delta_2,\tau\right) + aK\left(\Delta_3,\tau\right)\right.\\ \left. - cK\left(-(-\Delta_1-\Delta_2-\Delta_3),\tau\right) + (c-a)K\left(\Delta_2+\Delta_3,\tau\right) - (b-c)K\left(-(-\Delta_1-\Delta_2),\tau\right)\right],\end{aligned} \tag{3.2.17}$$

which, if we introduce $\Delta_4 = -\sum_{I=1}^{3}\Delta_I + 2\tau - 1$, can be simplified into:

$$\log \mathcal{I}(\tau;\Delta) = -\frac{i\pi N^2}{3\tau^2}\left[(a+b-c)\Delta_1\Delta_2\Delta_3 + a\Delta_2\Delta_3\Delta_4 + b\Delta_1\Delta_2\Delta_4 + c\Delta_1\Delta_3\Delta_4\right]. \tag{3.2.18}$$

3.3 Conclusions I

In this chapter we have explored the superconformal index of a large class of $\mathcal{N}=1$ toric quiver gauge theories. We have shown that a class of solutions can be extended to solve the BAEs for a large class of 4d $\mathcal{N}=1$ supersymmetric gauge theories. The BA approach that we have followed has the advantage that it does not require to take the Cardy-like limit and therefore provides a more complete large N expression. Indeed, for generic toric quiver gauge theories we determined that there is a region in the space of chemical potentials in which the $\mathcal{O}(N^2)$ result obtained in the Cardy-like limit can be recovered buttressing previous results in the literature [44–46].

By exploiting the BA approach to the topologically twisted index a systematic study of $1/N$ corrections for the ABJM index was performed in [109]. A similar study for a Chern-Simons matter theory dual to massive IIA black holes was reported in [110]. Such understanding of $1/N$ corrections will naturally translate into interesting aspects in the dual quantum gravity side for AdS_5 black holes. For example, the statistical entropy of certain magnetically charged AdS_4 black holes has recently been given a microscopic explanation in terms of the topologically twisted index [28] (see [111, 112] for a reviews with comprehensive lists of references). The investigation of sub-leading (logarithmic in N) corrections such as those performed recently [113–115] have helped clarify the nature of the degrees of freedom on the gravitational side of the duality. One would hope for similar developments in the context of AdS_5 black holes. Indeed, we will elaborate on this subject in the next chapter.

We have focused on the case of equal fugacities associated to angular momentum in the work [69] which shed some light on the inner workings of the evaluation of the SCI. In this chapter we

have completely avoided the subtle discussion concerning the space of solutions of the BAEs, we limited ourselves to just one class and showed that it yields a contribution sufficient to extract the dual black hole entropy and its potential corrections in the appropriate domain of chemical potentials. It would be very illuminating to have a better understanding of all the solutions and how one should weight their contributions to the index.

Finally, it is an important open problem to construct explicitly the black holes dual to the field theories discussed in this thesis. Our computation, as well as those in a number of recent publications [44–46], show that it is relatively easy to estimate the superconformal index in a large class of supersymmetric four-dimensional field theories some of which have known supergravity dual. Moreover, using $\log \mathcal{I}$ one can implement the Legendre transform of the entropy function and realize that it corresponds to that of large black holes in AdS_5. However, the explicit black hole construction on the gravity side is still in its infancy, not much is known beyond the AdS_5 black holes dual to $\mathcal{N} = 4$ SYM (and some of its orbifolds). It remains an outstanding challenge for the supergravity community to explicitly construct rotating electrically charged black holes which could be understood as dual of available field theory results. One particular example that comes to mind among the class discussed in this chapter would be the black holes in asymptotically $AdS_5 \times T^{1,1}$ and, more generally, $AdS_5 \times Y^{p,q}$.

CHAPTER 4

Logarithmic contribution to the SCI and underlying Chern-Simons matrix model

In this chapter we concentrate on systematically studying the SCI both from the BA approach and the saddle point approximation to evaluate the integral expression for SCI. Specifically, we keep track of logarithmic corrections in the rank of the gauge group and refine the Cardy-like limit computations by finding all perturbative corrections in inverse powers of the angular velocity. One of our key findings is the appearance of a matrix model associated to 3d Chern-Simons theory which can be solved exactly and uncovers a rich structure of sub-leading saddles.

Let us now precisely declare the two paths we follow to evaluate the SCI (2.1.8):

a) The saddle point method can be used to approximate $\mathcal{I}(p = q; v)$ provided we have a large control parameter. This is, in fact, the method pursued in various works [37, 42–46], where the evaluation was performed in the Cardy-like limit $q \to 1$ [8]. A different version of the saddle-point approach was applied in references [116, 117] where an Elliptic extension of the integrand in (2.1.8) was proposed as an alternative to the more common analytic extension.

b) One can evaluate the complex integral using the residue theorem and exploiting the properties of the pole structure of the integrand. This is the so-called BA approach which we have applied in chapter 3.

Approach *a*) provides, by definition, an approximate answer while approach *b*) is designed to yield an exact evaluation of the integral (2.1.8). There is, however, a catch in using the BA approach. As we have reviewed in section 2.1.2, the BA approach reduces the problem of evaluating (2.1.8) to the problem of finding *all solutions* of the Bethe-Ansatz Equations (BAEs). For the important question of matching the black hole entropy it has been sufficient to utilize a particular set of solutions to the BAEs. It is precisely in this sense that not *all BA solutions* have been used to evaluate $\mathcal{I}(p, q; v)$ that we talk about a BA truncation.

4.1 Saddle-point approach to the SCI

The classical gravity regime where the Bekenstein-Hawking entropy of the rotating, electrically charged, asymptotically AdS_5 black hole is known to correspond, on the field theory side, to the large-N regime. This situation motivates the study of the SCI in the large-N limit. Having an integral expression for the SCI of the form $\mathcal{I} \sim \int [du] \exp\big(N^2 S_{\text{eff}}(u_{ij})\big)$ (see (2.1.4) and (2.1.13)) makes it suitable for a saddle point evaluation. The pairwise nature of the full effective action, however, prevents us from directly applying standard matrix models techniques. Recall that standard matrix model effective actions have a typically attractive potential depending only on the matrix eigenvalues, thus playing the role of an external source and a Vandermonde-like repulsive term which is pairwise, specifically: $S_{\text{eff}}(u) = V_{\text{external}}(u_i) + W_{\text{pairs}}(u_{ij})$, such that the two terms V_{external} and W_{pairs} compete until the eigenvalues u_i stabilize in the equilibrium configuration [118] (For a pedagogical introduction and comprehensive list of reference see for example [119]). In contrast, for the SCI we have an effective action where V_{external} is absent, thus it is purely pairwise interaction $W_{\text{pairs}}(u_{ij})$. This structure resembles the so-called frustrated systems appearing in condensed matter. For these systems the building blocks of the full interaction term compete among themselves yielding structurally rich set of vacua and, consequently, a plethora of new phenomena

[8] Other ways of implementing the Cardy-like limit has been used in [59] where $q \to$ roots of unity.

[120]. Precisely because such frustrated systems have several equilibrium configurations beyond the dominant one, the application of saddle-point approaches becomes inefficient. Indeed, we found various such subdominant configurations when analyzing the SCI numerically in terms of elliptic gamma functions. It would be interesting to understand if there is a deeper and more explicit connection between the SCI and frustrated systems.

In [116, 117], the authors proposed to circumvent the difficulties of having only pairwise interaction by introducing an elliptic extension of the SCI. Such extensions exploit the central fact that W_{pairs} have saddle points configurations consisting of eigenvalues u_i uniformly distributed along the periodic directions of the interaction term.

The Cardy-like limit has resolved the question of saddle-points by simplifying the analysis of the SCI to a limit where it is easy to find the dominant saddle-point configuration. In our systematic Cardy-like expansion, we effectively depart from the leading Cardy-like limit in a way that automatically eliminates the pairwise nature of the effective potential. In this process we uncover an interesting connection with an effective $SU(N)$ Chern-Simons theory on S^3.

With these ideas in mind, we proceed to compute the index using the conventional saddle-point approach. For simplicity we start with $\mathcal{N}=4$ SYM and compute the corresponding index (2.1.14). Then we move on to a generic $\mathcal{N}=1$ SCFT and compute the corresponding index (2.1.13).

4.1.1 Saddle point approximation for $\mathcal{N}=4$ SYM

To compute the integral in (2.1.14) using the conventional saddle point approach, we introduce an effective action $S_{\text{eff}}(\hat{u};\Delta,\tau)$ as

$$\begin{aligned} N^2 S_{\text{eff}}(\hat{u};\Delta,\tau) = \sum_{i\neq j}\left(\sum_{a=1}^{3}\log\widetilde{\Gamma}(u_{ij}+\Delta_a;\tau)+\log\theta_0(u_{ij};\tau)\right) \\ +(N-1)\sum_{a=1}^{3}\log\widetilde{\Gamma}(\Delta_a;\tau)+2(N-1)\log(q;q)_\infty, \end{aligned} \tag{4.1.1}$$

such that the index (2.1.14) can be rewritten simply as

$$\mathcal{I}(\tau;\Delta)=\frac{1}{N!}\int_{-\frac{1}{2N}}^{1-\frac{1}{2N}}\prod_{\mu=1}^{N-1}du_\mu\,\exp\left[N^2 S_{\text{eff}}(\hat{u};\Delta,\tau)\right]. \tag{4.1.2}$$

Here $\hat{u}$ denotes a set of holonomies $\hat{u}=\{u_j|j=1,\cdots,N\}$ and we have chosen the above integration range for later convenience. Note that we have replaced $-\sum_{i\neq j}\log\widetilde{\Gamma}(u_{ij};\tau)$ with $\sum_{i\neq j}\log\theta_0(u_{ij};\tau)$ to get (4.1.1) and (4.1.2) from (2.1.14), using the quasi-double-periodicity (A.5a), (A.7) and the inversion formula (A.6), (A.8) of the elliptic functions.

Given the effective action (4.1.1) and the integral form of the index (4.1.2), we can now apply the saddle-point approach. First, we find solutions to the saddle point equations

$$0=\frac{\partial}{\partial u_\mu}S_{\text{eff}}(\hat{u};\Delta,\tau)\Big|_{\hat{u}=\hat{u}_*}\qquad(\mu=1,\cdots,N-1). \tag{4.1.3}$$

Then the index (4.1.2) can be approximated as

$$\mathcal{I}(\tau;\Delta)\sim\sum_{\hat{u}_*\in\mathcal{C}'}\frac{1}{N!}\int_{D_{\hat{u}_*}}\prod_{\mu=1}^{N-1}du_\mu\,\exp\left[N^2 S_{\text{eff}}(\hat{u};\Delta,\tau)\right], \tag{4.1.4}$$

where the integration is along the steepest descent contour $\mathcal{C}'$ passing through one or more saddle points. For each saddle point, $D_{\hat{u}_*}$ is a neighborhood of the corresponding saddle point solution $\hat{u}_*$. For a real saddle point, where $\hat{u}_*$ lies on the original contour $\mathcal{C}$ of (4.1.2), we have

$$\hat{u}_* \in D_{\hat{u}_*} \subseteq \mathcal{C} = \bigcup_{\mu=1}^{N-1} [-\frac{1}{2N}, 1-\frac{1}{2N}]. \tag{4.1.5}$$

However, in general, we may expect the saddle point to be complex, in which case the original contour $\mathcal{C}$ will have to be deformed to pass through the saddle point. Here we assume this to be the case, but will further comment on the contour deformation in section 4.1.3.

Note that (assuming contour deformation is possible) if we did not restrict the integral in (4.1.4) to the neighborhoods of the saddle points, but kept the full integration contour $\mathcal{C}'$, then we would still have an exact expression for the index. The approximation comes from integrating only near the saddle points, and this needs to be controlled by a large parameter. Such a parameter would naturally be N^2 in the 't Hooft expansion. But in the Cardy-like limit, $1/|\tau|$ can also play the role of a large parameter. In either case, the saddle point result (4.1.4) is valid up to exponentially suppressed terms in the large parameter. From here on, we choose $1/|\tau|$ as a large control parameter[9]

To make contact with the results in the literature we take the Cardy-like limit that imposes $|\tau| \ll 1$ from here on. In section 4.1.2, we revisit the leading term in the Cardy-like limit $|\tau| \to 0$ [37, 43]. In section 4.1.3, we keep track of sub-leading corrections in the finite Cardy-like expansion with $|\tau| \ll 1$. In both sections, our goal is to obtain an explicit expression for the SCI using the saddle-point approximation (4.1.4).

4.1.2 Leading term in the Cardy-like limit

In the Cardy-like limit, $|\tau| \to 0$, we substitute the asymptotic formulas of the Pochhammer symbol (A.12), the elliptic theta function (A.17), and the elliptic gamma function (A.21) into the effective action (4.1.1). The leading order term then scales as $\mathcal{O}(1/\tau^2)$, and we find

$$N^2 S_{\text{eff}}(\hat{u};\Delta,\tau) = -\frac{\pi i}{3\tau^2}\sum_{a=1}^{3}\left(\sum_{i\neq j} B_3(\{u_{ij}+\Delta_a\}_\tau) + (N-1)B_3(\{\Delta_a\}_\tau)\right) + \mathcal{O}(|\tau|^{-1}), \tag{4.1.6}$$

where $B_3(x)$ is the third Bernoulli polynomial. The definition of a τ-modded value $\{\cdot\}_\tau$ is given in (A.13). Here we assumed

$$\{\tilde{u}_{ij}+\tilde{\Delta}_a\} \not\to 0 \text{ or } 1 \tag{4.1.7}$$

for any u_i's and Δ_a's to use the asymptotic formula of the elliptic gamma function (A.21). The 'tilde' values $\tilde{u}_i$ and $\tilde{\Delta}_a$ are defined following (A.15) and the curly bracket $\{\cdot\}$ is defined in (A.16).

The saddle point equation (4.1.3) is given from the effective action (4.1.6) as

$$\begin{aligned} 0 = -\frac{\pi i}{\tau^2}\sum_{a=1}^{3}\sum_{j=1}^{N}\Big(&B_2(\{u_{\mu j}+\Delta_a\}_\tau) - B_2(\{u_{Nj}+\Delta_a\}_\tau) \\ &- B_2(\{-u_{\mu j}+\Delta_a\}_\tau) + B_2(\{-u_{Nj}+\Delta_a\}_\tau)\Big) + \mathcal{O}(|\tau|^{-1}), \end{aligned} \tag{4.1.8}$$

[9] We need this control parameter so we can safely place ourselves near the saddle point that dominates in the Cardy-like limit.

under the assumption (4.1.7). As we have commented in the beginning of this section, the pairwise saddle point equation (4.1.8) yields a rich set of solutions and we expect that one or a handful of solutions yields a dominant contribution to the index in the saddle point approximation (4.1.4). One of the most well known solutions is the one with all identical holonomies, namely $u_i = u_j$ for all $i, j \in \{1, \cdots, N\}$ [37, 43]. The effective action at this saddle point successfully counted the dual AdS_5 black hole microstates [37]. In the main text, we focus on the case where this particular saddle point with identical holonomies is dominant over the other saddle points and therefore this black hole microstate counting is valid. We put off the discussion on other types of saddle points, in particular the ones dubbed as C-center solutions[10] in [121], to Appendix B.

On the integration contour (4.1.5), there are N distinct sets of identical holonomies satisfying the $SU(N)$ constraint $\sum_{i=1}^{N} u_i \in \mathbb{Z}$, namely

$$\hat{u}^{(m)} = \left\{ u_j^{(m)} = \frac{m}{N} \,\middle|\, j = 1, \cdots, N \right\} \quad (m = 0, 1, \cdots, N-1). \tag{4.1.9}$$

We can compute the effective action (4.1.6) at this saddle point (4.1.9) as

$$N^2 S_{\text{eff}}(\hat{u}^{(m)}; \Delta, \tau) = -\frac{\pi i (N^2-1)}{\tau^2} \prod_{a=1}^{3} \left(\{\tilde{\Delta}_a\} - \frac{1+\eta}{2} \right) + \mathcal{O}(|\tau|^{-1}), \tag{4.1.10}$$

where we have introduced $\eta \in \{\pm 1\}$ as

$$\sum_{a=1}^{3} \{\Delta_a\}_\tau = 2\tau + \sum_{a=1}^{3} \{\tilde{\Delta}_a\} = 2\tau + \frac{3+\eta}{2}, \tag{4.1.11}$$

from the constraint $\sum_{a=1}^{3} \Delta_a - 2\tau \in \mathbb{Z}$ and the assumption (4.1.7). The SCI is then given by substituting (4.1.10) into the saddle point approximation (4.1.4) as

$$\begin{aligned} \mathcal{I}(\tau; \Delta) = N \exp\left[-\frac{\pi i (N^2-1)}{\tau^2} \prod_{a=1}^{3} \left(\{\tilde{\Delta}_a\} - \frac{1+\eta}{2} \right) + o\left(|\tau|^{-2}\right) \right] \\ + (\text{contribution from other saddles}). \end{aligned} \tag{4.1.12}$$

This reproduces the result of [37, 42, 43]. In the context of a 4d Cardy formula, equation (4.1.12) is also consistent with the result of [45] and closely related to the supersymmetric Casimir energy [105, 122] used to count the dual black hole microstates [36]. The factor of $N!$ in the denominator of (4.1.4) is removed by the degeneracy from permuting N holonomies within the saddle point (4.1.9).

4.1.3 Sub-leading terms in the Cardy-like expansion

The fact that the $|\tau|^{-2}$-leading term in the Cardy-like limit (4.1.12) also captures the N^2-leading term in the large-N limit is not clear *a priori*, since (4.1.12) could have terms of order N^2 but sub-leading in the Cardy-like expansion such as $\mathcal{O}(N^2|\tau|^{-1})$. In this subsection we clarify that such a correction does *not* show up and therefore (4.1.12) captures the N^2-leading term in the large-N limit correctly, by keeping track of all the sub-leading terms up to exponentially suppressed ones in the Cardy-like expansion.

[10] The C-center solution is related to the $\{C, N/C, 0\}$ BA solution in [68] and the $(C, N/C)$ saddle in [116].

To go beyond the leading term in the Cardy-like limit, we have to expand the special functions to higher order. In particular, we substitute the asymptotic formulas of the Pochhammer symbol (A.12), the elliptic theta function (A.17), and the elliptic gamma function (A.21) into (4.1.1) and keep track of sub-leading terms in the finite Cardy-like expansion. The result is given in terms of Bernoulli polynomials as

$$\begin{aligned}
N^2 S_{\text{eff}}(\hat{u};\Delta,\tau) = &-\frac{\pi i}{3\tau^2}\sum_{a=1}^{3}\left(\sum_{i\neq j}B_3(\{u_{ij}+\Delta_a\}_\tau)+(N-1)B_3(\{\Delta_a\}_\tau)\right)\\
&+\frac{\pi i}{\tau}\left(\sum_{a=1}^{3}\sum_{i\neq j}B_2(\{u_{ij}+\Delta_a\}_\tau)+(N-1)\sum_{a=1}^{3}B_2(\{\Delta_a\}_\tau)+\sum_{i\neq j}\{u_{ij}\}_\tau(1-\{u_{ij}\}_\tau)\right)\\
&-\frac{5\pi i}{6}\sum_{a=1}^{3}\left(\sum_{i\neq j}B_1(\{u_{ij}+\Delta_a\}_\tau)+(N-1)B_1(\{\Delta_a\}_\tau)\right)\\
&+\pi i\sum_{i\neq j}\{u_{ij}\}_\tau+\frac{\pi i(2\tau^2-3\tau-1)N^2}{6\tau}+\pi i N-\frac{\pi i(2\tau^2+3\tau-1)}{6\tau}\\
&-(N-1)\log\tau+\sum_{i\neq j}\log\left(1-e^{-\frac{2\pi i}{\tau}(1-\{u_{ij}\}_\tau)}\right)\left(1-e^{-\frac{2\pi i}{\tau}\{u_{ij}\}_\tau}\right)\\
&+\mathcal{O}\left(|\tau|^{-1}e^{\frac{2\pi\sin(\arg\tau)}{|\tau|}X}\right),
\end{aligned}\tag{4.1.13}$$

where the first line above is just the leading order term (4.1.6). As in the previous subsection, we follow the conventions in (A.13), (A.15), (A.16) and the assumption (4.1.7). The higher order terms are of $\mathcal{O}(|\tau|^{-1}e^{\frac{2\pi\sin(\arg\tau)}{|\tau|}X})$ where X is defined as

$$X=\min(\{\tilde{u}_{ij}+\tilde{\Delta}_a\},\ 1-\{\tilde{u}_{ij}+\tilde{\Delta}_a\}:a=1,2,3,\ i,j=1,\cdots,N).\tag{4.1.14}$$

This is exponentially suppressed under the assumption (4.1.7). Thus, we are treating the SCI in all powers of τ up to exponentially suppressed terms.

Using this finite Cardy-like expansion of the effective action (4.1.13), we would like to evaluate sub-leading corrections to the saddle point solution (4.1.9) and the index (4.1.12) obtained in the infinite Cardy-like limit. For that purpose, it suffices to focus on the effective action (4.1.13) *near* the leading saddle point solution (4.1.9). To be specific, we make the Ansatz for saddle point solutions in the finite Cardy-like expansion,

$$\hat{u}^{(m)}=\left\{u_j^{(m)}=\frac{m}{N}+v_j\tau\,\middle|\,v_j\sim\mathcal{O}(|\tau|^0),\ \sum_{j=1}^{N}v_j=0\right\}\quad(m=0,1,\cdots,N-1),\tag{4.1.15}$$

and investigate the effective action (4.1.13) around this Ansatz. This Ansatz is natural as it is equivalent to the leading order solution (4.1.9) up to sub-leading corrections given by v_j. Note that $\sum_{j=1}^{N}v_j=0$ is required to satisfy the $SU(N)$ constraint.

The effective action (4.1.13) *near* the saddle point Ansatz (4.1.15) can be simplified using

$$\begin{aligned}\{u_{ij}+\Delta_a\}_\tau &= u_{ij}+\{\Delta_a\}_\tau,\\ \{u_{ij}\}_\tau &= \begin{cases} u_{ij} & (\tilde{u}_i \geq \tilde{u}_j)\\ 1+u_{ij} & (\tilde{u}_i < \tilde{u}_j),\end{cases}\end{aligned} \tag{4.1.16}$$

since $u_{ij} = v_{ij}\tau$ is at most order $\mathcal{O}(|\tau|)$ and therefore we can factor it out from the modded values carefully. The resulting simplified effective action is given as

$$\begin{aligned}N^2 S_{\text{eff}}(\hat{u};\Delta,\tau) = &-\frac{\eta\pi i}{\tau^2} N\sum_{j=1}^{N}\left(u_j - \frac{\sum_{k=1}^{N} u_k}{N}\right)^2 + \sum_{j\neq k}\log\left(2\sin\frac{\pi u_{jk}}{\tau}\right)\\ &-\frac{\pi i}{\tau^2}(N^2-1)\prod_{a=1}^{3}\left(\{\Delta_a\}_\tau - \frac{1+\eta}{2}\right) + \frac{\pi i(6-5\eta)(N^2-1)}{12}\\ &-\frac{\pi i N(N-1)}{2} - (N-1)\log\tau + \mathcal{O}(|\tau|^{-1}e^{\frac{2\pi\sin(\arg\tau)}{|\tau|}X}),\end{aligned} \tag{4.1.17}$$

where we have used the same η introduced in (4.1.11).

The saddle point equation (4.1.3) is given from the effective action (4.1.17) and the Ansatz (4.1.15) as

$$i\eta\, v_j = \frac{1}{N}\sum_{k=1\,(\neq j)}^{N}\cot\pi v_{jk} \quad (i=1,\cdots,N) \tag{4.1.18}$$

and is valid up to exponentially suppressed terms. Note that the system of equations is τ-independent, thus justifying our assumption $v_j \sim \mathcal{O}(|\tau|^0)$. In addition, the log term in the first line of (4.1.17) leads to a repulsion between pairs of eigenvalues. It is this term that shows up away from the strict Cardy-like limit that pushes the eigenvalues apart and modifies the leading order solution, (4.1.9), of condensed eigenvalues. In fact, as will be highlighted below, this set of equations closely resemble those of an $SU(N)$ Chern-Simons model [123, 124].

The steepest descent contour

At leading order in the Cardy-like limit, we found N distinct real saddle points (4.1.9). However, at sub-leading order, while there are still N distinct saddle points, each one is now complex, as the solutions to (4.1.18) are complex. As a result, we seek to deform the original contour (4.1.5) to a new contour $\mathcal{C}'$ that passes through these N saddles.

To be more specific, we show a typical complex saddle point solution in Figure 17. The original contour integrates all eigenvalues along the real line, as shown by the red path. The first step is then to deform the contour so that the integration path of each eigenvalue u_μ passes through the corresponding saddle point solution as indicated by the green path in the figure. Since the contributions from the left and the right ends of green contours cancel each other, the deformed contour can be written simply as

$$\mathcal{C}' = \bigcup_{\mu=1}^{N-1}(v_\mu\tau - \frac{1}{2N}, v_\mu\tau + 1 - \frac{1}{2N}], \tag{4.1.19}$$

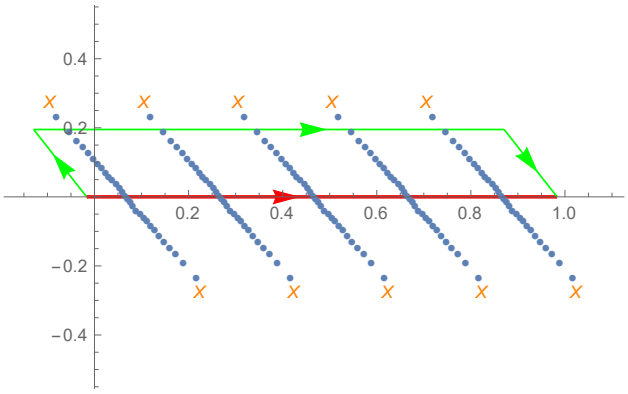


Figure 17: Numerical leading saddle points (blue dots) discussed in Appendix C.3 with $N = 30$ and $\tau = \frac{ie^{\pi i/6}}{\pi}$. There must be $N = 30$ distinct sets of holonomies in the above figure but here only 5 copies of them are shown for presentation. Orange crosses denote $\pm\tau + \frac{m}{N}$ $(m = 2, 8, 14, 20, 26)$ and therefore it is straightforward to see that each set of holonomies collapses to $\frac{m}{N}$ as $|\tau| \to 0$.

where $\{v_\mu\}$ is a solution to the saddle-point equation (4.1.18). Note that we are implicitly assuming that the effective action is analytic in this region so that the deformation is valid.

The saddle-point approximation to the SCI is then obtained from the effective action (4.1.17) as

$$\mathcal{I}(\tau;\Delta) \sim \sum_{m=0}^{N-1} \frac{\mathcal{A}}{N!} \int_{D_{\hat{u}^{(m)}}} \prod_{\mu=1}^{N-1} du_\mu \exp\left[-\frac{\eta\pi i}{\tau^2} N \sum_{j=1}^{N} \left(u_j - \frac{\sum_{k=1}^{N} u_k}{N} \right)^2 + \sum_{j\neq k} \log\left(2\sin\frac{\pi u_{jk}}{\tau} \right) \right] + (\text{contribution from other saddles}), \tag{4.1.20}$$

up to exponentially suppressed terms, where $D_{\hat{u}^{(m)}}$ denotes a small neighborhood of a saddle point solution $\hat{u}^{(m)}$ on the deformed contour (4.1.19), namely

$$D_{\hat{u}^{(m)}} = \bigcup_{\mu=1}^{N-1} (v_\mu\tau + \frac{m}{N} - \epsilon, v_\mu\tau + \frac{m}{N} + \epsilon] \subseteq \mathcal{C}', \tag{4.1.21}$$

for some small positive number ϵ. The prefactor $\mathcal{A}$ is defined as

$$\mathcal{A} = \exp\left[-\frac{\pi i}{\tau^2}(N^2-1) \prod_{a=1}^{3} \left(\{\Delta_a\}_\tau - \frac{1+\eta}{2} \right) + \frac{\pi i(6-5\eta)(N^2-1)}{12} - \frac{\pi i N(N-1)}{2} - (N-1)\log\tau + \mathcal{O}(|\tau^{-1}|e^{\frac{2\pi\sin(\arg\tau)}{|\tau|}X}) \right]. \tag{4.1.22}$$

Finally, it is convenient to introduce new integration variables λ_j with the constraint $\sum_{j=1}^{N} \lambda_j = 0$ as

$$u_j = u_j^{(m)} - (i\lambda_j + v_j)\tau = \frac{m}{N} - i\lambda_j\tau. \tag{4.1.23}$$

This allows us to rewrite (4.1.20) as

$$\mathcal{I}(\tau;\Delta) \sim N\tau^{N-1}e^{-\frac{\pi i(N^2-1)}{2}}\frac{\mathcal{A}}{N!}\int_{D_{\hat{\lambda}}}\prod_{\mu=1}^{N-1}d\lambda_\mu\,\exp\left[\eta\pi iN\sum_{j=1}^{N}\lambda_j^2+\sum_{j\neq k}\log(2\sinh\pi\lambda_{jk})\right] \\ +\,(\text{contribution from other saddles}), \tag{4.1.24}$$

where the integration contour $D_{\hat{\lambda}}$ is given from the contour (4.1.21) and the change of variables (4.1.23) as

$$D_{\hat{\lambda}} = \bigcup_{\mu=1}^{N-1}(iv_\mu - \frac{i\epsilon}{\tau}, iv_\mu + \frac{i\epsilon}{\tau}]. \tag{4.1.25}$$

Remarkably, the steepest descent integral in (4.1.24) is identical to that used to evaluate the S^3 sphere partition function of supersymmetric $\mathrm{SU}(N)_k$ Chern-Simons theory

$$Z^{CS}_{\mathrm{SU}(N)_k} = \frac{1}{N!}\int_{-\infty}^{\infty}\prod_{\mu=1}^{N-1}d\lambda_\mu\,\exp\left[-\pi ik\sum_{j=1}^{N}\lambda_j^2+\sum_{j\neq k}\log(2\sinh\pi\lambda_{jk})\right], \tag{4.1.26}$$

under the constraint $\sum_{j=1}^{N}\lambda_j = 0$, provided we make the identification $k = -\eta N$. This does depend on the ability to deform the contour of the Chern-Simons theory to pass through the $D_{\hat{\lambda}}$ contour, which we assume to be the case. We investigate this further in Appendix C. The final result is that the index can be written as

$$\mathcal{I}(\tau;\Delta) \sim N\tau^{N-1}e^{-\frac{\pi i(N^2-1)}{2}}\mathcal{A}\,Z^{CS}_{\mathrm{SU}(N)_{k=-\eta N}} \\ +\,(\text{contribution from other saddles}). \tag{4.1.27}$$

We have computed this $SU(N)$ partition function in Appendix D based on the $\mathrm{U}(N)$ partition function from [125]. Substituting the result (D.6) into (4.1.27), we get

$$\boxed{\mathcal{I}(\tau;\Delta) \sim N\exp\left[-\frac{\pi i(N^2-1)}{\tau^2}\prod_{a=1}^{3}\left(\{\Delta_a\}_\tau-\frac{1+\eta}{2}\right)+\mathcal{O}(e^{-1/|\tau|})\right] \\ +\,(\text{contribution from other saddles}).} \tag{4.1.28}$$

The leading Cardy-like limit of (4.1.28) reproduces the result obtained in the leading Cardy-like limit by [36, 37, 42–44]. One of the main results of this chapter is that there are no sub-leading τ-corrections besides exponentially suppressed contributions. We also obtain a $\log N$ contribution to the logarithm of the SCI, which comes directly from the degeneracy of N different saddle points contributing equally to the SCI [11]. This is in fact an important lesson we learn, and it will ensure the universality of the logarithmic correction for a large class of $\mathcal{N} = 1$ 4d SCFT's as we will see in subsequent sections.

[11] Note that we do not include contributions to $\log N$ that are present in the full quantum Chern-Simons theory [126]. These contributions arise from integration near the trivial connection which has a residual global gauge symmetry corresponding to $SU(N)$ gauge transformations and therefore contributes a factor of inverse volume of $SU(N)$ to the path integral. Our computation connects to the matrix model of $SU(N)$ Chern-Simons theory, not to the quantum path integral of Chern-Simons theory.

4.1.4 Saddle point approximation for $\mathcal{N}=1$ toric quiver gauge theories

We now generalize the previous set of results to the case of $\mathcal{N}=1$ toric quiver gauge theories discussed in chapter 2. Once again, we consider a toric quiver gauge theory whose gauge group G has $n_{\rm v}$ simple factors (in all the $\mathcal{N}=1$ quiver gauge theories we will deal with, the number of simple factors coincides with the number of vector multiplets). We focus, for concreteness, on the case in which all the gauge group factors are $SU(N_a)$, a goes from 1 to $n_{\rm v}$, with $N_a = N \ \forall\, a$. In these theories the weight vectors ρ are such that for any bi-fundamental field Φ_{ab}:

$$\rho_{ij}^{\Phi_{ab}}(u) \equiv u_{ij}^{ab} \equiv u_i^a - u_j^b. \tag{4.1.29}$$

There are $d-1$ fugacities corresponding to flavor symmetries appearing in the generic toric gauge theories that we will study, and recall that d is the number of external points of the toric diagram that are related to the quivers defining the theory (see chapter 2). The integrand of (2.1.8) can be now exponentiated and treated like an effective action:

$$\begin{aligned} S_{\rm eff}(u;\Delta,\tau) = &\sum_{\Phi_{ab}}\sum_{i_a\neq j_b}\log\widetilde{\Gamma}\left(u_{ij}^{ab}+\Delta_{ab};\tau\right) - \sum_{a=1}^{n_{\rm v}}\sum_{i_a\neq j_a}\widetilde{\Gamma}\left(u_{ij}^{a},\tau\right) \\ &+ 2n_{\rm v}(N-1)\log\left(q;q\right)_\infty + (N-1)\sum_{\Phi_{ab}}\widetilde{\Gamma}(\Delta_{ab};\tau), \end{aligned} \tag{4.1.30}$$

where we have denoted $u_{ij}^{ab} \equiv u_{i_a} - u_{j_b}$ for the holonomies associated to the chiral multiplets Φ_{ab} and $u_{ij}^{a} \equiv u_{i_a} - u_{j_a}$ for the vector multiplets. Making use of the expression for the elliptic gamma function in the $|\tau| \ll 1$ limit, the effective action can be expressed as:

$$\begin{aligned} S_{\rm eff}(u;\Delta,\tau) = &-\frac{\pi i}{3\tau^2}\sum_{\Phi_{ab}}\Bigg(\sum_{i_a\neq j_b}\{u_{ij}^{ab}+\Delta_{ab}\}_\tau(\{u_{ij}^{ab}+\Delta_{ab}\}_\tau-\frac{1}{2})(\{u_{ij}^{ab}+\Delta_{ab}\}_\tau-1) \\ &\qquad +(N-1)\{\Delta_{ab}\}_\tau(\{\Delta_{ab}\}_\tau-\frac{1}{2})(\{\Delta_{ab}\}_\tau-1)\Bigg) \\ &+\frac{\pi i}{\tau}\Bigg(\sum_{\Phi_{ab}}\sum_{i_a\neq j_b}(\{u_{ij}^{ab}+\Delta_{ab}\}_\tau^2-\{u_{ij}^{ab}+\Delta_{ab}\}_\tau+\frac{1}{6}) + \sum_{a=1}^{n_{\rm v}}\sum_{i_a\neq j_a}\{u_{ij}^{a}\}_\tau(1-\{u_{ij}^{a}\}_\tau) \\ &\qquad +(N-1)\sum_{\Phi_{ab}}(\{\Delta_{ab}\}_\tau^2-\{\Delta_{ab}\}_\tau+\frac{1}{6})\Bigg) \\ &-\frac{5\pi i}{6}\sum_{\Phi_{ab}}\Bigg(\sum_{i_a\neq j_b}(\{u_{ij}^{ab}+\Delta_{ab}\}_\tau-\frac{1}{2})+(N-1)(\{\Delta_{ab}\}_\tau-\frac{1}{2})\Bigg) \\ &+\pi i\sum_{a=1}^{n_{\rm v}}\sum_{i_a\neq j_a}\{u_{ij}^{a}\}_\tau + \sum_{a=1}^{n_{\rm v}}\sum_{i_a\neq j_a}\log\Big(1-e^{-\frac{2\pi i}{\tau}(1-\{u_{ij}^{a}\}_\tau)}\Big)\Big(1-e^{-\frac{2\pi i}{\tau}\{u_{ij}^{a}\}_\tau}\Big) \\ &+\frac{i\pi N^2}{6\tau}\left((n_\chi-n_{\rm v})\tau^2-n_{\rm v}\right)+\frac{i\pi N n_{\rm v}}{6\tau}\left(\tau^2+1\right)-\frac{i\pi n_\chi\tau}{6} \\ &+2n_{\rm v}(N-1)\log\left(q;q\right)_\infty+\mathcal{O}(e^{-1/|\tau|}). \end{aligned} \tag{4.1.31}$$

Using the asymptotic formula (A.12) valid for $|\tau| \ll 1$ and following section 4.1.3 we generalize the statement that u_{ij}^{ab} satisfy the Ansatz for the saddles (4.1.15), which allows us to rewrite the effective action as

$$\begin{aligned} S_{\text{eff}}(u;\Delta,\tau) = &-\frac{\pi i}{\tau^2}\sum_{\Phi_{ab}}(\{\Delta_{ab}\}_\tau - \tau - \frac{1}{2})\sum_{i_a\neq j_b}(u_{ij}^{ab})^2 - \frac{\pi i}{\tau}\sum_{a=1}^{n_{\text{v}}}\sum_{i_a\neq j_a}(u_{ij}^{a})^2 + \frac{2\pi i}{\tau}\sum_{a=1}^{n_{\text{v}}}\sum_{i_a>j_a}u_{ij}^{a} \\ &+ 2\sum_{a=1}^{n_{\text{v}}}\sum_{i_a>j_a}\log\left(1-e^{-\frac{2\pi i}{\tau}u_{ij}^{a}}\right) \\ &- \frac{\pi i}{3\tau^2}(N^2-1)\sum_{\Phi_{ab}}\left(B_3\left(\{\Delta_{ab}\}_\tau\right) - 3\tau B_2\left(\{\Delta_{ab}\}_\tau\right) + \frac{5\tau^2}{2}B_1\left(\{\Delta_{ab}\}_\tau\right)\right) \\ &+ \frac{i\pi N^2}{6\tau}\left((n_\chi - n_{\text{v}})\tau^2 - n_{\text{v}}\right) + \frac{i\pi n_{\text{v}}}{2}N \\ &- \frac{i\pi}{6\tau}\left((n_\chi - n_{\text{v}})\tau^2 + 3n_{\text{v}}\tau - n_{\text{v}}\right) - n_{\text{v}}(N-1)\log\tau + \mathcal{O}(e^{-1/|\tau|}). \end{aligned} \tag{4.1.32}$$

We have used Bernoulli polynomials for the sake of compactness. To simplify the terms depending on u_{ij} in (4.1.32), it will be convenient to rewrite the sum over the chiral multiplets $\sum_{\Phi_{ab}}$ as $\frac{1}{2}\sum_{a=1}^{n_{\text{v}}}\sum_{\phi_a=1}^{n_{\phi_a}}$, where ϕ_a labels an arrow connected to a and n_{ϕ_a} is the degree of incidence the node a in the graph representing the quiver. The effective action then simplifies to

$$\begin{aligned} S_{\text{eff}}(u;\Delta,\tau) = &\sum_{a=1}^{n_{\text{v}}}F_a(u;\eta_a,\tau) - \frac{\pi i}{3\tau^2}(N^2-1)\sum_{\Phi_{ab}}\left[B_3\left(\{\Delta_{ab}\}_\tau\right) - 3\tau\left(B_2\left(\{\Delta_{ab}\}_\tau\right) - \frac{1}{6}\right)\right. \\ &\left. - \frac{\tau}{2} + \frac{5\tau^2}{2}B_1\left(\{\Delta_{ab}\}_\tau\right)\right] + \frac{i\pi N^2}{6\tau}\left((n_\chi - n_{\text{v}})\tau^2 - n_{\text{v}}\right) + \frac{i\pi n_{\text{v}}}{2}N \\ &- \frac{i\pi}{6\tau}\left((n_\chi - n_{\text{v}})\tau^2 + 3n_{\text{v}}\tau - n_{\text{v}}\right) - n_{\text{v}}(N-1)\log\tau + \mathcal{O}(e^{-1/|\tau|}), \end{aligned} \tag{4.1.33}$$

where we have defined

$$F_a(u;\eta_a,\tau) \equiv -\frac{\pi i\eta_a}{\tau^2}N\sum_{i_a}u_{i_a}^2 + \sum_{i_a\neq j_a}\log\left(2\sin\frac{\pi u_{ij}^{a}}{\tau}\right). \tag{4.1.34}$$

Here the factors η_a are given by

$$\sum_{\phi_a=1}^{n_{\phi_a}}\{\Delta_{\phi_a}\}_\tau \equiv \tau(n_{\phi_a}-2) + \eta_a + \frac{n_{\phi_a}}{2}. \tag{4.1.35}$$

We have written Δ_{ϕ_a} to emphasize that we are summing over a very specific subset of Δ_{ab}, that is, for a fixed value of a, we sum only over chiral multiplets connected to a in the quiver. Let us further note that, upon the shifting (4.1.40), conservation of $U(1)$ global charge at each node of the quiver yields $\eta_a = 1$ as long as we remain within the domain of chemical potentials specified by:

$$\text{Im}\left(-\frac{1}{\tau}\right) > \text{Im}\left(\frac{\sum_{k=1}^{d-1}[\Delta_k]_\tau}{\tau}\right) > 0, \tag{4.1.36}$$

which is represented in 16. It is remarkable that the holonomy-dependent part of (4.1.33), namely (4.1.34), takes exactly the same form with the effective action in (4.1.20) for the $\mathcal{N}=4$ SYM case. Hence the arguments of section 4.1.3 can be applied here to solve the matrix model with the effective action (4.1.34). In the physics point of view, this implies that the relation between the sub-leading structures of the $\mathcal{N}=4$ SCI in the Cardy-like limit and the 3d Chern-Simons theory studied in the previous subsection 4.1.3 can be extended to more general 4D $\mathcal{N}=1$ quiver gauge theories. To be specific, we can use the expression for $Z_{\mathrm{SU}(N)}$ shown in Appendix D to compute the first term of (4.1.33):

$$\sum_{a=1}^{n_{\mathrm{v}}} \log Z^{(a)}_{SU(N)} = \frac{i n_{\mathrm{v}} \pi N(N-1)}{2} + \frac{5\pi i (N^2-1)}{12} \sum_{a=1}^{n_{\mathrm{v}}} \eta_a. \tag{4.1.37}$$

Even though we are restricting ourselves to the special case with $\eta_a = 1$ in this subsection, we do not replace η_a by 1 to be able to compare with the $\mathcal{N}=4$ case. The fact that $S_{\mathrm{eff}}(u;\Delta,\tau)$ contains the contribution of $Z^{(a)}_{SU(N)}$ is quite remarkable, and it indicates a nontrivial relation between the SCI and Chern-Simons theory living in 3d which could be understood from the effective field theory point of view, as recently done in [58, 59].

Before substituting (4.1.37) into (4.1.33), however, let us first simplify the remaining terms of (4.1.33). We rewrite (4.1.33) as

$$\begin{aligned} S_{\mathrm{eff}}(u;\Delta,\tau) = \sum_{a=1}^{n_{\mathrm{v}}} F_a(u;\eta_a,\tau) - \frac{\pi i}{3\tau^2}(N^2-1) \sum_{\Phi_{ab}} \Big[B_3\left([\Delta_{ab}]_\tau + 1\right) - 3\tau \left[\Delta_{ab}\right]_\tau \left([\Delta_{ab}]_\tau + 1\right) \\ - \frac{\tau}{2} + \frac{5\tau^2}{2}\left([\Delta_{ab}]_\tau + \frac{1}{2} \right) \Big] + \frac{i\pi N^2}{6\tau}\left((n_\chi - n_{\mathrm{v}})\tau^2 - n_{\mathrm{v}} \right) + \frac{i\pi n_{\mathrm{v}}}{2} N \\ - \frac{i\pi}{6\tau}\left((n_\chi - n_{\mathrm{v}})\tau^2 + 3n_{\mathrm{v}}\tau - n_{\mathrm{v}} \right) - n_{\mathrm{v}}(N-1)\log\tau + \mathcal{O}(e^{-1/|\tau|}). \end{aligned} \tag{4.1.38}$$

For the sake of compactness, we have used the relation $\{x\}_\tau = [x]_\tau + 1$ thus we will express our final answer in terms of $[\Delta]_\tau$. Let us now analyze separately the second term in (4.1.38):

$$\begin{aligned} \mathcal{K}([\Delta_{ab}]_\tau;\tau) &\equiv B_3\left([\Delta_{ab}]_\tau + 1\right) - 3\tau\left[\Delta_{ab}\right]_\tau \left([\Delta_{ab}]_\tau + 1\right) \\ &= B_3\left([\Delta_{ab}]_\tau - \tau + 1\right) - 3\tau^2 \left[\Delta_{ab}\right]_\tau + B_3\left(\tau\right), \\ \sum_{\Phi_{ab}} \mathcal{K}([\Delta_{ab}]_\tau;\tau) &= \sum_{\Phi_{ab}} B_3\left([\Delta_{ab}]_\tau - \tau + 1\right) - 3\tau^2 \sum_{\Phi_{ab}} [\Delta_{ab}]_\tau + n_\chi B_3(\tau). \end{aligned} \tag{4.1.39}$$

To simplify (4.1.39), first let us analyze the shifting of the chemical potentials

$$\Delta_k \to \Delta_k - \frac{2\tau}{d}. \tag{4.1.40}$$

For the chemical potentials defined in (2.1.11) we have:

$$\Delta_{ab} = \xi_{ab} + r_{ab}\tau = \sum_{l=1}^{d-1} Q_k^{ab} \Delta_k + r_{ab}\tau, \tag{4.1.41}$$

where r_{ab} is the R-charge assigned through a-maximization and Q_k^{ab}, Δ_k are the global charge, and chemical potentials respectively. As discussed in section 3.1.1, the shifting (4.1.40) ensures optimal

obstruction of bosonic-fermionic cancellation in the SCI by canceling the $(-1)^F$ in (2.1.1) and can be interpreted as a redefinition of R-charges such that only those chiral multiplets with negative $U(1)$ global charge acquire R-charge equals 2. This allows us to define d_{ab} as specified in equation (3.1.34). Detailed tables with the values for the global charges Q_k^{ab} are displayed in section 3.2.

The properties of the Bernoulli polynomials allows to write $\mathcal{K}([\Delta_{ab}]_\tau;\tau)$ after the shifting (4.1.40) in the following way:

$$\begin{aligned}\sum_{\Phi_{ab}}\mathcal{K}([\Delta_{ab}]_\tau;\tau) \to &\sum_{\Phi_{ab}}(-1)^{d_{ab}}B_3\left((-1)^{d_{ab}}\left[\bar{\xi}_{ab}\right]_\tau-\tau+1\right)-3\tau^2\sum_{\Phi_{ab}}\left[\bar{\xi}_{ab}\right]_\tau\\ &-6\tau^3 n_s+n_\chi B_3(\tau),\\ n_s\equiv&\sum_{\Phi_{ab}}d_{ab},\\ \sum_{\Phi_{ab}}\mathcal{K}(\left[\bar{\xi}_{ab}\right]_\tau;\tau)=&\sum_{\Phi_{ab}}(-1)^{d_{ab}}B_3\left((-1)^{d_{ab}}\left[\bar{\xi}_{ab}\right]_\tau+1\right)-3\tau\sum_{\Phi_{ab}}\left[\bar{\xi}_{ab}\right]_\tau^2\\ &-6\tau^3 n_s+(n_\chi-n_{\rm v})B_3(\tau).\end{aligned}\tag{4.1.42}$$

Using the fact that the quiver diagrams analyzed here can be drawn on a torus, and that $2n_s = n_F = n_\chi - n_{\rm v}$ is the number of monomial terms in the superpotential (which corresponds to the number of faces of the quiver representing the theory, see for example [1] and references therein), we obtain

$$\begin{aligned}\sum_{\Phi_{ab}}\mathcal{K}(\left[\bar{\xi}_{ab}\right]_\tau;\tau)=&\sum_{\Phi_{ab}}(-1)^{d_{ab}}B_3\left((-1)^{d_{ab}}\left[\bar{\xi}_{ab}\right]_\tau+1\right)-3\tau\sum_{\Phi_{ab}}\left[\bar{\xi}_{ab}\right]_\tau^2\\ &-(n_\chi-n_{\rm v})\left(3\tau^3-B_3(\tau)\right).\end{aligned}\tag{4.1.43}$$

Let us now analyze separately the following term:

$$\begin{aligned}\frac{5\tau^2}{2}\sum_{\Phi_{ab}}\left([\Delta_{ab}]_\tau+\frac{1}{2}\right)&=\frac{5\tau^2}{2}\sum_{a=1}^{n_{\rm v}}\left(\frac{1}{2}\sum_{\phi_a}^{n_{\phi_a}}[\Delta_{\phi_a}]_\tau+\frac{n_{\phi_a}}{4}\right)\\ &=\frac{5\tau^2}{2}\sum_{a=1}^{n_{\rm v}}\frac{\eta_a}{2}+\frac{5\tau^3}{2}(n_\chi-n_{\rm v}),\end{aligned}\tag{4.1.44}$$

where we have organized the sum over chiral multiplets $\sum_{\Phi_{ab}}\to\frac{1}{2}\sum_{a=1}^{n_{\rm v}}\sum_{\phi_a=1}^{n_{\phi_a}}$ and in the 2nd line we have used (4.1.35). Inserting (4.1.43) and (4.1.44) back into (4.1.38) yields:

$$\begin{aligned}S_{\rm eff}(u;\Delta,\tau)=&\sum_{a=1}^{n_{\rm v}}F_a(u;\eta_a,\tau)\\ &-\frac{i\pi(N^2-1)}{3\tau^2}\left\{\sum_{\Phi_{ab}}\left[K\left(\left[\bar{\xi}_{ab}\right]_\tau,\tau\right)\right]-\frac{n_\chi\tau}{2}-(n_\chi-n_{\rm v})\left(\frac{1}{2}\tau^3-B_3(\tau)\right)\right.\\ &\left.+\frac{5\tau^2}{2}\sum_{a=1}^{n_{\rm v}}\frac{\eta_a}{2}\right\}+\frac{i\pi N^2}{6\tau}\left((n_\chi-n_{\rm v})\tau^2-n_{\rm v}\right)+\frac{i\pi n_{\rm v}}{2}N\\ &-\frac{i\pi}{6\tau}\left((n_\chi-n_{\rm v})\tau^2+3n_{\rm v}\tau-n_{\rm v}\right)-n_{\rm v}(N-1)\log\tau+\mathcal{O}(e^{-1/|\tau|}).\end{aligned}\tag{4.1.45}$$

Here we have rewritten (3.1.25) as:

$$K(\Delta,\tau) \equiv B_3\,(\Delta+1) - 3\tau\Delta^2 \tag{4.1.46}$$

and the final equality holds when $|\Delta| < 1$. Upon simplification of (4.1.45) we obtain:

$$\begin{aligned} S_{\text{eff}}(u;\Delta,\tau) = &\sum_{a=1}^{n_{\text{v}}} F_a(u;\eta_a,\tau) - \frac{i\pi(N^2-1)}{3\tau^2}\sum_{\Phi_{ab}} K\left(\left[\bar{\xi}_{ab}\right]_\tau,\tau\right) \\ &- \frac{i\pi(N^2-1)}{12}5\left(\sum_{a=1}^{n_{\text{v}}}\eta_a\right) - \frac{\pi i n_{\text{v}} N(N-1)}{2} + \frac{i\pi n_\chi}{2}(N^2-1) \\ &- n_{\text{v}}(N-1)\log\tau + \mathcal{O}(e^{-1/|\tau|}). \end{aligned} \tag{4.1.47}$$

The term $-\frac{i\pi(N^2-1)}{3\tau^2}\sum_{\Phi_{ab}} K\left(\left[\bar{\xi}_{ab}\right]_\tau,\tau\right)$ gives the leading entropy function:

$$\begin{aligned} &S_E = -\frac{i\pi(N^2-1)}{6\tau^2}C_{IJK}\left[\Delta_I\right]_\tau\left[\Delta_J\right]_\tau\left[\Delta_K\right]_\tau \quad (I=1,\cdots,d), \\ &\sum_{I=1}^{d}\Delta_I - 2\tau = -1, \end{aligned} \tag{4.1.48}$$

as shown in the previous chapter (see also [1, 46, 55]). The coefficients C_{IJK} are the triangular 't Hooft anomaly coefficients which correspond, as pointed out originally in [53] and later in [46], to the Chern-Simons couplings of the holographic dual gravitational description as elucidated in [54]. Note that, as already pointed out in the previous subsection 4.1.2, (4.1.48) is closely related to the supersymmetric Casimir energy [36, 105, 122]. The structure (4.1.48) was derived on a case by case basis for a large class of toric quiver gauge theories in the domain of chemical potentials (4.1.36).

Inserting (4.1.37) back into (4.1.47), we have

$$\begin{aligned} S_{\text{eff}}(u;\Delta,\tau) = &-\frac{i\pi(N^2-1)}{6\tau^2}C_{IJK}\left[\Delta_I\right]_\tau\left[\Delta_J\right]_\tau\left[\Delta_K\right]_\tau \\ &+ \frac{i\pi n_\chi}{2}(N^2-1) - n_{\text{v}}(N-1)\log\tau + \mathcal{O}(e^{-1/|\tau|}). \end{aligned} \tag{4.1.49}$$

Therefore, we can write $\mathcal{I}(\tau;\Delta)$ by generalizing the expression (4.1.24) which yields

$$\begin{aligned} \mathcal{I}(\tau;\Delta) &= N\tau^{n_{\text{v}}(N-1)}e^{-\frac{n_{\text{v}}i\pi(N^2-1)}{2}}e^{S_{\text{eff}}(u;\Delta,\tau)} \\ &= n_{\text{v}}N\exp\left[-\frac{i\pi(N^2-1)}{6\tau^2}C_{IJK}\left[\Delta_I\right]_\tau\left[\Delta_J\right]_\tau\left[\Delta_K\right]_\tau + \frac{i\pi}{2}(n_\chi - n_{\text{v}})(N^2-1) + \mathcal{O}(e^{-1/|\tau|})\right], \end{aligned} \tag{4.1.50}$$

up to contribution from other saddles. Using the fact that $n_\chi - n_{\text{v}} = n_W = 2n_s$ (see equation (2.2.58)) we can ignore the term $\frac{i\pi}{2}(n_\chi - n_{\text{v}})(N^2-1)$ because it is a multiple of $2\pi i$ which does not affect the value of $\mathcal{I}(\tau;\Delta)$. Finally we can write

$$\boxed{\begin{aligned} \mathcal{I}(\tau;\Delta) = n_v N\exp&\left[-\frac{i\pi(N^2-1)}{6\tau^2}C_{IJK}\left[\Delta_I\right]_\tau\left[\Delta_J\right]_\tau\left[\Delta_K\right]_\tau + \mathcal{O}(e^{-1/|\tau|})\right] \\ &+ (\text{contribution from other saddles}). \end{aligned}} \tag{4.1.51}$$

The Cardy-like leading term in (4.1.51) reproduces the results of [1, 44–46, 55]. More importantly, the answer in (4.1.51) contains no sub-leading contributions in τ up to exponentially suppressed terms, justifying *a posteriori* the efficacy of the Cardy-like limit. The logarithmic correction has the same origin, arising from a normalization, as it did in the $\mathcal{N}=4$ case. Note that we can recover the case $\eta=1$ of (4.1.28) by setting $n_\chi=3$ and $n_{\rm v}=1$ in (4.1.51).

4.2 Bethe-Ansatz approach

We will now revisit the BA computation retaining sub-leading corrections on N. Firstly we discuss the simple case of $\mathcal{N}=4$ SYM and then we move forward to $\mathcal{N}=1$ toric quiver gauge theories. Moreover, we give a closer look to the properties of the BA solutions, specifically to their degeneracy, which plays a crucial role in determining a universal logarithmic correction to the SCI.

4.2.1 Bethe Ansatz approximation for $\mathcal{N}=4$ SYM

According to the BA formula [39], the integral representation of the SCI of the $\mathcal{N}=4$ $SU(N)$ SYM theory (2.1.14) can be rewritten in terms of a discrete sum (2.1.28) which we reproduce here for convenience:

$$\mathcal{I}(\tau;\Delta)=\kappa_N\sum_{\hat{u}\in \mathrm{BA}}\mathcal{Z}(\hat{u};\Delta,\tau)H(\hat{u};\Delta,\tau)^{-1}, \tag{4.2.1}$$

where the building blocks are given as

$$\kappa_N=\frac{1}{N!}\left((q;q)_\infty^2\prod_{a=1}^{3}\widetilde{\Gamma}(\Delta_a;\tau)\right)^{N-1} \tag{4.2.2a}$$

$$\mathcal{Z}\left(\hat{u};\Delta,\tau\right)=\prod_{i\neq j}^{N}\frac{\prod_{a=1}^{3}\widetilde{\Gamma}(u_{ij}+\Delta_a;\tau)}{\widetilde{\Gamma}\left(u_{ij};\tau\right)} \tag{4.2.2b}$$

$$H\left(\hat{u};\Delta,\tau\right)=\det\left[\frac{1}{2\pi i}\frac{\partial\left(Q_1,\cdots,Q_N\right)}{\partial\left(u_1,\cdots,u_{N-1},\lambda\right)}\right], \tag{4.2.2c}$$

and the BA operator Q_i (2.1.20) takes the explicit form:

$$Q_i(\hat{u};\Delta,\tau)\equiv e^{2\pi i\lambda}\prod_{j=1}^{N}\frac{\theta_1(u_{ji}+\Delta_1;\tau)\theta_1(u_{ji}+\Delta_2;\tau)\theta_1(u_{ji}-\Delta_1-\Delta_2;\tau)}{\theta_1(u_{ij}+\Delta_1;\tau)\theta_1(u_{ij}+\Delta_2;\tau)\theta_1(u_{ij}-\Delta_1-\Delta_2;\tau)}. \tag{4.2.3}$$

recalling that the BAEs are given as

$$Q_i(\hat{u};\Delta,\tau)=1. \tag{4.2.4}$$

As we reviewed in section 2.1, the BA operator has a double-periodicity, namely

$$Q_i(\hat{u};\Delta,\tau)=Q_i(\hat{u}';\Delta,\tau) \tag{4.2.5}$$

for two sets of holonomies

$$\begin{aligned}\hat{u}&=\{u_i|i=1,\cdots,N\},\\ \hat{u}'&=\{u_i+m_i+n_i\tau|\,m_i,n_i\in\mathbb{Z},\ i=1,\cdots,N\}.\end{aligned} \tag{4.2.6}$$

Hence, if we find one solution $\hat{u}$ to the BAEs (4.2.4), we can generate infinitely many solutions $\hat{u}'$ with different sets of integers m_i's and n_i's. Since the building blocks $\mathcal{Z}(\hat{u};\Delta,\tau)$ and $H(\hat{u};\Delta,\tau)$ are invariant under $\hat{u}\to\hat{u}'$ (4.2.6) provided $\hat{u}$ is a solution to the BAEs (4.2.4) [38], the contributions from these infinitely many BAE solutions to the index through (4.2.1) are all identical.

One of the simplest solution to the BAEs (4.2.4) is a so-called 'basic' solution, namely

$$\hat{u}_{\text{basic}}=\left\{u_i=\bar{u}+\frac{i}{N}\tau\,\middle|\,i=1,2,\cdots,N-1\right\}\bigcup\{u_N=\bar{u}\} \tag{4.2.7}$$

where $\bar{u}$ is determined as

$$N\bar{u}+\frac{N(N-1)}{2}\tau\in\mathbb{Z} \tag{4.2.8}$$

from the $SU(N)$ constraint $\sum_{i=1}^{N}u_i\in\mathbb{Z}$. Due to the double-periodicity of the BA operator (4.2.5), there are infinitely many basic solutions as

$$\hat{u}_{\text{basic}}=\left\{u_i=\bar{u}+\frac{i}{N}\tau+m_i+n_i\tau\,\middle|\,i=1,2,\cdots,N-1\right\}\bigcup\{u_N=\bar{u}+m_N+n_N\tau\} \tag{4.2.9}$$

with arbitrary integers m_i's and n_i's. Note that m_i's are redundant since u_i's are defined modulo integers in the first place in (2.1.14) due to periodicity (see the cylinder in Figure 1).

In this section, we will compute the contribution from these basic solutions to the SCI through the BA formula (4.2.1) in the large-N limit, assuming that it dominates the other contributions.

Degeneracy

To determine the contribution from infinitely many basic solutions (4.2.9) to the index through the BA formula (4.2.1), first we must figure out how many times we should add the contribution from a single basic solution: in short, we need the 'relevant degeneracy' of basic solutions. There are two possible origins of degeneracies:

$$i)\ \text{The \# of permuting } N \text{ holonomies within a given basic solution } \hat{u}_{\text{basic}} \tag{4.2.10a}$$

$$ii)\ \text{The \# of } \bar{u} \text{ and } n_i's \text{ which yield inequivalent basic solutions } \hat{u}_{\text{basic}}. \tag{4.2.10b}$$

The $i)$ factor is obviously $N!$. The $ii)$ factor should be treated more carefully. First, the number of $\bar{u}$ that yields inequivalent basic solutions is given from (4.2.8) as N, namely

$$\bar{u}\in\left\{\frac{k}{N}-\frac{N-1}{2}\tau\,\middle|\,k=0,1,\cdots,N-1\right\}. \tag{4.2.11}$$

The infinitely many inequivalent basic solutions obtained by manipulating n_i's, however, must *not* be taken into the 'relevant degeneracy' when we compute the index using (4.2.1). This is because, the equation (3.9) of [39] restricts u_i's to be inside the fundamental domain. To be specific, it requires

$$0\le\text{Im}[u_i]<\text{Im}\tau, \tag{4.2.12}$$

which uniquely fixes every n_i. Hence the relevant degeneracy of a basic solution is $N\times N!$. Consequently, the BA formula (4.2.1) reads

$$\begin{aligned}\mathcal{I}(\tau;\Delta)=N\times N!\times\kappa_N\mathcal{Z}(\hat{u}_{\text{basic}};\Delta,\tau)H(\hat{u}_{\text{basic}};\Delta,\tau)^{-1}\\+\,(\text{from other BA solutions}).\end{aligned} \tag{4.2.13}$$

We focus on the logarithm of the basic contribution, namely the first line of (4.2.13):

$$\begin{aligned}\log \mathcal{I}(\tau;\Delta)\big|_{\text{Basic BA}} &= \log N! + \log N + \log \kappa_N \\ &\quad + \log \mathcal{Z}(\hat{u}_{\text{basic}};\Delta,\tau) - \log H(\hat{u}_{\text{basic}};\Delta,\tau).\end{aligned} \tag{4.2.14}$$

The contribution $\log \kappa_N$ can be written explicitly from the definition (4.2.2a) as

$$\log \kappa_N = -\log N! + (N-1)\left(\sum_{a=1}^{3} \log \widetilde{\Gamma}(\Delta_a;\tau) + 2\log(q;q)_\infty\right). \tag{4.2.15}$$

In the remaining part of this section, we compute the remaining two contributions in the second line of (4.2.14) in order, mainly following the results of [38]. We omit the subscript 'basic' of $\hat{u}_{\text{basic}}$ for notational convenience from here on.

The contribution from $\log \mathcal{Z}(\hat{u};\Delta,\tau)$

The contribution $\log \mathcal{Z}(\hat{u};\Delta;\tau)$ to the index (4.2.14) can be written explicitly as

$$\log \mathcal{Z}(\hat{u};\Delta;\tau) = \sum_{i\neq j}^{N}\left(\sum_{a=1}^{3} \log \widetilde{\Gamma}(\frac{i-j}{N}\tau + \Delta_a;\tau) - \log \widetilde{\Gamma}(\frac{i-j}{N}\tau;\tau)\right). \tag{4.2.16}$$

To simplify the expression (4.2.16) further, recall that section 4 of [38] yields

$$\begin{aligned}\sum_{i\neq j}^{N} \log \widetilde{\Gamma}(\frac{i-j}{N}\tau + \Delta_a;\tau) &= 2\pi i \sum_{i\neq j}^{N} Q(\frac{i-j}{N}\tau + \{\Delta_a\}_\tau;\tau) - N\log\frac{\theta_0(\frac{N(\{\Delta_a\}_\tau-1)}{\tau};-\frac{N}{\tau})}{\theta_0(\frac{\{\Delta_a\}_\tau-1}{\tau};-\frac{1}{\tau})} \\ &\quad + \sum_{k=0}^{\infty}\left(\log\frac{\psi(\frac{N(k+\{\Delta_a\}_\tau)}{\tau})}{\psi(\frac{N(k+1-\{\Delta_a\}_\tau)}{\tau})} - N\log\frac{\psi(\frac{k+\{\Delta_a\}_\tau}{\tau})}{\psi(\frac{k+1-\{\Delta_a\}_\tau}{\tau})}\right),\end{aligned} \tag{4.2.17a}$$

$$\sum_{i\neq j}^{N} \log \widetilde{\Gamma}(\frac{i-j}{N}\tau;\tau) = 2\pi i \sum_{i\neq j}^{N} Q(\frac{i-j}{N}\tau + 1;\tau) - N\log N - 2N\log\frac{(\tilde{q}^N;\tilde{q}^N)_\infty}{(\tilde{q};\tilde{q})_\infty} + \frac{\pi i}{12}(N-1), \tag{4.2.17b}$$

where we have followed the conventions of $\theta_0(u;\tau)$ and $\psi(u)$ in Appendix A and also defined $\tilde{q} \equiv e^{-\frac{2\pi i}{\tau}}$ and

$$Q(u;\tau) \equiv -\frac{B_3(u)}{6\tau^2} + \frac{B_2(u)}{2\tau} - \frac{5}{12}B_1(u) + \frac{\tau}{12} \tag{4.2.18}$$

in terms of Bernoulli polynomials $B_n(x)$. Then, following the conventions introduced in Appendix A, we can show that some of the contributions in (4.2.17) are exponentially suppressed in the large-N limit as

$$\log\left(\tilde{q}^N;\tilde{q}^N\right)_\infty = \mathcal{O}(e^{-\frac{2\pi N \sin(\arg\tau)}{|\tau|}}), \tag{4.2.19a}$$

$$\theta_0(\frac{N(\{\Delta_a\}_\tau-1)}{\tau};-\frac{N}{\tau}) = \mathcal{O}(e^{-\frac{2\pi N \sin(\arg\tau)}{|\tau|}\min(\{\tilde{\Delta}_a\},1-\{\tilde{\Delta}_a\})}), \tag{4.2.19b}$$

$$\sum_{k=0}^{\infty}\log\psi(\frac{N(k+1-\{\Delta_a\}_\tau)}{\tau}) = \mathcal{O}(Ne^{-\frac{2\pi N \sin(\arg\tau)}{|\tau|}(1-\{\tilde{\Delta}_a\})}), \tag{4.2.19c}$$

$$\sum_{k=0}^{\infty}\log\psi(\frac{N(k+\{\Delta_a\}_\tau)}{\tau}) = \mathcal{O}(Ne^{-\frac{2\pi N \sin(\arg\tau)}{|\tau|}\{\tilde{\Delta}_a\}}), \tag{4.2.19d}$$

where we have assumed

$$\{\tilde{\Delta}_a\} \not\to 0, 1. \tag{4.2.20}$$

Ignoring the above exponentially suppressed terms and using the identity (A.10), we can simplify (4.2.17) as

$$\begin{aligned}\sum_{i\neq j}^{N} \log\widetilde{\Gamma}(\frac{i-j}{N}\tau+\Delta_a;\tau) = &-\frac{\pi i N^2(\{\Delta_a\}_\tau-\tau)(\{\Delta_a\}_\tau-\tau-\frac{1}{2})(\{\Delta_a\}_\tau-\tau-1)}{3\tau^2}\\ &+\frac{\pi i(\{\Delta_a\}_\tau-\tau-\frac{1}{2})}{6}-N\log\widetilde{\Gamma}(\Delta_a;\tau)\\ &+\mathcal{O}(Ne^{-\frac{2\pi N\sin(\arg\tau)}{|\tau|}\min(\{\tilde{\Delta}_a\},1-\{\tilde{\Delta}_a\})}),\end{aligned} \tag{4.2.21a}$$

$$\begin{aligned}\sum_{i\neq j}^{N} \log\widetilde{\Gamma}(\frac{i-j}{N}\tau;\tau) = &\frac{\pi i N^2(\tau-\frac{1}{2})(\tau-1)}{3\tau}-\frac{\pi i N(\tau^2-3\tau+1)}{6\tau}-\frac{\pi i\tau}{6}\\ &-N\log N+2N\log(\tilde{q};\tilde{q})_\infty+\mathcal{O}(e^{-\frac{2\pi N\sin(\arg\tau)}{|\tau|}}).\end{aligned} \tag{4.2.21b}$$

Finally, substituting (4.2.21) into (4.2.16) and introducing $\eta\in\{\pm1\}$ as (4.1.11), we obtain

$$\begin{aligned}\log\mathcal{Z}(\hat{u};\Delta_a,\tau) = &-\frac{\pi i N^2}{\tau^2}\prod_{a=1}^{3}\left(\{\Delta_a\}_\tau-\frac{1+\eta}{2}\right)+\frac{(1-\eta)\pi i}{2}N^2+\frac{\eta\pi i}{12}\\ &+N\log N-N\sum_{a=1}^{3}\log\widetilde{\Gamma}(\Delta_a;\tau,\tau)-2N\log(\tilde{q};\tilde{q})_\infty\\ &+\frac{\pi i N(\tau^2-3\tau+1)}{6\tau}+\mathcal{O}(Ne^{-\frac{2\pi N\sin(\arg\tau)}{|\tau|}\min(\{\tilde{\Delta}_a\},1-\{\tilde{\Delta}_a\})}).\end{aligned} \tag{4.2.22}$$

The contribution from $-\log H(\hat{u};\Delta,\tau)$

Next we consider the contribution from the Jacobian to the index (4.2.1), which has been already studied in [68]. In particular, section 2.2 of [68] yields[12]

$$\begin{aligned}-\log H(\hat{u};\Delta,\tau) = &-\log N-(N-1)\log\left(\frac{i}{\pi}\sum_{\Delta}\partial_\Delta\log\theta_1(\Delta;\frac{\tau}{N})\right)\\ &+\log\det\Big(I_{N-1}+\tilde{H}(\hat{u};\Delta,\tau)\Big),\end{aligned} \tag{4.2.23}$$

where Δ take values in $\{\Delta_1,\Delta_2,-\Delta_1-\Delta_2\}$ and we have defined an $(N-1)\times(N-1)$ square matrix $\tilde{H}$ as

$$\Big[\tilde{H}(\hat{u};\Delta,\tau)\Big]_{\mu\nu} \equiv \frac{g(\mu;\Delta,\tau)-g(\mu-\nu;\Delta,\tau)}{\sum_{k=1}^{N}g(k;\Delta,\tau)}, \tag{4.2.24a}$$

$$g(j;\Delta,\tau) \equiv \frac{i}{2\pi}\sum_{\Delta}\partial_\Delta\log\left[\theta_1(\frac{j}{N}\tau+\Delta;\tau)\theta_1(-\frac{j}{N}\tau+\Delta;\tau)\right]. \tag{4.2.24b}$$

[12] Note $\Delta_a^{\text{there}} = 2\pi\Delta_a^{\text{here}}$ $(a=1,2)$ and $\theta_1(2\pi u;\tau)^{\text{there}} = \theta_1(u;\tau)^{\text{here}}$.

The second term of (4.2.23) can be computed explicitly in the large-N limit using the asymptotic expansion of the elliptic theta function (A.19) as

$$\frac{i}{\pi}\sum_{\Delta}\partial_{\Delta}\log\theta_1(\Delta;\frac{\tau}{N})=\eta\frac{N}{\tau}+\mathcal{O}(e^{-\frac{2\pi N\sin(\arg\tau)}{|\tau|}\min(\{\tilde{\Delta}_a\},1-\{\tilde{\Delta}_a\})}) \tag{4.2.25}$$

under the assumption (4.2.20). Here we have used $\sum_{\Delta}\{\Delta\}_\tau=\frac{3+\eta}{2}$ from (4.1.11) and $\Delta\in\{\Delta_1,\Delta_2,-\Delta_1-\Delta_2\}$. Substituting (4.2.25) into (4.2.23) then gives

$$\begin{aligned}-\log H(\hat{u};\Delta,\tau)=&-N\log N+(N-1)\log\frac{\tau}{\eta}-\log\det\Big(I_{N-1}+\tilde{H}(\hat{u};\Delta,\tau)\Big)\\&+\mathcal{O}(e^{-\frac{2\pi N\sin(\arg\tau)}{|\tau|}\min(\{\tilde{\Delta}_a\},1-\{\tilde{\Delta}_a\})}).\end{aligned} \tag{4.2.26}$$

The final step would be therefore estimating $-\log\det(I_{N-1}+\tilde{H})$.

Since it is difficult to estimate $-\log\det(I_{N-1}+\tilde{H})$ in general, first we take the Cardy-like limit $|\tau|\ll 1$. Using the asymptotic formula (A.19), we can obtain the Cardy-like expansion of the g-function (4.2.24b) under the assumption (4.2.20) as

$$g(j;\Delta,\tau)=\frac{\eta}{\tau}+\mathcal{O}(e^{-\frac{2\pi\sin(\arg\tau)}{|\tau|}\min(\{\tilde{\Delta}_a\},1-\{\tilde{\Delta}_a\})}), \tag{4.2.27}$$

where we have used $\sum_{\Delta}\{\Delta\}_\tau=\frac{3+\eta}{2}$ as before. Substituting (4.2.27) back into $[\tilde{H}(\hat{u};\Delta,\tau)]_{\mu\nu}$ (4.2.24a) then gives

$$\tilde{H}_{\mu\nu}=\mathcal{O}(N^{-1}e^{-\frac{2\pi\sin(\arg\tau)}{|\tau|}\min(\{\tilde{\Delta}_a\},1-\{\tilde{\Delta}_a\})}). \tag{4.2.28}$$

The contribution from the Jacobian (4.2.26) is then simplified as

$$-\log H(\hat{u};\Delta,\tau)=-N\log N+(N-1)\log\frac{\tau}{\eta}+\mathcal{O}(e^{-\frac{2\pi\sin(\arg\tau)}{|\tau|}\min(\{\tilde{\Delta}_a\},1-\{\tilde{\Delta}_a\})}) \tag{4.2.29}$$

in the Cardy-like limit [68].

We want to estimate $-\log\det(I_{N-1}+\tilde{H})$ in the large-N limit, however, not in the Cardy-like limit. To do that, we use the Gershgorin Circle Theorem: every eigenvalue of $\tilde{H}$ lies within at least one of the $N-1$ Gershgorin discs ($\mu=1,2,\cdots,N-1$)

$$D(\tilde{H}_{\mu\mu},\sum_{\nu=1\,(\neq\mu)}^{N-1}|\tilde{H}_{\mu\nu}|), \tag{4.2.30}$$

where the first and the second argument of $D(\cdot,\cdot)$ denotes the center and the radius of a disk respectively. Due to (4.2.28), every Gershgorin disc can be located within the unit disk whose center is at the origin for a small enough but finite $|\tau|$, and therefore every eigenvalue of the matrix $\tilde{H}$ has modulus less than 1 in that regime. Hence we can estimate $-\log\det(I_{N-1}+\tilde{H})$ for a small enough $|\tau|$ as

$$-\log\det(I_{N-1}+\tilde{H})=-\mathrm{Tr}\Big[\log(I_{N-1}+\tilde{H})\Big]=\mathrm{Tr}\Big(\sum_{n=1}^{\infty}\frac{1}{n}(-\tilde{H})^n\Big)=\mathcal{O}(N^0). \tag{4.2.31}$$

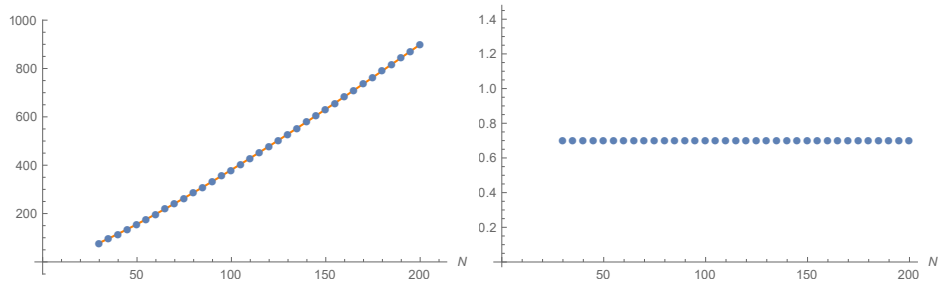


Figure 18: In the left hand side, blue dots represent numerical values of the real part of the Jacobian contribution $\mathrm{Re}\log H(\hat{u};\Delta,\tau)$ and an orange line shows the first two leading terms read from (4.2.26), namely $N\log N-(N-1)\log|\tau|$. The figure in the right hand side shows numerical values of $\mathrm{Re}\log\det(I_{N-1}+\tilde{H})$, obtained by subtracting an orange line from blue dots in the left hand side. It converges to a certain finite value and therefore we can conclude it is of order $\mathcal{O}(N^0)$.

Here we have used that every eigenvalue of $\tilde{H}_{\mu\nu}$ has modulus less than 1 for the taylor expansion of a logarithm in the 2nd equation. The Jacobian contribution (4.2.26) is then estimated as

$$-\log H(\hat{u};\Delta,\tau)=-N\log N+(N-1)\log\frac{\tau}{\eta}+\mathcal{O}(N^0). \tag{4.2.32}$$

for a small enough but finite $|\tau|$.

We have not been able to estimate $-\log\det(I_{N-1}+\tilde{H})$ analytically for a generic finite τ, which allows for some eigenvalues of $\tilde{H}$ to be greater than equal to 1. Hence we move on to a numerical analysis: we investigate $-\log\det(I_{N-1}+\tilde{H})$ with $\Delta_1=\frac{1}{\pi}$, $\Delta_2=\frac{1}{e}$, and $\tau=2+i$ for $N=30,35,\cdots,200$ numerically. In this case the corresponding matrix $\tilde{H}$ (4.2.24a) has some eigenvalues greater than 1 so we cannot rely on the analytic argument (4.2.31). As one can see in Figure 18, however, $-\log\det(I_{N-1}+\tilde{H})$ still seems to be of order $\mathcal{O}(N^0)$. We obtained similar results with other chemical potentials Δ_a's and τ. Based on this numerical analysis, we believe that (4.2.31) and (4.2.32) are valid for a generic finite τ in fact.

The sum of all contributions

Substituting (4.2.15), (4.2.22), (4.2.26) into (4.2.14) and using the identity (A.9a), finally we have

$$\begin{aligned}\log\mathcal{I}(\tau;\Delta)\big|_{\text{Basic BA}}=&-\frac{\pi iN^2}{\tau^2}\prod_{a=1}^{3}\left(\{\Delta_a\}_\tau-\frac{1+\eta}{2}\right)+\log N-\sum_{a=1}^{3}\log\widetilde{\Gamma}(\Delta_a;\tau)\\&-2\log(q;q)_\infty+\frac{(1-\eta)\pi iN(N-1)}{2}+\frac{\pi i(6-5\eta)}{12}\\&-\log\tau-\log\det(I_{N-1}+\tilde{H}(\hat{u};\Delta,\tau))\\&+\mathcal{O}(e^{-\frac{2\pi N\sin(\arg\tau)}{|\tau|}\min(\{\tilde{\Delta}_a\},1-\{\tilde{\Delta}_a\})}).\end{aligned} \tag{4.2.33}$$

Recall that $\log\det(I_{N-1}+\tilde{H})$ is of order $\mathcal{O}(N^0)$ as we have discussed in (4.2.31) so this can be written simply as

$$\boxed{\log\mathcal{I}(\tau;\Delta)\big|_{\text{Basic BA}}=-\frac{\pi iN^2}{\tau^2}\prod_{a=1}^{3}\left(\{\Delta_a\}_\tau-\frac{1+\eta}{2}\right)+\log N+\mathcal{O}(N^0)} \tag{4.2.34}$$

in the large-N limit, where we have neglected the pure imaginary term $\frac{(1-\eta)\pi i N(N-1)}{2}$ since it is of the form $2\pi i\mathbb{Z}$ due to $\eta \in \{\pm 1\}$.

If we take the Cardy-like limit after the large-N limit, we can simplify (4.2.33) further using the Cardy-like Jacobian contribution (4.2.29), the asymptotic expansion of a Pochhammer symbol (A.12), and the following expansion

$$\sum_{a=1}^{3}\log\widetilde{\Gamma}(\Delta_a;\tau) = -\frac{\pi i}{\tau^2}\prod_{a=1}^{3}\left(\{\Delta_a\}_\tau - \frac{1+\eta}{2}\right) + \frac{\pi i(\tau-2\eta)(2\tau-\eta)}{12\tau} + \mathcal{O}(e^{-\frac{2\pi\sin(\arg\tau)}{|\tau|}\min(\{\tilde{\Delta}_a\},1-\{\tilde{\Delta}_a\})}) \tag{4.2.35}$$

derived from (A.21). The result is given as

$$\boxed{\log\mathcal{I}(\tau;\Delta)\big|_{\text{Basic BA}} = -\frac{\pi i(N^2-1)}{\tau^2}\prod_{a=1}^{3}\left(\{\Delta_a\}_\tau - \frac{1+\eta}{2}\right) + \log N + \mathcal{O}(e^{-\frac{2\pi\sin(\arg\tau)}{|\tau|}\min(\{\tilde{\Delta}_a\},1-\{\tilde{\Delta}_a\})}).} \tag{4.2.36}$$

Similarly to what we obtained in section 4.1, the $\frac{1}{\tau^2}$ contribution coincides with the one reported in [38] and the logarithmic correction agrees perfectly with the result derived using the saddle-point approach. The origin of the $\log N$ term can be found in the 'relevant degeneracy' of the BA solutions and we will show a similar result for more generic SCFT's.

4.2.2 Bethe Ansatz approximation for generic $\mathcal{N}=1$ SCFT

The goal of this section is to extend the results obtained for the SCI of $\mathcal{N}=4$ SYM to the SCI of more generic quiver gauge theories following the techniques applied in [1, 55]. The formula for the SCI in terms of solutions to the BAEs [39, 40]:

$$\begin{aligned}
\mathcal{I}(\tau;\Delta) &= \kappa_G \sum_{\hat{u}\in\text{BA}} \mathcal{Z}_{tot}(\hat{u};\Delta,\tau)\, H(\hat{u};\Delta,\tau)^{-1}, \\
\kappa_G &= \bar{\kappa}_G \times \left(\prod_{\Phi_{ab}}\widetilde{\Gamma}(\Delta_{ab};\tau)\right)^{\text{rk}(G)}, \\
\mathcal{Z}_{tot}(u;\Delta,\tau) &= \frac{\prod_{\Phi_{ab}}\prod_{i_a\neq j_b}\widetilde{\Gamma}(u_{i_a}-u_{j_b}+\Delta_{ab};\tau)}{\prod_{a=1}^{n_v}\prod_{i_a\neq j_a}\widetilde{\Gamma}\left(u^a_{ij};\tau,\tau\right)}, \\
H(u;\Delta,\tau) &= \det\left[\frac{1}{2\pi i}\frac{\partial Q_{i_a}(u;,\Delta,\tau)}{\partial u_{j_b}}\right]_{i_a j_b}.
\end{aligned} \tag{4.2.37}$$

Where we are interested in solutions of the BA equations, which we write as:

$$Q_{i_a}(u;\Delta,\tau) = e^{2\pi i\left(\sum_b\lambda_b - \sum_{j_b}u^{ab}_{ij}\right)}\prod_{\langle a,b\rangle}\prod_{j_b}\frac{\theta_0\left(-u^{ab}_{ij}+\Delta_{ab};\tau\right)}{\theta_0\left(-u^{ba}_{ji}+\Delta_{ab};\tau\right)} = 1, \tag{4.2.38}$$

where the notation is such that $\langle a,b\rangle$ represents the set of chiral multiplets Φ_{ab} for a fixed value of a. We evaluate in BA solutions of the form: $u^{ab}_{ij} = \frac{\tau}{N}(i_a - j_b)$. These solutions appeared first

in [52] while evaluating the topologically twisted of 4d $\mathcal{N}=1$ theories on $T^2\times S^2$ in the high temperature limit; it was later shown in [68] that such configuration provides an exact solution to the BAEs. We showed in section 3.1 that this type of solution indeed satisfies the BA equations (4.2.38) and provides the expected leading contribution of the form (4.1.48) (see also [1, 55]). Let us now proceed to take the large N limit of (4.2.37) keeping track of corrections of sub-leading corrections.

The contribution from κ_G and degeneracy

Starting from κ_G in (4.2.37) we take the large N limit:

$$n_{\rm v}N|\mathcal{W}_G|\kappa_G = n_{\rm v}N\,(q;q)_\infty^{2n_{\rm v}(N-1)}\left(\prod_{\Phi_{ab}}\widetilde{\Gamma}\left(\Delta_{ab};\tau\right)\right)^{N-1}, \tag{4.2.39}$$
$$\log n_{\rm v}N+\log\left(|\mathcal{W}_G|\kappa_G\right) = \log n_{\rm v}N+2n_{\rm v}(N-1)\log\left(q;q\right)_\infty+(N-1)\sum_{\Phi_{ab}}\log\widetilde{\Gamma}\left(\Delta_{ab};\tau\right).$$

The factor $n_{\rm v}N$ in (4.2.39) enters if we include the possibility of shifting each holonomy in the BA solution N of times yielding inequivalent basic solutions .

The contribution from $\mathcal{Z}_{tot}$

Let us now consider the expression for $\log\mathcal{Z}_{tot}$:

$$\begin{aligned}\log\mathcal{Z}_{tot} &= \log\left(\frac{\prod_{\Phi_{ab}}\prod_{i_a\neq j_b}\widetilde{\Gamma}\left(u_{i_a}-u_{j_b}+\Delta_{ab};\tau\right)}{\prod_{a=1}^{n_{\rm v}}\prod_{i_a\neq j_a}\widetilde{\Gamma}\left(u^a_{ij};\tau,\tau\right)}\right)\\ &= \sum_{\Phi_{ab}}\sum_{i_a\neq j_b}\log\widetilde{\Gamma}\left(u_{i_a}-u_{j_b}+\Delta_{ab};\tau\right)-\sum_{a=1}^{n_{\rm v}}\sum_{i_a\neq j_a}\log\widetilde{\Gamma}\left(u^a_{ij};\tau\right).\end{aligned} \tag{4.2.40}$$

Taking the large N limit here requires just to reproduce the same calculation of section 4.2.1, only there are $n_{\rm v}$ contributions coming from the vector multiplets and we sum over n_χ chiral multiplets. Explicitly we have:

$$\widetilde{\Gamma}\left(u^{ab}_{ij}+\Delta_{ab};\tau\right) = \frac{e^{-\pi i\widetilde{\mathcal{Q}}\left(u^{ab}_{ij}+\Delta_{ab};\tau\right)}}{\theta_0\left(\frac{u^{ab}_{ij}+\Delta_{ab}}{\tau};-\frac{1}{\tau}\right)}\times\prod_{k=0}^{\infty}\frac{\psi\left(\frac{k+1+u^{ab}_{ij}}{\tau}\right)}{\psi\left(\frac{k-u^{ab}_{ij}-\Delta_{ab}}{\tau}\right)}, \tag{4.2.41}$$
$$\begin{aligned}\widetilde{\mathcal{Q}}\left(u+\Delta;\tau,\tau\right) = {}& \frac{u^3}{3\tau^2}+u^2\left(\frac{\Delta}{\tau^2}-\frac{2\tau-1}{2\tau^2}\right)+u\left(\frac{1-6\tau+5\tau^2}{6\tau^2}+\frac{\Delta^2}{\tau^2}-\frac{2\tau-1}{\tau^2}\Delta\right)-\\ &-\frac{\Delta^2}{2\tau^2}\left(2\tau-1\right)+\frac{\Delta}{6\tau^2}\left(5\tau^2-6\tau+1\right)+\frac{1}{12\tau^2}\left(2\tau-1\right)\left(2\tau-\tau^2\right)+\frac{\Delta^3}{\tau^2}.\end{aligned}$$

Note that, the leading contribution coming from vector multiplets can be obtained from (4.2.41) by setting $\Delta_{ab}=0$. We can write:

$$\begin{aligned}
\log \mathcal{Z}_{tot} &= \sum_{\Phi_{ab}} \sum_{i_a \neq j_b} \log \widetilde{\Gamma}\left(u_{ij}^{ab}+\Delta_{ab};\tau,\tau\right) - \sum_{a=1}^{n_{\rm v}} \sum_{i_a \neq j_a} \widetilde{\Gamma}\left(u_{ij}^{a},\tau,\tau\right) \\
&= -i\pi \sum_{\Phi_{ab}} \sum_{i_a \neq j_b} \widetilde{\mathcal{Q}}\left(u_{ij}^{ab}+\Delta_{ab};\tau,\tau\right) + \sum_{\Phi_{ab}} \sum_{i_a \neq j_b} \sum_{k=0}^{\infty} \log \frac{\psi\left(\frac{k+1+u_{ij}^{ab}}{\tau}\right)}{\psi\left(\frac{k-u_{ij}^{ab}-\Delta_{ab}}{\tau}\right)} \\
&\quad - \sum_{\Phi_{ab}} \sum_{i_a \neq j_b} \log \theta_0\left(\frac{u_{ij}^{ab}+\Delta_{ab}}{\tau};-\frac{1}{\tau}\right) \\
&\quad + i\pi n_{\rm v} \sum_{i\neq j}^{N} \widetilde{\mathcal{Q}}\left(u_{ij};\tau\right) + n_{\rm v} N \log N + 2 n_{\rm v} N \log \frac{\left(\widetilde{q}^N;\widetilde{q}^N\right)_\infty}{\left(\widetilde{q};\widetilde{q}\right)_\infty} - \frac{i n_{\rm v}\pi}{12}\left(N-1\right) \\
&= -\frac{i\pi N^2}{3\tau^2} \sum_{\Phi_{ab}} B_3\left(\left[\Delta_{ab}\right]_\tau - \tau + 1\right) + i\pi \sum_{\Phi_{ab}} \frac{\left(\left[\Delta_{ab}\right]_\tau - \tau + \frac{1}{2}\right)}{6} \\
&\quad - N \sum_{\Phi_{ab}} \log \widetilde{\Gamma}\left(\Delta_{ab};\tau,\tau\right) - n_{\rm v} \frac{i\pi}{3\tau^2} N(N-1) B_3(\tau) - n_{\rm v} \frac{i\pi}{6}(N-1)\tau \\
&\quad + n_{\rm v} N \log N - 2 n_{\rm v} N \log\left(\widetilde{q};\widetilde{q}\right)_\infty + \mathcal{O}\left(N e^{-\frac{N}{|\tau|}}\right),
\end{aligned} \tag{4.2.42}$$

where once again we have used the relation $\{x\}_\tau = [x]_\tau + 1$. Equation (4.2.42) can be simplified making use of (4.1.35) in the following way

$$\begin{aligned}
\log \mathcal{Z}_{tot} &= -\frac{i\pi N^2}{3\tau^2} \sum_{\Phi_{ab}} B_3\left(\left[\Delta_{ab}\right]_\tau - \tau + 1\right) + \frac{i\pi}{12} \sum_{a=1}^{n_{\rm v}} \eta_a \\
&\quad - N \sum_{\Phi_{ab}} \log \widetilde{\Gamma}\left(\Delta_{ab};\tau\right) - n_{\rm v} \frac{i\pi}{3\tau^2} N(N-1) B_3(\tau) - n_{\rm v} \frac{i\pi}{6} N\tau \\
&\quad + n_{\rm v} N \log N - 2 n_{\rm v} N \log\left(\widetilde{q};\widetilde{q}\right)_\infty + \mathcal{O}\left(N e^{-\frac{N}{|\tau|}}\right).
\end{aligned} \tag{4.2.43}$$

If we remain within the domain of chemical potentials (4.1.36), which in the case of $\mathcal{N}=4$ SYM corresponds to taking $\eta=1$, and perform the shifting $\Delta_l \to \Delta_l - \frac{2\tau}{d}$, we have

$$\begin{aligned}
\log \mathcal{Z}_{tot} &= -\frac{i\pi N^2}{6\tau^2} C_{IJK} \left[\Delta_I\right]_\tau \left[\Delta_J\right]_\tau \left[\Delta_K\right]_\tau + \frac{i\pi}{12} \sum_{a=1}^{n_{\rm v}} \eta_a + \frac{i\pi n_{\rm v} N}{3\tau^2} B_3(\tau) - n_{\rm v} \frac{i\pi}{6} N\tau \\
&\quad - N \sum_{\Phi_{ab}} \log \widetilde{\Gamma}\left(\Delta_{ab};\tau\right) + n_{\rm v} N \log N - 2 n_{\rm v} N \log\left(\widetilde{q};\widetilde{q}\right)_\infty + \mathcal{O}\left(N e^{-\frac{N}{|\tau|}}\right).
\end{aligned} \tag{4.2.44}$$

The contribution from the Jacobian

Let us consider the contribution from the Jacobian H in (4.2.38). We need to study the large N behavior of the matrix elements of the Jacobian matrix. The explicit form of the Jacobian is the following:

$$H = \det\left[\frac{1}{2\pi i} \frac{\partial\left(Q_{1_1},\cdots,Q_{N_1},\cdots,Q_{1_{n_{\rm v}}},\cdots,Q_{N_{n_{\rm v}}}\right)}{\partial\left(u_{1_1},\cdots,u_{N_1-1},\lambda_1,\cdots,u_{1_{n_{\rm v}}},\cdots,u_{N_{n_{\rm v}}-1},\lambda_{n_{\rm v}}\right)}\right], \tag{4.2.45}$$

where the BA operator is given as

$$Q_{i_a}\left(u;\Delta,\tau\right)=e^{2\pi i\left(\sum_b \lambda_b-\sum_{j_b} u_{ij}^{ab}\right)}\prod_{\langle a,b\rangle}\prod_{j_b}\frac{\theta_0\left(-u_{ij}^{ab}+\Delta_{ab};\tau\right)}{\theta_0\left(-u_{ji}^{ba}+\Delta_{ba};\tau\right)}. \tag{4.2.46}$$

Equation (4.2.45) is the determinant of an $n_{\rm v}N\times n_{\rm v}N$ matrix that can be seen as $n_{\rm v}\times n_{\rm v}$ blocks of $N\times N$ matrices. For each fixed values of a,b, one can run the argument in section 4.2.1 to show that the determinant is factorized as

$$H=\det H_{i_a,j_b}=N^{n_{\rm v}}\det H_{\mu_a\nu_b}, \tag{4.2.47}$$

where Greek letters take values $\mu_a=1,\cdots,N-1$ for each $a\in\{1,\cdots,n_v\}$. Consider now the following matrix element evaluated in the BA solutions:

$$\begin{aligned}H_{\mu_a,\nu_b}\Big|_{\rm BA}&=\frac{1}{2\pi i}\frac{\partial\log Q_{\mu_a}}{\partial u_{\nu_b}}\Big|_{\rm BA}\\&=\sum_{\langle a,c\rangle}\sum_{\nu_b}\left[\left(-\frac{\partial u_{\mu,\sigma}^{ac}}{\partial u_{\nu_b}}\right)\Big|_{\rm BA}+\frac{1}{2\pi i}\frac{\partial}{\partial u_{\nu_b}}\log\frac{\theta_0\left(-u_{\mu,\sigma}^{ac}+\Delta_{ac};\tau\right)}{\theta_0\left(-u_{\sigma,\mu}^{ca}+\Delta_{ca};\tau\right)}\Big|_{\rm BA}\right].\end{aligned} \tag{4.2.48}$$

As already seen in 4.2.1, the only important contribution in the large N limit of (4.2.48) comes from the sum $\sum_{\nu_b}$ and it is of the form $\sim N-1$. Moreover, the structure of (4.2.48) thus, we have:

$$\begin{aligned}-\log\det H_{\mu_a,\nu_b}&=(N-1)\log\left(\prod_{a=1}^{n_{\rm v}}\frac{i}{2\pi}\sum_{\phi_a=1}^{n_{\phi a}}\partial_{\Delta_{\phi_a}}\log\theta_1(\Delta_{\phi_a};\frac{\tau}{N})\right)+\mathcal{O}(N^0)\\&=(N-1)\log\left(\prod_{a=1}^{n_{\rm v}}\frac{\tau}{N\eta_a}\right)+\mathcal{O}(N^0)\\&=-n_{\rm v}N\log N+n_{\rm v}\log N+n_{\rm v}(N-1)\log\tau+\mathcal{O}(N^0),\end{aligned} \tag{4.2.49}$$

which is an immediate generalization of (4.2.32). We have used $\eta_a=1,\ \forall\ a=1,\cdots,n_{\rm v}$, which can be proven using (4.1.35) and the conservation of flavor $U(1)$ charges. Inserting (4.2.49) into the log of (4.2.47), we obtain

$$-\log H=-\log\det H_{i_aj_b}=-n_{\rm v}N\log N+n_{\rm v}(N-1)\log\tau+\mathcal{O}(N^0). \tag{4.2.50}$$

The sum of all contributions

After collecting the results (4.2.39), (4.2.44), and (4.2.50) all together, we obtain

$$\begin{aligned}\log\mathcal{I}(\tau,\Delta)\big|_{\text{Basic BA}}&=\log\left(n_{\rm v}N|\mathcal{W}_G|\kappa_G\right)+\log\mathcal{Z}_{tot}-\log H\\&=-\frac{i\pi N^2}{6\tau^2}C_{IJK}\left[\Delta_I\right]_\tau\left[\Delta_J\right]_\tau\left[\Delta_K\right]_\tau+\log n_{\rm v}N+\frac{i\pi n_{\rm v}}{12}\\&\quad-2n_{\rm v}\left(\log\left(q;q\right)_\infty+\frac{1}{2}\log\tau\right)-\sum_{\Phi_{ab}}\log\widetilde{\Gamma}\left(\Delta_{ab};\tau\right)+\mathcal{O}\left(N^0\right)\end{aligned} \tag{4.2.51}$$

in the large-N limit where we have used the identity (A.9a).

Taking the Cardy-like limit, we can simplify further using the asymptotic expansion of the q-Pochhammer symbol (A.12) and the Elliptic Gamma function (A.21), hence

$$\boxed{\log \mathcal{I}(\tau;\Delta)\big|_{\text{Basic BA}} = -\frac{i\pi(N^2-1)}{6\tau^2} C_{IJK}\,[\Delta_I]_\tau\,[\Delta_J]_\tau\,[\Delta_K]_\tau + \log n_{\text{v}} N + \mathcal{O}(e^{-1/|\tau|}).} \tag{4.2.52}$$

The first term in (4.2.52) reproduces the result of [1, 45, 46, 55]. Note that even in the $\mathcal{N}=1$ case the coefficient of the $\log N$ term is 1 and it appears crucially due to the degeneracy factor.

4.3 Conclusions II

One of the main results of this thesis is the exploration of the $\mathcal{N}=4$ SCI beyond the leading orders in Cardy-like and large-N limit, respectively. One motivation was to obtain a reliable estimation of logarithmic corrections. We have demonstrated by direct computation that the two main approaches to the SCI, namely the saddle point approach for the Cardy-like limit and the BA approach for the large-N limit, are consistent with each other up to exponentially suppressed terms in the Cardy-like limit. This result was expected but it is highly nontrivial given the different approximation schemes involved in each computation. Our result can best be summarized as:

$$\mathcal{I}(\tau;\Delta) = \begin{cases} \mathcal{I}(\tau;\Delta)\big|_{\text{Main Saddle}} + \text{contribution from other saddles}, \\ \mathcal{I}(\tau;\Delta)\big|_{\text{Basic BA}} + \text{contribution from other BA solutions}, \end{cases} \tag{4.3.1}$$

where $\log \mathcal{I}(\tau;\Delta)\big|_{\text{Main Saddle}}$ and $\log \mathcal{I}(\tau;\Delta)\big|_{\text{Basic BA}}$ are given explicitly in (1.3.6) and (1.3.7) respectively. Some of the contribution from other saddles and BA solutions have been studied in Appendix B.

The nature of other contributions in the BA approach were recently discussed in [121] where it was noticed that the structure of BA solutions might include entire continuous families beyond the naturally expected $\text{SL}(2,\mathbb{Z})$ type. This result indicates that the full expression for the SCI in the BA approach might require new techniques. As far as we are aware, there were no results regarding what the existence of a continuous family of BA solutions means in the saddle point approach to the SCI. Our work in Appendix C.2 shows the existence of a saddle whose contribution to the SCI does not look like the contribution from any $\text{SL}(2,\mathbb{Z})$ type BA solution, and therefore it is natural to expect that this saddle is related to a certain continuous family of BA solutions. Investigating this relation further may set the stage for a full understanding of the SCI.

One central product of our analysis for the saddle point approximation is a direct window into the *effective* theory of the SCI. Namely, some important elements of the effective field theory approach were originally proposed in [48] and subsequently developed and extended in [49, 51]. The main paradigm is that at high temperatures the 4d theory is described by an effective 3d theory. Starting from 4d theories and taking the Cardy-like expansion, we have directly uncovered the matrix model connected with the 3d Chern-Simons theory. Recent works [58, 59], presented advances from this effective field theory approach. It would be quite interesting to formulate dynamical questions in terms of degrees of freedom defined in the 3d Chern-Simons gauge theory. It is worth noticing that aspects of such effective field theory approach might have powerful implications for the gravitational side as recently suggested in [127–129].

Throughout our work in this project we relied heavily on numerical studies to inform us at crucial analytical turns. The ultimate product of our investigation can be entirely understood analytically. We relegated some of our numerical discussion to various appendices because the results have been mostly geared to confirm and motivate analytical results in the large-N limit. There have been, however, two recent studies exploiting a numerical approach to the index with the main goal of better understanding finite N aspects [130, 131]. It would be interesting to explore the structure of the index in more details, in particular, to gain an understanding of the combinations governing the convergence of the expressions to aspects of black hole physics. The recent numerical experiments reported in [130, 131] discuss finite N aspects and indicate convergence of the numerical result to the saddle point expression. It would be quite interesting to explore, for example, how the convergence rates compare among the various approaches to the SCI, such analysis might possibly shed light on the expansion in Eq. (4.3.1). The works [2, 132] pursues the direction of studying the BA approach for low rank of the gauge group, which shed some light on general aspects of the BA approach and its role in recovering the full index.

The AdS/CFT correspondence posits that $\mathcal{N} = 4$ SYM is the UV complete description of the gravity theory containing the AdS_5 black holes of interest. To the level of approximations described in this thesis we have obtained a term of the form $\log N$. The precise coefficient of this term is very robust, it is present in this identical form in the generic case of 4d $\mathcal{N} = 1$ theories with, for example, $SU(N)^{n_v}$ gauge group. This answer should pass the litmus test of being reproduced from low energy supergravity. At the moment, the gravity side of this litmus test seems much more formidable. There are a number of difficulties along this road. For example, the particular advantages of working in an odd-dimensional space that were crucial for clarifying the AdS_4 cases [66, 113, 114] are now gone as the dual theory is 10d IIB supergravity. Nevertheless, the simplicity of the field theory answer indicates that the gravity answer might be achieved by carefully considering a small set of fields. Moreover, the fact that the result is universal for a large class of asymptotically $AdS_5 \times SE_5$ black holes indicates that, most likely, the answer is the contribution of certain zero modes. It would be quite interesting to pursue this computation fully. The gravitational side has been explored in [133] where the gravitational interpretation to the BA solutions has been given in terms of orbifolds in the Euclidean black holes solutions.

It would be quite natural to elucidate similar aspects in 3d theories. Although there is currently no BA approach to the SCI in 3d, there are two approaches to the SCI: one using a continuum approximation for the monopole charge sums in the conformal index [61] and the other based on localization [64]; they both exploit a Cardy-like limit. It would be interesting to elucidate the relation between these two approaches along the lines of the work presented here. The situation in 3d is quite peculiar because many of the computations are essentially reduced to the matrix model for the topologically twisted index, discussed in [28]. For a class of matrix models describing topologically twisted indices, numerical results for the $\log N$ contribution have been worked out in [109, 110, 134] and precise agreement with the logarithmic entropy corrections for magnetically charged black holes was shown in [113, 114]. For a general class of rotating, electrically charged, black holes and their 3d SCI, agreement of the logarithmic corrections was established in [66]. Quite remarkably, certain universality of the logarithmic terms in 3d partition functions was established in [135] and its dual side matched in [136]; it would be quite enlightening to have such universal understanding extended to the topologically twisted index and the 3d SCI.

Let us finally remark that another approach to the SCI has been proposed via doubly-periodic extension of the index for $\mathcal{N} = 4$ SYM [116] and in subsequent work for the generic $\mathcal{N} = 1$ case [117]. The leading N^2 term in this approach matches the other two approximations to the SCI. The methods used in this manuscript that allow to go beyond the leading order rely heavily on the analytical structure which is precisely lost in this doubly-periodic approach. It would be quite interesting to penetrate the sub-leading structures in that approach where one might naturally hope that some aspects of modularity will be a powerful guiding principle.

CHAPTER 5
Appendix A

A Elliptic functions

Here we gather definitions and useful identities of elliptic functions.

A.1 Definitions

The Pochhammer symbol is defined as

$$(z;q)_\infty = \prod_{k=0}^{\infty}(1-zq^k). \tag{A.1}$$

The elliptic theta functions used in this paper have the following product forms:

$$\theta_0(u;\tau) = \prod_{k=0}^{\infty}(1-e^{2\pi i(u+k\tau)})(1-e^{2\pi i(-u+(k+1)\tau)}), \tag{A.2a}$$

$$\begin{aligned}\theta_1(u;\tau) &= -ie^{\frac{\pi i\tau}{4}}(e^{\pi i\tau}-e^{-\pi i\tau})\prod_{k=1}^{\infty}(1-e^{2\pi ik\tau})(1-e^{2\pi i(k\tau+u)})(1-e^{2\pi i(k\tau-u)}) \\ &= ie^{\frac{\pi i\tau}{4}}e^{-\pi iu}\theta_0(u;\tau)\prod_{k=1}^{\infty}(1-e^{2\pi ik\tau}).\end{aligned} \tag{A.2b}$$

The elliptic gamma function and the 'tilde' elliptic gamma function are defined as

$$\Gamma(z;p,q) = \prod_{j,k=0}^{\infty}\frac{1-p^{j+1}q^{k+1}z^{-1}}{1-p^jq^kz}, \tag{A.3a}$$

$$\widetilde{\Gamma}(u;\sigma,\tau) = \prod_{j,k=0}^{\infty}\frac{1-e^{2\pi i[(j+1)\sigma+(k+1)\tau-u]}}{1-e^{2\pi i[j\sigma+k\tau+u]}}. \tag{A.3b}$$

In this paper, we are mainly interested in the case with $\sigma=\tau$ and abbreviate $\Gamma(z;q,q)$ and $\widetilde{\Gamma}(u;\tau,\tau)$ as $\Gamma(z,q)$ and $\widetilde{\Gamma}(u;\tau)$ respectively. We also define a special function $\psi(u)$ as

$$\psi(u) \equiv \exp\left[u\log\left(1-e^{-2\pi iu}\right) - \frac{1}{2\pi i}\mathrm{Li}_2(e^{-2\pi iu})\right]. \tag{A.4}$$

A.2 Basic properties

The elliptic theta functions have quasi-double-periodicity, namely

$$\theta_0(u+m+n\tau;\tau) = (-1)^n e^{-2\pi inu}e^{-\pi in(n-1)\tau}\theta_0(u;\tau), \tag{A.5a}$$

$$\theta_1(u+m+n\tau;\tau) = (-1)^{m+n} e^{-2\pi inu}e^{-\pi in^2\tau}\theta_1(u;\tau), \tag{A.5b}$$

for $m,n\in\mathbb{Z}$. The inversion formula of $\theta_0(u;\tau)$ can be written simply as

$$\theta_0(-u;\tau) = -e^{-2\pi iu}\theta_0(u;\tau). \tag{A.6}$$

The elliptic gamma function also has quasi-double-periodicity, namely

$$\widetilde{\Gamma}(u;\sigma,\tau) = \widetilde{\Gamma}(u+1;\sigma,\tau) = \theta_0(u;\tau)^{-1}\widetilde{\Gamma}(u+\sigma;\sigma,\tau) = \theta_0(u;\sigma)^{-1}\widetilde{\Gamma}(u+\tau;\sigma,\tau). \tag{A.7}$$

It also satisfies the inversion formula

$$\widetilde{\Gamma}(u;\sigma,\tau)=\widetilde{\Gamma}(\sigma+\tau-u;\sigma,\tau)^{-1}. \tag{A.8}$$

The Pochhammer symbol and the elliptic theta functions are transformed under the S-transformation as ($q=e^{2\pi i\tau}$, $\tilde{q}=e^{-\frac{2\pi i}{\tau}}$)

$$(\tilde{q};\tilde{q})_\infty=(-i\tau)^{\frac{1}{2}}e^{\frac{\pi i}{12}(\tau+\frac{1}{\tau})}(q;q)_\infty, \tag{A.9a}$$

$$\theta_0(u/\tau;-1/\tau)=e^{\frac{\pi i}{\tau}(u^2+u+\frac{1}{6})-\pi i(u+\frac{1}{2})+\frac{\pi i\tau}{6}}\theta_0(u;\tau), \tag{A.9b}$$

$$\theta_1(u/\tau;-1/\tau)=-i(-i\tau)^{\frac{1}{2}}e^{\frac{\pi i u^2}{\tau}}\theta_1(u;\tau). \tag{A.9c}$$

The elliptic gamma function can be written in terms of these S-transformed elliptic theta functions and the ψ-function (A.4) as (see [42] for example)

$$\widetilde{\Gamma}(\Delta_a;\tau)=\frac{e^{2\pi i Q(\{\Delta_a\}_\tau;\tau)}}{\theta_0(\frac{\{\Delta_a\}_\tau-1}{\tau};-\frac{1}{\tau})}\prod_{k=0}^{\infty}\frac{\psi(\frac{k+\{\Delta_a\}_\tau}{\tau})}{\psi(\frac{k+1-\{\Delta_a\}_\tau}{\tau})}, \tag{A.10}$$

where $Q(\cdot;\cdot)$ is defined in (4.2.18) and repeated here as

$$Q(u;\tau)\equiv-\frac{B_3(u)}{6\tau^2}+\frac{B_2(u)}{2\tau}-\frac{5}{12}B_1(u)+\frac{\tau}{12}. \tag{A.11}$$

A.3 Asymptotic behaviors

For a small $|\tau|$ with fixed $0<\arg\tau<\pi$, the Pochhammer symbol can be approximated as

$$\log(q;q)_\infty=-\frac{\pi i}{12}(\tau+\frac{1}{\tau})-\frac{1}{2}\log(-i\tau)+\mathcal{O}(e^{\frac{2\pi\sin(\arg\tau)}{|\tau|}}). \tag{A.12}$$

To study asymptotic behaviors of elliptic functions, first we introduce a τ-modded value of a complex number u, namely $\{u\}_\tau$, as

$$\{u\}_\tau\equiv u-\lfloor\mathrm{Re}\,u-\cot(\arg\tau)\,\mathrm{Im}\,u\rfloor\quad(u\in\mathbb{C}). \tag{A.13}$$

By definition, the τ-modded value satisfies

$$\{u\}_\tau=\{\tilde{u}\}_\tau+\check{u}\tau,\qquad\{-u\}_\tau=\begin{cases}1-\{u\}_\tau & (\tilde{u}\notin\mathbb{Z})\\ -\{u\}_\tau & (\tilde{u}\in\mathbb{Z}),\end{cases} \tag{A.14}$$

where we have defined $\tilde{u},\check{u}\in\mathbb{R}$ as

$$u=\tilde{u}+\check{u}\tau. \tag{A.15}$$

Note that, for a real number x, a τ-modded value $\{x\}_\tau$ reduces to a normal modded value $\{x\}$ defined as

$$\{x\}\equiv x-\lfloor x\rfloor\quad(x\in\mathbb{R}). \tag{A.16}$$

Now, the elliptic theta function $\theta_0(u;\tau)$ can be approximated for a small $|\tau|$ with fixed $0<\arg\tau<\pi$ as

$$\begin{aligned}\log\theta_0(u;\tau)=&\frac{\pi i}{\tau}\{u\}_\tau(1-\{u\}_\tau)+\pi i\{u\}_\tau-\frac{\pi i}{6\tau}(1+3\tau+\tau^2)\\&+\log\left(1-e^{-\frac{2\pi i}{\tau}(1-\{u\}_\tau)}\right)\left(1-e^{-\frac{2\pi i}{\tau}\{u\}_\tau}\right)+\mathcal{O}(e^{\frac{2\pi\sin(\arg\tau)}{|\tau|}}),\end{aligned} \tag{A.17}$$

based on an alternative product form of $\theta_0(u;\tau)$:

$$\begin{aligned}\theta_0(u;\tau) = -ie^{-\frac{\pi i}{6}(\tau+\frac{1}{\tau})}e^{\frac{\pi i}{\tau}\{u\}_\tau(1-\{u\}_\tau)}e^{\pi i\{u\}_\tau} \\ \times\prod_{k=1}^{\infty}(1-e^{-\frac{2\pi i}{\tau}(k-\{u\}_\tau)})(1-e^{-\frac{2\pi i}{\tau}(k-1+\{u\}_\tau)}).\end{aligned} \tag{A.18}$$

This product form can be derived by combining (A.2a) with the S-transformation (A.9b) and following the definition (A.13).

Similarly, the elliptic theta function $\theta_1(u;\tau)$ is approximated for a small $|\tau|$ with fixed $0 < \arg\tau < \pi$ as

$$\begin{aligned}\log\theta_1(u;\tau) = \frac{\pi i}{\tau}\{u\}_\tau(1-\{u\}_\tau) - \frac{\pi i}{4\tau}(1+\tau) + \pi i\lfloor \operatorname{Re} u - \cot(\arg\tau)\operatorname{Im} u\rfloor + \frac{1}{2}\log\tau \\ + \log\Big(1-e^{-\frac{2\pi i}{\tau}(1-\{u\}_\tau)}\Big)\Big(1-e^{-\frac{2\pi i}{\tau}\{u\}_\tau}\Big) + \mathcal{O}(e^{\frac{2\pi\sin(\arg\tau)}{|\tau|}}),\end{aligned} \tag{A.19}$$

based on an alternative product form of $\theta_1(u;\tau)$:

$$\begin{aligned}\theta_1(u;\tau) = (-i\tau)^{\frac{1}{2}}e^{-\frac{\pi i}{4\tau}}e^{\pi i\lfloor \operatorname{Re} u-\cot(\arg\tau)\operatorname{Im} u\rfloor}e^{\frac{\pi i}{\tau}\{u\}_\tau(1-\{u\}_\tau)} \\ \times\prod_{k=1}^{\infty}(1-e^{-\frac{2\pi i}{\tau}k})(1-e^{-\frac{2\pi i}{\tau}(k-\{u\}_\tau)})(1-e^{-\frac{2\pi i}{\tau}(k-1+\{u\}_\tau)}).\end{aligned} \tag{A.20}$$

This product form can be derived by combining (A.2b) with the S-transformation (A.9c) and following the definition (A.13).

For a small $|\tau|$ with fixed $0 < \arg\tau < \pi$, the elliptic gamma function can be approximated as

$$\log\widetilde{\Gamma}(u;\tau) = 2\pi i\, Q(\{u\}_\tau;\tau) + \mathcal{O}(|\tau|^{-1}e^{\frac{2\pi\sin(\arg\tau)}{|\tau|}\min(\{\tilde{u}\},1-\{\tilde{u}\})}), \tag{A.21}$$

provided $\tilde{u} \not\to \mathbb{Z}$ (see [42] for example). See (4.2.18) or (A.11) for the definition of $Q(\cdot;\cdot)$.

B Contribution from C-center solutions

In this Appendix we repeat the same procedures in 4.1.1 and 4.2.1 for a more general class of saddle point solutions and the BA solutions respectively. Both solutions are denoted by a *finite*, positive divisor of N, namely C, and the solution with $C = 1$ corresponds to what we have discussed in the main text.

The final results of this Appendix, namely (B.13) and (B.18), are consistent with each other for the first three terms. The remaining pure imaginary or order $\mathcal{O}(N^0)$ terms do not match apparently: more detailed analysis on contour deformations in the saddle point approach and on the Jacobian contribution in the Bethe-Ansatz approach (see section 4.2 of [68] for example) would be required for a perfect match and we leave it for future research.

Another important implication of this Appendix is that 3d $SU(N)$ Chern-Simons theory arises from $\mathcal{N} = 4$ $SU(N)$ SYM on $S^1 \times S^3$ in the Cardy-like limit *independently* of saddle point solutions. In the main text we have observed it for a particular saddle point (4.1.15) and the following section B.1 will generalize this result to C-center saddle points (B.1).

Lastly, it is worth highlighting the robustness of the universal $\log N$ term. We will demonstrate that these C-center solutions, which can be dominant in certain domain of chemical potentials Δ_a, still contribute $\log\left(\frac{N}{C}\right)$ to the SCI which is compatible with the result in the main body of the manuscript.

B.1 Saddle point approach

In 4.1.3, we have investigated the contribution from a particular saddle point Ansatz (4.1.15) to the index through the saddle point approximation (4.1.4). Here we repeat the same procedure but with a more general Ansatz for C-center solutions [121], namely

$$\hat{u}^{(C,m)} = \left\{ u_j^{(C,m)} = \frac{m}{N} + \frac{\lfloor \frac{j-1}{N/C} \rfloor - \frac{C-1}{2}}{C} + v_j\tau \,\middle|\, v_j \sim \mathcal{O}(|\tau|^0),\ \sum_{j=1}^{N} v_j = 0 \right\} \tag{B.1}$$

with $m \in \{0, 1, \cdots, \frac{N}{C} - 1\}$. The range of m is for the integration contour deformed from (4.1.5) as

$$\bigcup_{\mu=1}^{N-1} (v_\mu\tau - \frac{1}{2N} - \frac{C-1}{2C},\ v_\mu\tau + 1 - \frac{1}{2N} - \frac{C-1}{2C}], \tag{B.2}$$

which passes through the above saddle point $\hat{u}^{(C,m)}$. The C-center solution Ansatz (B.1) and the corresponding deformed contour (B.2) reduce to the ones in the main text (4.1.15) and (4.1.19) respectively for $C = 1$.

In the strict Cardy-like limit $|\tau| \to 0$, the C-center solution Ansatz (B.1) reduces to C groups of holonomies, where each group has equal number (N/C) of condensed holonomies and is separated from adjacent groups by $1/C$ along the domain $(0, 1]$ with 0 identified with 1. The name 'C-center' comes from its symmetry breaking pattern $\mathbb{Z}_N \to \mathbb{Z}_C$ [121].

Following 4.1.3 and using the following identity of Bernoulli polynomials

$$\sum_{J=0}^{C-1} B_n(\{\frac{J}{C} + u\}_\tau) = \frac{1}{C^{n-1}} B_n(\{Cu\}_\tau) \quad (u \in \mathbb{C}), \tag{B.3}$$

we simplify the effective action (4.1.13) near the C-center Ansatz (B.1) up to exponentially suppressed terms as

$$\begin{aligned} N^2 S_{\text{eff}}(\hat{u};\Delta,\tau) \sim & \sum_{I=0}^{C-1}\left(-\frac{\pi i \eta_C N}{C\tau^2}\sum_{i=1}^{N/C}(u_{I,i}-\bar{u}_I)^2+\sum_{i\neq j}^{N/C}\log\left(2\sin\frac{\pi(u_{I,i}-u_{I,j})}{\tau}\right)\right) \\ & -\frac{\pi i}{2\tau^2}\frac{N^2}{C^2}\sum_{I,J=0}^{C-1}\xi_{I-J}(\bar{u}_{IJ})^2-\frac{\pi i N^2}{C^3\tau^2}\prod_{a=1}^{3}\left(\{C\Delta_a\}_\tau-\frac{1+\eta_C}{2}\right) \\ & +\frac{\pi i}{\tau^2}\prod_{a=1}^{3}\left(\{\Delta_a\}_\tau-\frac{1+\eta_1}{2}\right)-\frac{5\pi i\eta_C N^2}{12C}+\frac{\pi i N}{2}-\frac{\pi i(6-5\eta_1)}{12} \\ & -(N-1)\log\tau, \end{aligned} \tag{B.4}$$

where we have introduced $u_{I,i}$ and $\bar{u}_I$ as

$$\begin{aligned} u_i &= \frac{m}{N}+\frac{I-\frac{C-1}{2}}{C}+u_{I,i-(N/C)I} \quad \left(I=\left\lfloor\frac{i-1}{N/C}\right\rfloor,\ i=1,\cdots,N\right), \\ \bar{u}_I &= \frac{1}{N/C}\sum_{i=1}^{N/C}u_{I,i}. \end{aligned} \tag{B.5}$$

Note that $\sum_{I=0}^{C-1}\bar{u}_I=0$ from the $SU(N)$ constraint. We have also defined ξ_J and η_C as

$$\begin{aligned} \sum_{a=1}^{3}\{\frac{J}{C}+\Delta_a\}_\tau &= 2\tau+\frac{3+\xi_J}{2}, \\ \sum_{a=1}^{3}\{C\Delta_a\}_\tau &= 2C\tau+\frac{3+\eta_C}{2}, \end{aligned} \tag{B.6}$$

which are related with each other as $\eta_C=\sum_{J=0}^{C-1}\xi_J\in\{\pm1\}$ under the assumption $\{C\tilde{\Delta}_a\}\neq 0$. Note that η_1 is equivalent to the η introduced in the main text (4.1.11).

Substituting the effective action (B.4) into the saddle point approximation (4.1.4) gives the SCI as

$$\begin{aligned} \mathcal{I}(\tau;\Delta) \sim & \sum_{m=0}^{N/C-1}\frac{\mathcal{A}}{((N/C)!)^C}\int_{D_{\hat{u}^{(C,m)}}}\prod_{\mu=1}^{N-1}du_\mu\, e^{N^2 S_{\text{eff},u\text{-dept}}(\hat{u};\Delta_a,\tau)} \\ & +(\text{contribution from the other saddles}), \end{aligned} \tag{B.7}$$

where $D_{\hat{u}^{(C,m)}}$ denotes a small neighborhood of a saddle point solution $\hat{u}^{(C,m)}$ (B.1) on the contour (B.2), namely

$$\bigcup_{\mu=1}^{N-1}(v_\mu\tau+\frac{m}{N}+\frac{\lfloor\frac{\mu-1}{N/C}\rfloor-\frac{C-1}{2}}{C}-\epsilon, v_\mu\tau+\frac{m}{N}+\frac{\lfloor\frac{\mu-1}{N/C}\rfloor-\frac{C-1}{2}}{C}+\epsilon] \tag{B.8}$$

with some small positive number ϵ. The u-dependent part of the effective action, namely $N^2 S_{\text{eff},u\text{-dept}}(\hat{u};\Delta,\tau)$, denotes the first three terms of (B.4) and the prefactor $\mathcal{A}$ is related to the remaining u-independent

part of (B.4) as

$$\mathcal{A} = \exp\left[-\frac{\pi i N^2}{C^3\tau^2}\prod_{a=1}^{3}\left(\{C\Delta_a\}_\tau - \frac{1+\eta_C}{2}\right) + \frac{\pi i}{\tau^2}\prod_{a=1}^{3}\left(\{\Delta_a\}_\tau - \frac{1+\eta_1}{2}\right) - \frac{5\pi i\eta_C N^2}{12C} + \frac{\pi i N}{2} - \frac{\pi i(6-5\eta_1)}{12} - (N-1)\log\tau\right]. \tag{B.9}$$

Note that we have $((N/C)!)^C$ instead of the original $N!$ in the denominator of (B.7) taking an extra factor of $\frac{N!}{((N/C)!)^C}$ into account, which corresponds to the number of distributing N holonomies into C groups as (B.5).

Introducing new integration variables $\lambda_{I,i}$ and $\bar{\lambda}_I$ as

$$\begin{aligned} -i\lambda_{I,i}\tau &= u_{I,i} - \bar{u}_I \qquad (I = 0,\cdots,C-1 \text{ and } i = 1,\cdots,N/C-1), \\ -i\bar{\lambda}_I\tau &= \bar{u}_I \qquad (I = 0,\cdots,C-2), \end{aligned} \tag{B.10}$$

whose Jacobian is given as

$$\left|\frac{\partial(u_1,\cdots,u_{N-1})}{\partial(\lambda_{0,1},\cdots,\lambda_{0,N/C-1},\bar{\lambda}_0,\lambda_{1,1},\cdots,\lambda_{C-1,N/C-1})}\right| = e^{-\frac{\pi i(N-1)}{2}}\left(\frac{N}{C}\right)^{C-1}\tau^{N-1}, \tag{B.11}$$

the index (B.7) can be rewritten as

$$\mathcal{I}(\tau;\Delta) = \frac{N}{C}\tau^{N-1}\mathcal{A}\,e^{-\frac{\pi i(N^2/C-1)}{2}}\left(Z^{CS}_{\mathrm{SU}(N/C)}\right)^C\int\prod_{I=0}^{C-2}d\bar{\lambda}_I\,e^{\frac{\pi i}{2}\sum_{I,J=0}^{C-1}\xi_{I-J}(\bar{\lambda}_{IJ})^2} + (\text{contribution from other saddles}). \tag{B.12}$$

Here we have assumed smooth deformations of contours as we have done from (4.1.25) to real lines in the main text. Note that the original $SU(N)$ group breaks down into C copies of $\mathrm{SU}(N/C)$ groups and the remaining $C-1$ copies of U(1) groups: accordingly, we obtained C copies of the $\mathrm{SU}(N/C)$ Chern-Simons partition function together with the extra $(C-1)$-dimensional integral for U(1) terms. We denote the latter simply as $Z_{\mathrm{U}(1)\text{'s}}$. Finally, substituting the partition function of $SU(N)$ CS theory (D.6) with $N \to N/C$ into (B.12) gives

$$\mathcal{I}(\tau;\Delta) = \frac{N}{C}\exp\left[-\frac{\pi i N^2}{C^3\tau^2}\prod_{a=1}^{3}\left(\{C\Delta_a\}_\tau - \frac{1+\eta_C}{2}\right) + \frac{\pi i}{\tau^2}\prod_{a=1}^{3}\left(\{\Delta_a\}_\tau - \frac{1+\eta_1}{2}\right) + \frac{5\pi i(\eta_1 - C\eta_C)}{12}\right]\times Z_{\mathrm{U}(1)\text{'s}} + (\text{contribution from other saddles}). \tag{B.13}$$

B.2 Bethe-Ansatz approach

In 4.2.1, we have investigated the contribution from basic solutions (4.2.9) to the index through the Bethe-Ansatz formula (2.1.28). Here we generalize it with a larger set of solutions denoted by a positive divisor of N, namely C, as

$$\hat{u}_C = \left\{u_i = \bar{u} + \frac{I}{C} + \frac{i-(N/C)I}{N/C}\tau + m_i + n_i\tau \,\middle|\, I = \left\lfloor\frac{i}{N/C}\right\rfloor,\ i = 1,\cdots,N\right\} \tag{B.14}$$

with arbitrary integers m_i's and n_i's. Note that this solution is equivalent to the $\{C, N/C, 0\}$ solution in [68] and the $(C, N/C)$ saddle in [116]. Since the calculation is parallel to the one in the main text, we summarize the key intermediate results only.

First, the degeneracy gives $\log N! + \log N$ by the same token we discussed in the beginning of 4.2.1. The prefactor contribution also remains the same as (4.2.15). Calculating the contribution from $\log \mathcal{Z}(\hat{u}_C; \Delta, \tau)$ is more involved but does not require extra techniques other than using (4.2.21) and (B.3). The result is given as

$$\begin{aligned}
\log \mathcal{Z}(\hat{u}_C; \Delta, \tau) &= C \sum_{J=0}^{C-1} \sum_{i,j=0}^{N/C-1} \sum_{a=1}^{3} \log \tilde{\Gamma}(\frac{i-j}{N/C}\tau + \frac{J}{C} + \Delta_a; \tau) - N \sum_{a=1}^{3} \log \tilde{\Gamma}(\Delta_a; \tau) \\
&\quad - C \sum_{J=1}^{C-1} \sum_{i,j=0}^{N/C-1} \log \tilde{\Gamma}(\frac{i-j}{N/C}\tau + \frac{J}{C}; \tau) - C \sum_{i,j=0\,(i\neq j)}^{N/C-1} \log \tilde{\Gamma}(\frac{i-j}{N/C}\tau; \tau) \\
&= -\frac{\pi i N^2}{C^3 \tau^2} \prod_{a=1}^{3} \left(\{C\Delta_a\}_\tau - \frac{1+\eta_C}{2} \right) + \frac{\pi i (1-\eta_C) N^2}{2C} + \frac{\pi i (1 - 3\tau + \tau^2) N}{6\tau} \\
&\quad + \frac{\pi i \eta_C C}{12} - N \sum_{a=1}^{3} \log \tilde{\Gamma}(\Delta_a; \tau) + N \log \frac{N}{C} - 2N \log(\tilde{q}; \tilde{q})_\infty \\
&\quad + \mathcal{O}(N e^{-\frac{2\pi N \sin(\arg \tau)}{|\tau|} \min(\{\frac{J}{C} + \tilde{\Delta}_a\}, 1 - \{\frac{J}{C} + \tilde{\Delta}_a\} |\, J = 0, 1, \cdots, C-1)}),
\end{aligned} \tag{B.15}$$

where we have introduced the quantities η_C as in (B.6). The contribution from the Jacobian $-\log H(\hat{u}_C; \Delta, \tau)$ can also be obtained by following the procedure in 4.2.1 and the detailed discussion on the Jacobian matrix in [68] as

$$\begin{aligned}
-\log H(\hat{u}_C; \Delta, \tau) &= -\log N - (N-1) \log \left(\frac{i}{\pi} \sum_{\Delta} \partial_\Delta \log \theta_1(C\Delta; \frac{\tau}{N/C^2}) \right) - \log \det \left(I_{N-1} + \tilde{H} \right) \\
&= -N \log N + (N-1) \log \frac{C\tau}{\eta_C} - \log \det \left(I_{N-1} + \tilde{H} \right) \\
&\quad + \mathcal{O}(e^{-\frac{2\pi N \sin(\arg \tau)}{|\tau|} \min(\{\frac{J}{C} + \tilde{\Delta}_a\}, 1 - \{\frac{J}{C} + \tilde{\Delta}_a\} |\, J = 0, 1, \cdots, C-1)}).
\end{aligned} \tag{B.16}$$

Substituting all the contributions to the BA formula (2.1.28) and using (A.9a), finally we have the contribution from the BA solutions (B.14):

$$\begin{aligned}
\log \mathcal{I}(\tau; \Delta)\big|_{\{C, N/C, 0\}} &= -\frac{\pi i N^2}{C^3 \tau^2} \prod_{a=1}^{3} \left(\{C\Delta_a\}_\tau - \frac{1+\eta_C}{2} \right) + \log \frac{N}{C} + \frac{\pi i (1-\eta_C) N^2}{2C} \\
&\quad + \frac{\pi i \eta_C C}{12} - \frac{\pi i (1-\eta_C)(N-1)}{2} \\
&\quad - \sum_{a=1}^{3} \log \tilde{\Gamma}(\Delta_a; \tau) - 2 \log(q; q)_\infty - \log \tau - \log \det \left(I_{N-1} + \tilde{H} \right) \\
&\quad + \mathcal{O}(N e^{-\frac{2\pi N \sin(\arg \tau)}{|\tau|} \min(\{\frac{J}{C} + \tilde{\Delta}_a\}, 1 - \{\frac{J}{C} + \tilde{\Delta}_a\} |\, J = 0, 1, \cdots, C-1)}).
\end{aligned} \tag{B.17}$$

In the Cardy-like limit that imposes $|\tau| \ll 1$, this reduces to

$$\begin{aligned}\log \mathcal{I}(\tau;\Delta)\big|_{\{C,N/C,0\}} \sim & -\frac{\pi i N^2}{C^3\tau^2}\prod_{a=1}^{3}\left(\{C\Delta_a\}_\tau - \frac{1+\eta_C}{2}\right) + \frac{\pi i}{\tau^2}\prod_{a=1}^{3}\left(\{\Delta_a\}_\tau - \frac{1+\eta_1}{2}\right) \\ & + \log\frac{N}{C} + \frac{\pi i(1-\eta_C)N^2}{2C} - \frac{\pi i(1-\eta_C)(N-1)}{2} + \frac{\pi i \eta_C C}{12} \\ & - \frac{\pi i(6-5\eta_1)}{12} - \log\det\Big(I_{N-1} + \tilde{H}\Big).\end{aligned} \tag{B.18}$$

up to exponentially suppressed terms.

C Saddle point solutions of 3d Chern-Simons theory

In this Appendix we investigate the saddle point equation (4.1.18) from the effective action of the $\mathcal{N}=4$ $SU(N)$ SYM theory in the Cardy-like expansion (4.1.17), namely

$$i\eta\, v_j = \frac{1}{N}\sum_{k=1\,(\neq j)}^{N} \cot \pi v_{jk} \quad (i=1,\cdots,N). \tag{C.1}$$

This equation is in fact equivalent to the saddle point equation of 3d Chern-Simons theory with a 't Hooft coupling t [123, 124],

$$\frac{1}{t}u_j = \frac{1}{N}\sum_{k=1\,(\neq j)}^{N} \coth \frac{u_{jk}}{2}, \tag{C.2}$$

under $v_j \to iu_j/2\pi$ and $t = 2\pi i/\eta$. We solve this saddle point equation in the planar limit, or equivalently in the large-N limit.

The partition function of 3d Chern-Simons theory on S^3 can be written as [123, 124]

$$Z = \frac{1}{N!}\int \prod_i du_i \prod_{i<j}\left(2\sinh\frac{u_{ij}}{2}\right)^2 \exp\left(-\frac{1}{2g_s}\sum_i u_i^2\right), \tag{C.3}$$

where $g_s = 2\pi i/\hat{k}$ and $\hat{k}$ is the effective Chern-Simons level. As we have seen in (4.1.17), the fluctuations around the dominant saddle point of the $\mathcal{N}=4$ SYM theory are described by such a Chern-Simons theory, provide we make the identification $t = 2\pi i/\eta$ where $t = g_s N$ is the 't Hooft coupling. Although this partition function can be evaluated directly [125], as detailed in Appendix D, it is important to note that our starting point is a saddle point evaluation of the $\mathcal{N}=4$ SYM index. Hence, in principle, we should seek a saddle point evaluation of the 3d Chern-Simons partition function. As we demonstrate in this Appendix, the saddle point result coincides with the exact partition function in the large-N limit, so in practice this distinction is immaterial. However, we highlight an interesting observation that there are, in fact, multiple saddle point solutions to the Chern-Simons model and that it is important to properly identify the dominant saddle in order to find agreement.

C.1 The dominant saddle point

The saddle point equation obtained by varying the action in (C.3) takes the form

$$\frac{1}{t}u_j = \frac{1}{N}\sum_{k=1\,(\neq j)}^{N} \coth \frac{u_{jk}}{2}. \tag{C.4}$$

As in [137], it is convenient to introduce the exponentiated eigenvalues $X_j = e^{u_j}$, so that the saddle point equation becomes

$$\log X_j = \frac{t}{N}\sum_{k=1\,(\neq j)}^{N}\left(-1+\frac{2X_j}{X_j - X_k}\right). \tag{C.5}$$

As usual, in the large-N limit, we assume the eigenvalues condense along a single cut, $x \in [a,b]$ on the real axis, provided the 't Hooft parameter t is real. (Later on we will analytically continue to

complex t.) We then introduce the density of eigenvalues $\rho(x)$ such that

$$\sum_i f(x_i) \quad \longrightarrow \quad N \int_a^b dx\, \rho(x) f(x). \tag{C.6}$$

The important properties of the matrix partition function are now encoded in the eigenvalue density. In order to determine $\rho(x)$, we introduce the resolvent

$$\omega(X) \equiv -t + 2t \int_a^b dy\, \rho(y) \frac{X}{X - Y} \qquad (X \in \mathbb{C} \setminus \mathcal{C}). \tag{C.7}$$

This function is analytic in the complex X plane except for a cut $\mathcal{C}$ from $[e^a, e^b]$ on the positive real axis. By studying $\omega(X)$ on both sides of the cut, we can reproduce the saddle point equation

$$\log X = \frac{1}{2}[\omega_+(X) + \omega_-(X)] \qquad (X \in \mathcal{C}), \tag{C.8}$$

and also recover the eigenvalue density

$$\rho(x) = -\frac{1}{4\pi i t}[\omega_+(X) - \omega_-(X)] \qquad (X \in \mathcal{C}). \tag{C.9}$$

Here we have defined

$$\omega_\pm(X) = \omega(e^{x \pm i\epsilon}) = \omega(X \pm i\epsilon) \qquad (X \in \mathcal{C}). \tag{C.10}$$

Following [137], we can use the following trick to derive the resolvent $\omega(X)$. Recall that $\omega(X)$ is analytic on $X \in \mathbb{C} \setminus \mathcal{C}$. Then it is straightforward to check that the function $g(X)$ defined as

$$g(X) \equiv e^{\omega(X)/2} + X e^{-\omega(X)/2} \qquad (X \in \mathbb{C} \setminus \mathcal{C}), \tag{C.11}$$

can be analytically continued to the entire complex plane including $\mathcal{C}$ since

$$g_+(X) = e^{\omega_+(X)/2} + X e^{-\omega_+(X)} = X e^{-\omega_-(X)} + e^{\omega_-(X)} = g_-(X) \quad (X \in \mathcal{C}), \tag{C.12}$$

where the middle equality corresponds to the saddle point equation, (C.8). Furthermore, using the asymptotic behavior of (C.7)

$$\lim_{X \to 0} \omega(X) = -t, \qquad \lim_{|X| \to \infty} \omega(X) = t, \tag{C.13}$$

we deduce the form of $g(X)$ as

$$g(X) = e^{-t/2}(X + 1) \qquad (X \in \mathbb{C}). \tag{C.14}$$

Substituting this into (C.11) then gives

$$e^{\omega(X)/2} = \frac{1}{2}\left(g(X) \pm \sqrt{g(X)^2 - 4X}\right). \tag{C.15}$$

Consistency of this solution demands that the branch cut of the square root is along $\mathcal{C}$. In particular, note that the branch points of the square root are given by

$$X_\pm = 2e^t - 1 \pm 2(e^{2t} - e^t)^{\frac{1}{2}}, \tag{C.16}$$

with the product $X_+ X_- = 1$.

C.1.1 The solution for $t > 0$

Although we have assumed that the eigenvalues condense along the real line, the endpoints $X_\pm$ are only real for real $t > 0$. Assuming this to be the case, the resolvent (C.15) can be written as

$$e^{\omega(X)/2} = \frac{1}{2}\left(e^{-t/2}(X+1) - e^{-t/2}(X-X_+)^{\frac{1}{2}}(X-X_-)^{\frac{1}{2}}\right), \tag{C.17}$$

where the principal branch is taken for both square roots. The eigenvalue density can then be recovered from the discontinuity across the cut using (C.9), with the result [137]

$$\rho(x) = \frac{1}{\pi t}\tan^{-1}\frac{\sqrt{e^t - \cosh^2\frac{x}{2}}}{\cosh\frac{x}{2}} \quad (x \in [a,b]), \tag{C.18}$$

where the endpoints are given by $-a = b = 2\cosh^{-1}(e^{t/2})$.

Substituting this eigenvalue density into the saddle point action is non-trivial, but can be shown to give the genus-zero free energy (see *e.g.* Appendix A of [124])

$$\log Z = N^2\left(\frac{\zeta(3) - \mathrm{Li}_3(e^{-t})}{t^2} + \frac{t}{6} - \frac{\pi^2}{6t}\right) + o(N^2). \tag{C.19}$$

This has a simple expansion in the large-t limit

$$\log Z/N^2 \sim \frac{t}{6} - \frac{\pi^2}{6t} + \frac{\zeta(3)}{t^2} + \mathcal{O}(e^{-t}) \qquad (t \gg 1), \tag{C.20}$$

but remains valid for real $t > 0$. For small t, it has an expansion

$$\log Z/N^2 = \frac{1}{2}\log t - \frac{3}{4} + \frac{t}{12} + \frac{t^2}{288} + \cdots \qquad (t \to 0^+), \tag{C.21}$$

which diverges logarithmically as $t \to 0$.

C.1.2 The solution for $t = 2\pi i/\eta$ with $\eta = \pm 1$

While we have worked with real t above, in order to connect to $\mathcal{N} = 4$ SYM, we want to analytically continue to a purely imaginary value $t = 2\pi i/\eta$ where $\eta = \pm 1$. However, this continuation is subtle, since $\eta = \pm 1$ turns out to be the endpoints of a singular region of the Chern-Simons matrix model. In particular, there is a divergence for $t = 2\pi i/\eta$ with $-1 < \eta < 1$ [138]. This subtlety can also be seen by noting that the endpoints of the cut, $X_\pm$ in (C.16), collapse to $X_\pm = 1$ when $\eta = \pm 1$.

To avoid this singularity issue for $\eta = \pm 1$, we take $t = 2\pi i/\eta + \epsilon^2$ where ϵ is a small positive number. Although we have assumed real t above, it was not strictly needed in order to obtain the resolvent (C.15). We thus start from there and analytically continue to imaginary eigenvalues, $x \to ix$. In particular, we take $X = e^{ix}$, in which case the resolvent takes the form

$$e^{\omega(X)/2} = \frac{1}{2}\left(e^{-t/2}(e^{ix}+1) + (e^{-t/2}(e^{ix}+1) + 2e^{ix/2})^{\frac{1}{2}}(e^{-t/2}(e^{ix}+1) - 2e^{ix/2})^{\frac{1}{2}}\right). \tag{C.22}$$

For $t = \pm 2\pi i + \epsilon^2$, the square root factors have the following branch cuts:

$$\begin{aligned} h_+(x) &\equiv (e^{-t/2}(e^{ix}+1) + 2e^{ix/2})^{\frac{1}{2}} : \bigcup_{n\in\mathbb{Z}}[(4n+2)\pi - x_*, (4n+2)\pi + x_*], \\ h_-(x) &\equiv (e^{-t/2}(e^{ix}+1) - 2e^{ix/2})^{\frac{1}{2}} : \bigcup_{n\in\mathbb{Z}}[4n\pi - x_*, 4n\pi + x_*], \end{aligned} \tag{C.23}$$

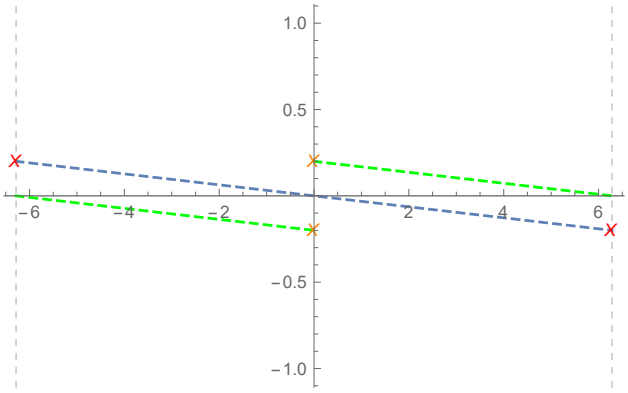


Figure 19: Orange (red) crosses are branch points and green (blue) lines are branch cuts of $h_+(x)$ and $h_-(x)$, respectively. Here we chose $\epsilon = 1/10$ for presentation.

where $x_* = 2\pi - 2i\epsilon + \mathcal{O}(\epsilon^2)$ (see Figure 19). Using[13]

$$h_\pm(x) = (-(1 \mp e^{ix/2})^2)^{\frac{1}{2}} + \mathcal{O}(\epsilon^2), \tag{C.24}$$

we can write down $h_\pm(x)$ more explicitly with the above specified branch cuts as

$$h_+(x) = \begin{cases} \pm i(1 - e^{ix/2}) + \mathcal{O}(\epsilon^2) & \text{(above the cuts of } h_+(x)) \\ \mp i(1 - e^{ix/2}) + \mathcal{O}(\epsilon^2) & \text{(below the cuts of } h_+(x)), \end{cases} \tag{C.25a}$$

$$h_-(x) = \begin{cases} \pm i(1 + e^{ix/2}) + \mathcal{O}(\epsilon^2) & \text{(above the cuts of } h_-(x)) \\ \mp i(1 + e^{ix/2}) + \mathcal{O}(\epsilon^2) & \text{(below the cuts of } h_-(x)). \end{cases} \tag{C.25b}$$

We now rewrite the resolvent (C.22) using (C.25) within the strip $\mathrm{Re}\, x \in (-2\pi, 2\pi)$ explicitly as

$$e^{\omega(X)/2} = \begin{cases} -1 + \mathcal{O}(\epsilon^2) & \text{(above the cuts of } h_\pm(x)) \\ -e^{ix} + \mathcal{O}(\epsilon^2) & \text{(between the cuts of } h_\pm(x)) \\ -1 + \mathcal{O}(\epsilon^2) & \text{(below the cuts of } h_\pm(x)), \end{cases} \tag{C.26a}$$

$$\to \quad \omega(X) = \begin{cases} -\frac{2\pi i}{\eta} + \mathcal{O}(\epsilon^2) & \text{(above the cuts of } h_\pm(x)) \\ -\frac{2\pi i}{\eta}(1 - \frac{x}{\pi}) + \mathcal{O}(\epsilon^2) & \text{(between the cuts of } h_\pm(x),\ \mathrm{Re}\, x \in [0, 2\pi)) \\ \frac{2\pi i}{\eta}(1 + \frac{x}{\pi}) + \mathcal{O}(\epsilon^2) & \text{(between the cuts of } h_\pm(x),\ \mathrm{Re}\, x \in (-2\pi, 0)) \\ \frac{2\pi i}{\eta} + \mathcal{O}(\epsilon^2) & \text{(below the cuts of } h_\pm(x)). \end{cases} \tag{C.26b}$$

Since (C.26a) determines $\omega(X)$ only up to $4\pi i\mathbb{Z}$, we have used the asymptotic conditions from (C.13) along with continuity outside of the branch cuts to fix $\omega(X)$. Finally, the eigenvalue density can be obtained by substituting (C.26b) into (C.9)

$$\rho(x) = \begin{cases} \frac{1}{2\pi}\left(1 - \frac{x}{2\pi}\right) + \mathcal{O}(\epsilon^2) & x \in [0, x_*) \\ \frac{1}{2\pi}\left(1 + \frac{x}{2\pi}\right) + \mathcal{O}(\epsilon^2) & x \in (-x_*, 0). \end{cases} \tag{C.27}$$

[13]This Taylor expansion becomes subtle as $x \to 2\pi\mathbb{Z}$ where the leading order vanishes. So we focus on the bulk and ignore this subtle issue near the endpoints $x = 2\pi\mathbb{Z}$.

Taking the limit $\epsilon \to 0$ then gives the simple expression

$$\rho(x) = \frac{1}{2\pi}\left(1 - \frac{|x|}{2\pi}\right) \qquad x \in (-2\pi, 2\pi), \tag{C.28}$$

which satisfies the normalization condition $\int_{-2\pi}^{2\pi} dx\, \rho(x) = 1$ as expected. Recall that, since we have analytically continued, the actual eigenvalues $u = ix$ are now distributed between $\pm 2\pi i$ along the imaginary axis.

The genus-zero free energy can be obtained by evaluating the saddle point action

$$S_{\text{eff}}/N^2 = \left[-\frac{1}{2t}\int dx \rho(x) u^2 + \frac{1}{2}\int \rho(x)\rho(\tilde{x}) dx\, d\tilde{x} \log\left(4\sinh^2\frac{u-\tilde{u}}{2}\right)^2\right]_{u=ix,\, \tilde{u}=i\tilde{x}} \tag{C.29}$$

on the solution given by (C.27). Here some care must be taken in keeping the ϵ regulator while integrating the log term because of branch issues. The result is simply

$$\log Z/N^2\big|_{t=\pm 2\pi i} = \frac{5\pi i}{12}\eta, \tag{C.30}$$

which is purely imaginary. This result can also be obtained directly by analytic continuation, namely by inserting $t = 2\pi i/\eta$ into (C.19) but our careful analysis provides some direct insight into the structure of eigenvalues.

C.2 The sub-leading saddle point

In deriving the resolvent, (C.15), we assumed a one-cut solution with the cut extending along $[X_-, X_+]$. The function $g(X)$ defined in (C.11) is then argued to be analytic in the complex plane. For $t > 0$, this picture is evident as the cut is on the positive real axis in the X plane. However, for $t = \pm 2\pi i$, the cut starts at $1 - 2\epsilon$, wraps twice along the unit circle, and ends at $1 + 2\epsilon$, where ϵ prevents the cut from overlapping with itself.

This picture of a cut wrapping twice around the unit circle in the X plane suggests the possibility of another solution where the cut extends only once around the circle. We have in fact identified such a solution where the cut starts at $X = -1$, goes around the circle, and ends again at $X = -1$. What is special about this solution is that the double endpoint $X = -1$ may be singular, and this allows for $g(X)$ defined in (C.11) to have a pole at $X = -1$. In particular, we find that

$$g(X) = e^{-t/2}(X+1) + e^{t/2}\frac{X}{X+1} \qquad (X \in \mathbb{C} \setminus \{-1\}), \tag{C.31}$$

is consistent with analyticity except for a pole at $X = -1$. The regular (first) term is identical to that of the standard solution, (C.14), while the pole (second) term is new but does not modify the asymptotic conditions (C.13).

C.2.1 The solution for $t > 0$

For $t > 0$, we choose the cut to lie along the unit circle, starting and ending at the singular point $X = -1$. Using (C.15), we obtain the resolvent

$$\omega(X) = \begin{cases} -t + 2\log(1+X) & (|X| < 1) \\ t - 2\log(1 + 1/X) & (|X| > 1), \end{cases} \tag{C.32}$$

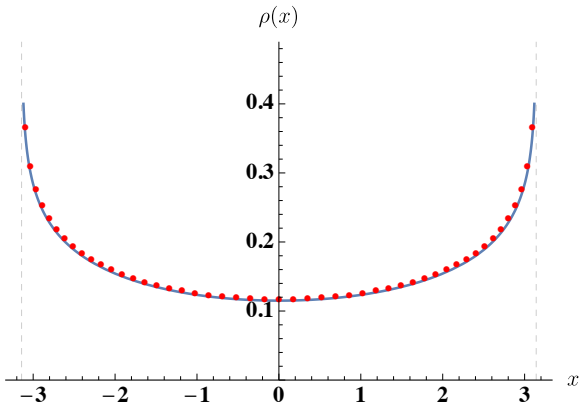


Figure 20: The numerically determined eigenvalue density, $\rho(x)$, for $N = 50$ and $t = 5$ (red dots) along with the large-N analytic solution (blue line), (C.33). The numerical density is obtained by finite differencing.

where the principal branch is taken for the log. Here the 'inside' and 'outside' solutions are chosen to satisfy the asymptotic conditions (C.13). In this case, the matrix eigenvalues are imaginary and lie in the interval $(-i\pi, i\pi)$. The eigenvalue density is obtained from (C.9), and is given by

$$\rho(x) = \frac{1}{2\pi}\left(1 - \frac{1}{t}\log\left(4\cos^2\frac{x}{2}\right)\right) \qquad (x \in (-\pi, \pi)), \tag{C.33}$$

and the eigenvalues themselves are $u = ix$. Although the 't Hooft coupling multiplies the log term, it averages to zero over the interval $(-\pi, \pi)$, so the normalization condition is satisfied with an average eigenvalue density of $1/2\pi$. This sub-leading solution is somewhat unusual as $\rho(x)$ diverges logarithmically at the endpoints, as highlighted in Figure 20.

The genus-zero free energy can be obtained by using the above eigenvalue density in (C.29), with the result

$$\log Z/N^2 = \frac{\zeta(3)}{t^2} + \frac{\pi^2}{6t} + (t\text{-independent imaginary term}), \tag{C.34}$$

where we have not been careful enough to keep track of the log branch issues that go into computing the imaginary term. Note that, even though here we have taken real $t > 0$, the saddle point free energy is complex since this sub-leading saddle itself is complex.

C.2.2 The solution for $t = 2\pi i/\eta$ with $\eta = \pm 1$

For connection to the $\mathcal{N} = 4$ SYM saddle, we are interested in analytically continuing to $t = 2\pi i/\eta$ with $\eta = \pm 1$. While in the previous cases the eigenvalues either lie entirely on the real or imaginary axis, this is no longer the case for the sub-leading saddle with $t = 2\pi i/\eta$. Instead, from numerical observations, the eigenvalues lie along a curve connecting $u \in (-i\pi, i\pi)$. We have been unable to obtain an analytic form of this curve. However, it can be examined numerically, as shown in Figure 21, where the 't Hooft coupling is analytically continued from $t = 5$ to $t = 2\pi i$.

The genus-zero free energy for the sub-leading saddle with $t = \pm 2\pi i$ may be obtained by analytic continuation of (C.34)

$$\log Z/N^2\big|_{t=\pm 2\pi i} = -\frac{\zeta(3)}{4\pi^2} + (\text{imaginary}). \tag{C.35}$$

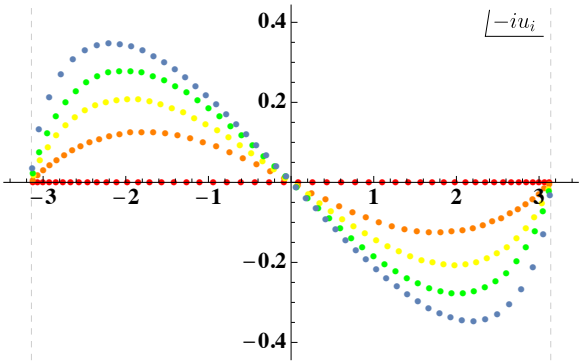


Figure 21: The numerically determined eigenvalues, $-iu_j$ for $N = 50$. The family of solutions correspond to $t = 5$ (red), $t = 5 + \pi i/2$ (orange), $t = 5 + 2\pi i$ (yellow), $t = 3 + 2\pi i$ (green), and $t = 2\pi i$ (blue), respectively.

Since this has a negative real part, it is always sub-dominant to the leading saddle whose free energy, (C.30), has vanishing real part.

C.3 Saddle point solutions of $\mathcal{N} = 4$ SYM from direct numerical evaluation

We now return to the original problem at hand, namely the saddle point evaluation of the $\mathcal{N} = 4$ SYM index in the Cardy-like limit. As we have shown in (4.1.24), the effective action reduces to that of 3d $SU(N)$ Chern-Simons theory. As a result, we may simply apply the saddle point solution of the latter theory to the $\mathcal{N} = 4$ SYM index. However, it is instructive to see how this works in practice. To do so, *we have numerically solved the saddle point equation arising from the effective action in (4.1.1)*. This was performed using FindRoot in Mathematica, where the elliptic gamma function was approximated by truncating its product representation, (A.3a).

We find that numerical solutions to the saddle point equation for the $\mathcal{N} = 4$ SYM index are sensitive to the initial trial configuration for the eigenvalues. Based on large-N investigations of the index that suggest the eigenvalues are distributed along the 'thermal' circle [116, 121], it is natural to start with an initial configuration distributed uniformly along the interval $(-\tau/2, \tau/2)$. This starting point, however, converges to the sub-leading saddle point solution corresponding to that discussed in section C.2. In order to find the dominant saddle point corresponding to section C.1, we have to instead start with an initial configuration mirroring (C.28) of the 3d Chern-Simons theory. Here the initial eigenvalues go twice around the 'thermal' circle, and are distributed non-uniformly in the interval $(-\tau, \tau)$.

As an example, we compare the numerical solution to the $\mathcal{N} = 4$ SYM saddle point equations with those from the 3d Chern-Simons theory in Figure 22 for the leading saddle and Figure 23 for the sub-dominant saddle. For $\mathcal{N} = 4$ SYM, we take $\tau = ie^{i\pi/6}$ and chemical potentials such that $\eta = 1$, so that $t = 2\pi i$ in the Chern-Simons theory. Since $|\tau| = 1$, the numerical results are not taken in the Cardy-like limit. Nevertheless, the similarity of the full SYM solution with that of the corresponding Chern-Simons theory is apparent. We have observed numerically that the sub-leading saddle point solution becomes indistinguishable from that of the Chern-Simons theory in the Cardy-like limit. However, the leading order saddle is more sensitive to $1/N$ effects arising from the repulsion between eigenvalues on the inner and outer circles of Figure 22. In any case, the

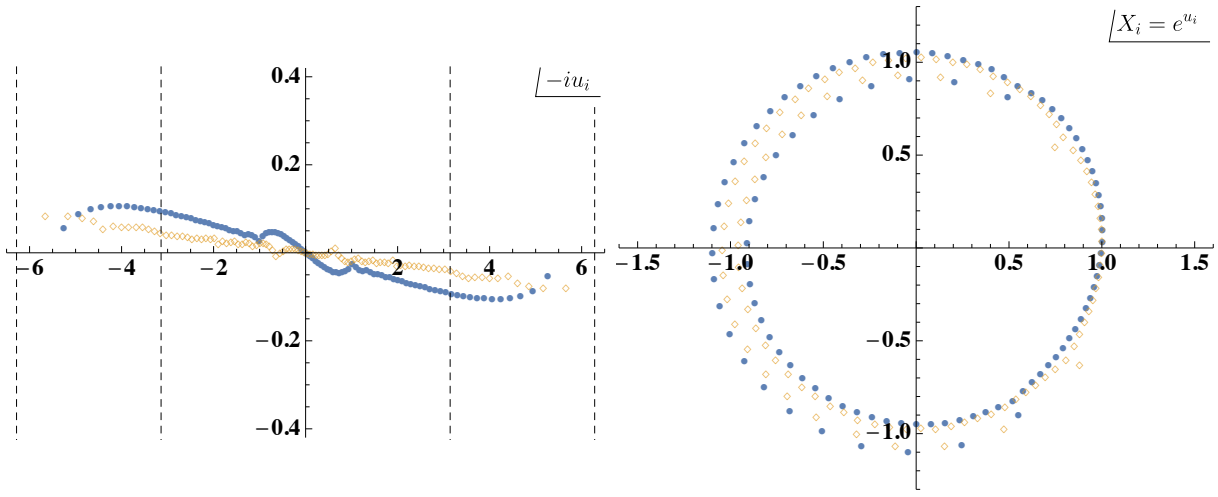


Figure 22: Comparison between the $\mathcal{N} = 4$ SYM (blue dots) and 3d Chern-Simons (orange diamonds) solutions for the dominant saddle point. Here we have taken $N = 100$ along with $\tau = ie^{i\pi/6}$ and $\Delta_a = (2/3, 2/3, 2/3 + 2\tau)$, which maps to $t = 2\pi i$ in the Chern-Simons theory. As seen in the figure on the right, the exponentiated eigenvalues go twice around the circle. The 3d Chern-Simons eigenvalues u_i are given as in (C.3), while the $\mathcal{N} = 4$ SYM eigenvalues $\tilde{u}_i$ are mapped according to $u_i = 2\pi i\tilde{u}_i/\tau$.

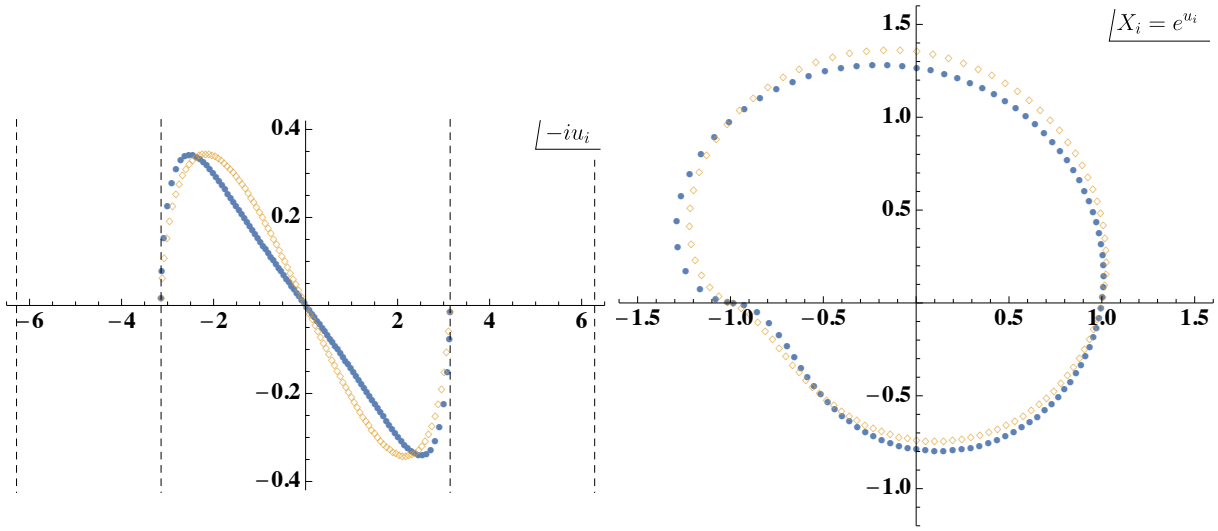


Figure 23: Comparison between the $\mathcal{N} = 4$ SYM (blue dots) and 3d Chern-Simons (orange diamonds) solutions for the sub-leading saddle point. The parameters are the same as in Figure 22, but for the sub-leading saddle the exponentiated eigenvalues go only once around the (distorted) circle.

distinction between $\mathcal{N} = 4$ SYM and 3d Chern-Simons solutions is small compared to the difference between the dominant and sub-leading saddles which is clearly evident when comparing Figure 22 with Figure 23.

D The S^3 partition function of $SU(N)$ Chern-Simons theory

Here we compute the S^3 partition function of $SU(N)$ Chern-Simons theory, namely

$$Z^{CS}_{\mathrm{SU}(N)} = \frac{1}{N!}\int_{-\infty}^{\infty}\Big(\prod_{j=1}^{N-1} d\lambda_j\Big)\, e^{-ik\pi\sum_{j=1}^{N}\lambda_j^2}\prod_{i\neq j} 2\sinh\pi\lambda_{ij} \tag{D.1}$$

with the constraint $\sum_{j=1}^{N}\lambda_j = 0$, where $k = -\eta N$ ($\eta = \pm 1$).

Recall that the S^3 partition function of U(N) Chern-Simons theory is given in Appendix B of [125] as

$$\begin{aligned} Z^{CS}_{\mathrm{U(N)}} &= \frac{1}{N!}\int_{-\infty}^{\infty}\Big(\prod_{j=1}^{N} d\lambda_j\Big)\, e^{-ik\pi\sum_{j=1}^{N}\lambda_j^2}\prod_{i\neq j} 2\sinh\pi\lambda_{ij} \\ &= \frac{(-1)^{\frac{N(N-1)}{2}} e^{-\frac{\pi i N(N-1)}{4}} e^{-\frac{\pi i}{6k}N(N^2-1)}}{(ik)^{N/2}}\prod_{m=1}^{N-1}\Big(2\sin\frac{\pi m}{k}\Big)^{N-m}. \end{aligned} \tag{D.2}$$

Under the change of variables $\lambda_\mu \to \lambda_\mu + \sum_{j=1}^{N}\lambda_j$ ($\mu = 1, \cdots, N-1$), whose Jacobian is given as

$$\prod_{j=1}^{N} d\lambda_j \quad \to \quad N\prod_{j=1}^{N} d\lambda_j, \tag{D.3}$$

the U(N) partition function (D.2) can be rewritten as

$$\begin{aligned} Z^{CS}_{\mathrm{U(N)}} &= \frac{1}{(N-1)!}\int_{-\infty}^{\infty}\Big(\prod_{j=1}^{N} d\lambda_j\Big)\, e^{-ik\pi\sum_{\mu=1}^{N-1}(\lambda_\mu+\sum_{j=1}^{N}\lambda_j)^2 - ik\pi\lambda_N^2}\prod_{\mu\neq\nu}^{N-1} 2\sinh\pi\lambda_{\mu\nu} \\ &\qquad\times\prod_{\mu=1}^{N-1} 2\sinh\pi(\lambda_\mu + \Sigma_j\lambda_j - \lambda_N)2\sinh\pi(\lambda_N - \lambda_\mu - \Sigma_j\lambda_j) \\ &= \frac{1}{(N-1)!}\int_{-\infty}^{\infty}\Big(\prod_{\mu=1}^{N-1} d\lambda_\mu\Big)\prod_{i\neq j}^{N} 2\sinh\pi\lambda_{ij}\Big|_{\lambda_N = -\sum_{\mu=1}^{N-1}\lambda_\mu} \\ &\qquad\times\int_{-\infty}^{\infty} d\lambda_N\, e^{-ik\pi N(\lambda_N+\sum_{\mu=1}^{N-1}\lambda_\mu)^2} e^{-ik\pi(\sum_{\mu=1}^{N-1}\lambda_\mu^2 + (\sum_{\mu=1}^{N-1}\lambda_\mu)^2)} \\ &= \Big(\frac{N}{ik}\Big)^{\frac{1}{2}} Z^{CS}_{\mathrm{SU}(N)}. \end{aligned} \tag{D.4}$$

For $k = -\eta N$ with $\eta = \pm 1$, substituting the identity

$$\prod_{m=1}^{N-1}\Big(2\sin\frac{\pi m}{N}\Big)^{N-m} = N^{N/2} \tag{D.5}$$

into the U(N) partition function (D.2) and using the relation (D.4), we have

$$\begin{aligned} Z^{CS}_{\mathrm{SU}(N)} &= e^{-\frac{\pi i\eta}{4}}\frac{e^{\frac{\pi i N(N-1)}{2}} e^{-\frac{\pi i N(N-1)}{4}} e^{\frac{\pi i\eta}{6}(N^2-1)}}{e^{-\frac{\pi i\eta N}{4}}} e^{\frac{\pi i(1+\eta)N(N-1)}{4}} \\ &= \exp\Big[\frac{\pi i N(N-1)}{2} + \frac{5\pi i\eta(N^2-1)}{12}\Big]. \end{aligned} \tag{D.6}$$

References

[1] A. González Lezcano and L. A. Pando Zayas, *Microstate counting via Bethe Ansätze in the 4d $\mathcal{N}$ = 1 superconformal index*, *JHEP* **03** (2020) 088 [1907.12841].

[2] A. González Lezcano, J. Hong, J. T. Liu and L. A. Pando Zayas, *Sub-leading Structures in Superconformal Indices: Subdominant Saddles and Logarithmic Contributions*, *JHEP* **01** (2021) 001 [2007.12604].

[3] A. G. Lezcano, J. Hong, J. T. Liu and L. A. P. Zayas, *The Bethe-Ansatz approach to the $\mathcal{N} = 4$ superconformal index at finite rank*, 2101.12233.

[4] S. W. Hawking, *Black hole explosions?*, *Nature* **248** (1974) 30.

[5] J. D. Bekenstein, *Black holes and the second law*, *Lettere al Nuovo Cimento (1971-1985)* **4** (1972) 737.

[6] J. D. Bekenstein, *Black holes and entropy*, *Phys. Rev. D* **7** (1973) 2333.

[7] J. D. Bekenstein, *Generalized second law of thermodynamics in black-hole physics*, *Phys. Rev. D* **9** (1974) 3292.

[8] S. W. Hawking, *Particle Creation by Black Holes*, *Commun. Math. Phys.* **43** (1975) 199.

[9] A. Strominger and C. Vafa, *Microscopic origin of the Bekenstein-Hawking entropy*, *Phys. Lett.* **B379** (1996) 99 [hep-th/9601029].

[10] J. Polchinski, *Dirichlet Branes and Ramond-Ramond charges*, *Phys. Rev. Lett.* **75** (1995) 4724 [hep-th/9510017].

[11] E. Witten, *Bound states of strings and p-branes*, *Nucl. Phys. B* **460** (1996) 335 [hep-th/9510135].

[12] A. Sen, *A Note on marginally stable bound states in type II string theory*, *Phys. Rev. D* **54** (1996) 2964 [hep-th/9510229].

[13] A. Sen, *U duality and intersecting Dirichlet branes*, *Phys. Rev. D* **53** (1996) 2874 [hep-th/9511026].

[14] C. Vafa, *Gas of d-branes and Hagedorn density of BPS states*, *Nucl. Phys. B* **463** (1996) 415 [hep-th/9511088].

[15] M. Bershadsky, C. Vafa and V. Sadov, *D-branes and topological field theories*, *Nucl. Phys. B* **463** (1996) 420 [hep-th/9511222].

[16] C. Vafa, *Instantons on D-branes*, *Nucl. Phys. B* **463** (1996) 435 [hep-th/9512078].

[17] M. Dine, N. Seiberg, X. G. Wen and E. Witten, *Nonperturbative Effects on the String World Sheet. 2.*, *Nucl. Phys. B* **289** (1987) 319.

[18] A. N. Schellekens and N. P. Warner, *Anomalies and Modular Invariance in String Theory*, *Phys. Lett. B* **177** (1986) 317.

[19] R. Dijkgraaf, E. P. Verlinde and H. L. Verlinde, *BPS spectrum of the five-brane and black hole entropy*, *Nucl. Phys. B* **486** (1997) 77 [hep-th/9603126].

[20] R. Dijkgraaf, E. P. Verlinde and H. L. Verlinde, *Counting dyons in N=4 string theory*, *Nucl. Phys. B* **484** (1997) 543 [hep-th/9607026].

[21] R. Dijkgraaf, G. W. Moore, E. P. Verlinde and H. L. Verlinde, *Elliptic genera of symmetric products and second quantized strings*, *Commun. Math. Phys.* **185** (1997) 197 [hep-th/9608096].

[22] A. Dabholkar, S. Murthy and D. Zagier, *Quantum Black Holes, Wall Crossing, and Mock Modular Forms*, 1208.4074.

[23] A. Dabholkar and S. Nampuri, *Quantum black holes*, *Lect. Notes Phys.* **851** (2012) 165 [1208.4814].

[24] A. Dabholkar, *Ramanujan and Quantum Black Holes*, 1905.04060.

[25] J. M. Maldacena, *The large N limit of superconformal field theories and supergravity*, *Adv. Theor. Math. Phys.* **2** (1998) 231 [hep-th/9711200].

[26] E. Witten, *Anti-de Sitter space and holography*, *Adv. Theor. Math. Phys.* **2** (1998) 253 [hep-th/9802150].

[27] J. L. Cardy, *Operator Content of Two-Dimensional Conformally Invariant Theories*, *Nucl. Phys. B* **270** (1986) 186.

[28] F. Benini, K. Hristov and A. Zaffaroni, *Black hole microstates in AdS_4 from supersymmetric localization*, *JHEP* **05** (2016) 054 [1511.04085].

[29] F. Benini, K. Hristov and A. Zaffaroni, *Exact microstate counting for dyonic black holes in AdS_4*, *Phys. Lett.* **B771** (2017) 462 [1608.07294].

[30] M. J. Duff and J. T. Liu, *Anti-de Sitter black holes in gauged $N = 8$ supergravity*, *Nucl. Phys. B* **554** (1999) 237 [hep-th/9901149].

[31] O. Aharony, O. Bergman, D. L. Jafferis and J. Maldacena, *$\mathcal{N} = 6$ superconformal Chern-Simons-matter theories, M2-branes and their gravity duals*, *JHEP* **10** (2008) 091 [0806.1218].

[32] E. Witten, *Topological Quantum Field Theory*, *Commun. Math. Phys.* **117** (1988) 353.

[33] E. Witten, *Constraints on Supersymmetry Breaking*, *Nucl. Phys. B* **202** (1982) 253.

[34] J. Kinney, J. M. Maldacena, S. Minwalla and S. Raju, *An Index for 4 dimensional super conformal theories*, *Commun. Math. Phys.* **275** (2007) 209 [hep-th/0510251].

[35] C. Romelsberger, *Counting chiral primaries in $N = 1$, $d=4$ superconformal field theories*, *Nucl. Phys. B* **747** (2006) 329 [hep-th/0510060].

[36] A. Cabo-Bizet, D. Cassani, D. Martelli and S. Murthy, *Microscopic origin of the Bekenstein-Hawking entropy of supersymmetric AdS_5 black holes*, *JHEP* **10** (2019) 062 [1810.11442].

[37] S. Choi, J. Kim, S. Kim and J. Nahmgoong, *Large AdS black holes from QFT*, 1810.12067.

[38] F. Benini and P. Milan, *Black Holes in 4D $\mathcal{N}=4$ Super-Yang-Mills Field Theory*, *Phys. Rev. X* **10** (2020) 021037 [1812.09613].

[39] F. Benini and P. Milan, *A Bethe Ansatz type formula for the superconformal index*, *Commun. Math. Phys.* **376** (2020) 1413 [1811.04107].

[40] C. Closset, H. Kim and B. Willett, *$\mathcal{N} = 1$ supersymmetric indices and the four-dimensional A-model*, *JHEP* **08** (2017) 090 [1707.05774].

[41] C. Closset, H. Kim and B. Willett, *Supersymmetric partition functions and the three-dimensional A-twist*, *JHEP* **03** (2017) 074 [1701.03171].

[42] A. Arabi Ardehali, *Cardy-like asymptotics of the 4d $\mathcal{N} = 4$ index and AdS_5 blackholes*, *JHEP* **06** (2019) 134 [1902.06619].

[43] M. Honda, *Quantum Black Hole Entropy from 4d Supersymmetric Cardy formula*, *Phys. Rev. D* **100** (2019) 026008 [1901.08091].

[44] A. Cabo-Bizet, D. Cassani, D. Martelli and S. Murthy, *The asymptotic growth of states of the 4d $\mathcal{N} = 1$ superconformal index*, *JHEP* **08** (2019) 120 [1904.05865].

[45] J. Kim, S. Kim and J. Song, *A 4d N=1 Cardy Formula*, *JHEP* **01** (2021) 025 [1904.03455].

[46] A. Amariti, I. Garozzo and G. Lo Monaco, *Entropy function from toric geometry*, 1904.10009.

[47] A. Arabi Ardehali, J. T. Liu and P. Szepietowski, *c - a from the $\mathcal{N} = 1$ superconformal index*, *JHEP* **12** (2014) 145 [1407.6024].

[48] L. Di Pietro and Z. Komargodski, *Cardy formulae for SUSY theories in $d = 4$ and $d = 6$*, *JHEP* **12** (2014) 031 [1407.6061].

[49] A. Arabi Ardehali, *High-temperature asymptotics of supersymmetric partition functions*, *JHEP* **07** (2016) 025 [1512.03376].

[50] A. Arabi Ardehali, *High-temperature asymptotics of the 4d superconformal index*, Ph.D. thesis, Michigan U., 2016. 1605.06100.

[51] L. Di Pietro and M. Honda, *Cardy Formula for 4d SUSY Theories and Localization*, *JHEP* **04** (2017) 055 [1611.00380].

[52] S. M. Hosseini, A. Nedelin and A. Zaffaroni, *The Cardy limit of the topologically twisted index and black strings in AdS_5*, *JHEP* **04** (2017) 014 [1611.09374].

[53] S. M. Hosseini, K. Hristov and A. Zaffaroni, *A note on the entropy of rotating BPS $AdS_7 \times S^4$ black holes*, *JHEP* **05** (2018) 121 [1803.07568].

[54] S. Benvenuti, L. A. Pando Zayas and Y. Tachikawa, *Triangle anomalies from Einstein manifolds*, *Adv. Theor. Math. Phys.* **10** (2006) 395 [hep-th/0601054].

[55] A. Lanir, A. Nedelin and O. Sela, *Black hole entropy function for toric theories via Bethe Ansatz*, *JHEP* **04** (2020) 091 [1908.01737].

[56] A. Amariti, M. Fazzi and A. Segati, *The SCI of $\mathcal{N} = 4$ $USp(2N_c)$ and $SO(N_c)$ SYM as a matrix integral*, 2012.15208.

[57] A. Amariti, M. Fazzi and A. Segati, *Expanding on the Cardy-like limit of the superconformal index of the SCI of 4d $\mathcal{N} = 1$ ABCD SCFTs*, 2103.15853.

[58] D. Cassani and Z. Komargodski, *EFT and the SUSY Index on the 2nd Sheet*, 2104.01464.

[59] A. Arabi Ardehali and S. Murthy, *The 4d superconformal index near roots of unity and 3d Chern-Simons theory*, 2104.02051.

[60] S. Choi and S. Kim, *Large AdS_6 black holes from CFT_5*, 1904.01164.

[61] S. Choi, C. Hwang and S. Kim, *Quantum vortices, M2-branes and black holes*, 1908.02470.

[62] G. Kántor, C. Papageorgakis and P. Richmond, *AdS_7 black-hole entropy and 5D $\mathcal{N} = 2$ Yang-Mills*, *JHEP* **01** (2020) 017 [1907.02923].

[63] J. Nahmgoong, *6d superconformal Cardy formulas*, 1907.12582.

[64] J. Nian and L. A. Pando Zayas, *Microscopic entropy of rotating electrically charged AdS_4 black holes from field theory localization*, *JHEP* **03** (2020) 081 [1909.07943].

[65] N. Bobev and P. M. Crichigno, *Universal spinning black holes and theories of class $\mathcal{R}$*, *JHEP* **12** (2019) 054 [1909.05873].

[66] F. Benini, D. Gang and L. A. Pando Zayas, *Rotating Black Hole Entropy from M5 Branes*, *JHEP* **03** (2020) 057 [1909.11612].

[67] P. M. Crichigno and D. Jain, *The 5d Superconformal Index at Large N and Black Holes*, 2005.00550.

[68] J. Hong and J. T. Liu, *The topologically twisted index of $\mathcal{N} = 4$ super-Yang-Mills on $T^2 \times S^2$ and the elliptic genus*, *JHEP* **07** (2018) 018 [1804.04592].

[69] F. Benini, E. Colombo, S. Soltani, A. Zaffaroni and Z. Zhang, *Superconformal indices at large N and the entropy of $AdS_5 \times SE_5$ black holes*, *Class. Quant. Grav.* **37** (2020) 215021 [2005.12308].

[70] A. Sen, *Logarithmic Corrections to $\mathcal{N} = 2$ Black Hole Entropy: An Infrared Window into the Microstates*, *Gen. Rel. Grav.* **44** (2012) 1207 [1108.3842].

[71] S. Benvenuti, B. Feng, A. Hanany and Y.-H. He, *Counting BPS Operators in Gauge Theories: Quivers, Syzygies and Plethystics*, *JHEP* **11** (2007) 050 [hep-th/0608050].

[72] B. Feng, A. Hanany and Y.-H. He, *Counting gauge invariants: The Plethystic program*, *JHEP* **03** (2007) 090 [hep-th/0701063].

[73] O. Aharony, J. Marsano, S. Minwalla, K. Papadodimas and M. Van Raamsdonk, *The Hagedorn - deconfinement phase transition in weakly coupled large N gauge theories*, *Adv. Theor. Math. Phys.* **8** (2004) 603 [hep-th/0310285].

[74] C. Romelsberger, *Calculating the Superconformal Index and Seiberg Duality*, 0707.3702.

[75] F. Dolan and H. Osborn, *Applications of the Superconformal Index for Protected Operators and q-Hypergeometric Identities to N=1 Dual Theories*, *Nucl. Phys. B* **818** (2009) 137 [0801.4947].

[76] B. S. Acharya, J. M. Figueroa-O'Farrill, C. M. Hull and B. J. Spence, *Branes at conical singularities and holography*, *Adv. Theor. Math. Phys.* **2** (1999) 1249 [hep-th/9808014].

[77] L. Castellani, A. Ceresole, R. D'Auria, S. Ferrara, P. Fre and M. Trigiante, *G / H M-branes and AdS(p+2) geometries*, *Nucl. Phys. B* **527** (1998) 142 [hep-th/9803039].

[78] C. Bar, *Real Killing Spinors and Holonomy*, *Commun. Math. Phys.* **154** (1993) 509.

[79] J. P. Gauntlett, D. Martelli, J. Sparks and D. Waldram, *Sasaki-Einstein metrics on S(2) x S(3)*, *Adv. Theor. Math. Phys.* **8** (2004) 711 [hep-th/0403002].

[80] D. Martelli and J. Sparks, *Toric geometry, Sasaki-Einstein manifolds and a new infinite class of AdS/CFT duals*, *Commun. Math. Phys.* **262** (2006) 51 [hep-th/0411238].

[81] I. R. Klebanov and E. Witten, *Superconformal field theory on threebranes at a Calabi-Yau singularity*, *Nucl. Phys.* **B536** (1998) 199 [hep-th/9807080].

[82] D. R. Morrison and M. R. Plesser, *Nonspherical horizons. 1.*, *Adv. Theor. Math. Phys.* **3** (1999) 1 [hep-th/9810201].

[83] S. Benvenuti, S. Franco, A. Hanany, D. Martelli and J. Sparks, *An infinite family of superconformal quiver gauge theories with Sasaki-Einstein duals*, *JHEP* **06** (2005) 064 [hep-th/0411264].

[84] B. Feng, A. Hanany and Y.-H. He, *D-brane gauge theories from toric singularities and toric duality*, *Nucl. Phys. B* **595** (2001) 165 [hep-th/0003085].

[85] M. Bertolini, F. Bigazzi and A. L. Cotrone, *New checks and subtleties for AdS/CFT and a-maximization*, *JHEP* **12** (2004) 024 [hep-th/0411249].

[86] K. A. Intriligator and B. Wecht, *The Exact superconformal R symmetry maximizes a*, *Nucl. Phys. B* **667** (2003) 183 [hep-th/0304128].

[87] D. A. Cox and B. John, *Little, and donal o'shea. using algebraic geometry*, *Graduate texts in mathematics. Springer, New York* (1998) .

[88] W. Fulton, *Introduction to Toric Varieties.(AM-131), Volume 131*. Princeton university press, 2016.

[89] T. Delzant, *P 'e riodic hamiltonians and convex images of the moment map*, *Bulletin de la Soci 'e t é math 'e matique de France* **116** (1988) 315.

[90] E. Witten, *Phases of N=2 theories in two-dimensions*, *Nucl. Phys. B* **403** (1993) 159 [hep-th/9301042].

[91] K. Hori, R. Thomas, S. Katz, C. Vafa, R. Pandharipande, A. Klemm et al., *Mirror symmetry*, vol. 1. American Mathematical Soc., 2003.

[92] B. Feng, S. Franco, A. Hanany and Y.-H. He, *Symmetries of toric duality*, *JHEP* **12** (2002) 076 [hep-th/0205144].

[93] J. P. Gauntlett, D. Martelli, J. F. Sparks and D. Waldram, *A new infinite class of Sasaki-Einstein manifolds*, *Adv. Theor. Math. Phys.* **8** (2006) 987 [hep-th/0403038].

[94] A. Hanany and A. Iqbal, *Quiver theories from D6 branes via mirror symmetry*, *JHEP* **04** (2002) 009 [hep-th/0108137].

[95] A. Hanany and Y.-H. He, *NonAbelian finite gauge theories*, *JHEP* **02** (1999) 013 [hep-th/9811183].

[96] A. Hanany, P. Kazakopoulos and B. Wecht, *A New infinite class of quiver gauge theories*, *JHEP* **08** (2005) 054 [hep-th/0503177].

[97] D. Martelli and J. Sparks, *Toric Sasaki-Einstein metrics on S**2 x S**3*, *Phys. Lett. B* **621** (2005) 208 [hep-th/0505027].

[98] J. F. Plebanski and M. Demianski, *Rotating, charged, and uniformly accelerating mass in general relativity*, *Annals of Physics* **98** (1976) 98.

[99] M. Cvetic, H. Lu, D. N. Page and C. N. Pope, *New Einstein-Sasaki and Einstein spaces from Kerr-de Sitter*, *JHEP* **07** (2009) 082 [hep-th/0505223].

[100] S. Benvenuti and M. Kruczenski, *From Sasaki-Einstein spaces to quivers via BPS geodesics: L**p,q—r*, *JHEP* **04** (2006) 033 [hep-th/0505206].

[101] S. Franco, A. Hanany, K. D. Kennaway, D. Vegh and B. Wecht, *Brane dimers and quiver gauge theories*, *JHEP* **01** (2006) 096 [hep-th/0504110].

[102] A. Hanany and K. D. Kennaway, *Dimer models and toric diagrams*, hep-th/0503149.

[103] A. Butti and A. Zaffaroni, *From toric geometry to quiver gauge theory: The Equivalence of a-maximization and Z-minimization*, *Fortsch. Phys.* **54** (2006) 309 [hep-th/0512240].

[104] S. M. Hosseini, K. Hristov and A. Zaffaroni, *An extremization principle for the entropy of rotating BPS black holes in AdS_5*, *JHEP* **07** (2017) 106 [1705.05383].

[105] B. Assel, D. Cassani, L. Di Pietro, Z. Komargodski, J. Lorenzen and D. Martelli, *The Casimir Energy in Curved Space and its Supersymmetric Counterpart*, *JHEP* **07** (2015) 043 [1503.05537].

[106] B. Assel, D. Cassani and D. Martelli, *Supersymmetric counterterms from new minimal supergravity*, 1410.6487.

[107] J. Lorenzen and D. Martelli, *Comments on the Casimir energy in supersymmetric field theories*, *JHEP* **07** (2015) 001 [1412.7463].

[108] A. Arabi Ardehali, *High-temperature asymptotics of the 4d superconformal index*, Ph.D. thesis, Michigan U., 2016. 1605.06100.

[109] J. T. Liu, L. A. Pando Zayas, V. Rathee and W. Zhao, *Toward Microstate Counting Beyond Large N in Localization and the Dual One-loop Quantum Supergravity*, *JHEP* **01** (2018) 026 [1707.04197].

[110] J. T. Liu, L. A. Pando Zayas and S. Zhou, *Subleading Microstate Counting in the Dual to Massive Type IIA*, 1808.10445.

[111] S. M. Hosseini, *Black hole microstates and supersymmetric localization*, Ph.D. thesis, Milan Bicocca U., 2018-02. 1803.01863.

[112] A. Zaffaroni, *Lectures on AdS Black Holes, Holography and Localization*, 2019, 1902.07176.

[113] J. T. Liu, L. A. Pando Zayas, V. Rathee and W. Zhao, *One-Loop Test of Quantum Black Holes in anti–de Sitter Space*, *Phys. Rev. Lett.* **120** (2018) 221602 [1711.01076].

[114] D. Gang, N. Kim and L. A. Pando Zayas, *Precision Microstate Counting for the Entropy of Wrapped M5-branes*, *JHEP* **03** (2020) 164 [1905.01559].

[115] L. A. Pando Zayas and Y. Xin, *Universal logarithmic behavior in microstate counting and the dual one-loop entropy of AdS_4 black holes*, *Phys. Rev. D* **103** (2021) 026003 [2008.03239].

[116] A. Cabo-Bizet and S. Murthy, *Supersymmetric phases of 4d $\mathcal{N} = 4$ SYM at large N*, *JHEP* **09** (2020) 184 [1909.09597].

[117] A. Cabo-Bizet, D. Cassani, D. Martelli and S. Murthy, *The large-N limit of the 4d $\mathcal{N} = 1$ superconformal index*, 2005.10654.

[118] E. Brézin, C. Itzykson, G. Parisi and J.-B. Zuber, *Planar diagrams*, in *The Large N Expansion In Quantum Field Theory And Statistical Physics: From Spin Systems to 2-Dimensional Gravity*, pp. 567–583, World Scientific, (1993).

[119] B. Eynard, T. Kimura and S. Ribault, *Random matrices*, 1510.04430.

[120] H.-T. Diep, *Frustrated Spin Systems*. 2004, 10.1142/5697.

[121] A. Arabi Ardehali, J. Hong and J. T. Liu, *Asymptotic growth of the 4d $\mathcal{N} = 4$ index and partially deconfined phases*, *JHEP* **07** (2020) 073 [1912.04169].

[122] N. Bobev, M. Bullimore and H.-C. Kim, *Supersymmetric Casimir Energy and the Anomaly Polynomial*, *JHEP* **09** (2015) 142 [1507.08553].

[123] M. Aganagic, A. Klemm, M. Marino and C. Vafa, *Matrix model as a mirror of Chern-Simons theory*, *JHEP* **02** (2004) 010 [hep-th/0211098].

[124] N. Halmagyi and V. Yasnov, *The spectral curve of the lens space matrix model*, hep-th/0311117v3.

[125] A. Kapustin, B. Willett and I. Yaakov, *Exact Results for Wilson Loops in Superconformal Chern-Simons Theories with Matter*, *JHEP* **03** (2010) 089 [0909.4559].

[126] H. Ooguri and C. Vafa, *World sheet derivation of a large N duality*, *Nucl. Phys.* **B641** (2002) 3 [hep-th/0205297].

[127] F. Larsen, J. Nian and Y. Zeng, *AdS_5 black hole entropy near the BPS limit*, *JHEP* **06** (2020) 001 [1907.02505].

[128] J. Nian and L. A. Pando Zayas, *Toward an Effective CFT_2 from $\mathcal{N} = 4$ Super Yang-Mills and Aspects of Hawking Radiation*, 2003.02770.

[129] M. David, J. Nian and L. A. Pando Zayas, *Gravitational Cardy Limit and AdS Black Hole Entropy*, 2005.10251.

[130] S. Murthy, *The growth of the $\frac{1}{16}$-BPS index in 4d $\mathcal{N} = 4$ SYM*, 2005.10843.

[131] P. Agarwal, S. Choi, J. Kim, S. Kim and J. Nahmgoong, *AdS black holes and finite N indices*, 2005.11240.

[132] F. Benini and G. Rizi, *Superconformal index of low-rank gauge theories via the Bethe Ansatz*, 2102.03638.

[133] O. Aharony, F. Benini, O. Mamroud and P. Milan, *A gravity interpretation for the Bethe Ansatz expansion of the $\mathcal{N} = 4$ SYM index*, 2104.13932.

[134] L. A. Pando Zayas and Y. Xin, *Topologically twisted index in the 't Hooft limit and the dual AdS_4 black hole entropy*, *Phys. Rev. D* **100** (2019) 126019 [1908.01194].

[135] M. Marino and P. Putrov, *ABJM theory as a Fermi gas*, *J. Stat. Mech.* **1203** (2012) P03001 [1110.4066].

[136] S. Bhattacharyya, A. Grassi, M. Marino and A. Sen, *A One-Loop Test of Quantum Supergravity*, *Class. Quant. Grav.* **31** (2014) 015012 [1210.6057].

[137] M. Marino, *Lectures on localization and matrix models in supersymmetric Chern-Simons-matter theories*, *J.Phys.* **A44** (2011) 463001 [1104.0783].

[138] T. Morita and V. Niarchos, *F-theorem, duality and SUSY breaking in one-adjoint Chern-Simons-Matter theories*, *Nucl. Phys. B* **858** (2012) 84 [1108.4963].